An Investigation of Homo and Heterodimerization of the human delta opioid receptor

A THESIS PRESENTED FOR
THE DEGREE OF
DOCTOR OF PHILOSOPHY

BY

MARY McVEY

DIVISION OF BIOCHEMISTRY AND MOLECULAR BIOLOGY
INSTITUTE OF BIOMEDICAL AND LIFE SCIENCES
UNIVERSITY OF GLASGOW

AUGUST 2001

Abstract

Homo and heterodimerization of G-protein coupled receptors (GPCRs) is a concept which has gained credibility as another mechanism by which GPCR signalling can increase in complexity.

The generation of Flag and c-myc N-terminally tagged forms of the human δOR, with and without GFP fused to the C-terminus, has allowed identification of each receptor form after transient transfection in HEK293 cells. Stable cell lines expressing Flag-δOR or Flag-δOR-GFP were generated in HEK293cells. High affinity [^{3}H]antagonist binding and agonist stimulated inhibition of adenylyl cyclase activity was observed. Agonist stimulated internalization of Flag-δOR-GFP was followed in live cells with a $t_{½}$ of < 10min.

Constitutively formed (mouse) δOR homodimers were identified using co-immunprecipitation techniques (Cvejic and Devi 1997). The human δOR is demonstrated here to also form constitutive homodimers using co-immunoprecipitation techniques. Constitutive heterodimerization of human δOR with the μOR, IP prostanoid receptor, IP prostaniod receptor-GFP, β_1AR-GFP and β_2AR-GFP was also observed. Further investigations of the lysis procedures and antibodies used for immunoprecipitation indicated that the heterodimers were not a reflection of the experimental conditions used.

Fluorescently labelled antibodies were used to specifically label N-terminally tagged GPCRs expressed at the cell-surface. The spectral overlap property of the fluorescent labels chosen allowed fluorescence resonance energy transfer (FRET) to be used to determine homo and heterodimerization of antibody-bound GPCRs. The fluorescent donor molecule, Europium, also has the property of long-lived fluorescence after excitation. Thus allowing the FRET to be time-resolved (TR-FRET) increasing the sensitivity of the developed assay.

Constitutively formed cell-surface δOR homodimers were identified using TR-FRET. The presence of agonist was unable to modulate this interaction.

Heterodimerization between the δOR and β_2AR-GFP, which had been observed using co-immunoprecipitation techniques, was not evident using the cell-surface TR-FRET in intact cells. The presence of agonist for each receptor within the dimer or the presence of both agonists together did not generate any heterodimerization between the δOR and β_2AR-GFP receptors. No significant level of heterodimers between the δOR and μOR was observed using TR-FRET.

Optimisation of the TR-FRET assay has allowed the assay to be performed in a homogeneous format although this is less sensitive than the heterogeneous assay described.

Aknowledgements

Firstly, I would like to thank my supervisor, Professor Graeme Milligan for his assistance and guidance throughout my project, and for his patience during my writing of this thesis. I would also like to thank everyone in A20 and A3 for their scientific input, help and moral support. Special thanks go to Tomas Drmota for much needed words of encouragement, even if some of them were in Czech, and Elaine Kellet who patiently listens to all my complaints. I would also like to thank Craig Carr for his unique moral boosting technique more commonly known as sarcasm, I hope you were only joking Craig.

Funding for my project was provided by the BBSRC and SmithKline Beecham Pharmaceuticals and was gratefully received. I also spent some time at SmithKline Beecham in Harlow and would like to extend my thanks to everyone there, especially my supervisor Dr Andrew Pope and to Lucy Mensah for their help and support not only during my time in Harlow but throughout the project.

I would not have managed to achieve any of this without the help and support of my friends and family. My parents, who have been loving and supportive and all my brothers for their words of encouragement.

Lastly I wish to thank my husband Gerry who has been continually supportive throughout this project and while I have been writing this thesis as without your love and patience I would not have got this far.

Contents

List of Figures

List of Tables

Abbreviations

ADP	Adenosine 5'-diphosphate
APC	Cross-linked Allophycocyanin
APP(NH)p	Adenylyl 5'-imidodiphosphate
β_2AR	β_2-adrenergic receptor
B_{max}	Maximal binding capacity
BFP	Blue fluorescent protein
cAMP	Adenosine 3', 5'-cyclic monophosphate
cDNA	Complementary deoxyribonucleic acid
CHAPS	3-[(3-cholamidopropyl)-dimethylammonio]-1-propanesulfonate
CHO	Chinese hamster ovary
cpm	Counts per minute
DADLE	[d]Ala^2, [d]Leu^5, enkephalin
DALCE	[D-Ala2, Leu5, Cys6]enkephalin
DAMGO	Tyr-D-Ala-Gly-NMe-Phe-Gly-ol
DMEM	Dulbecco's modified Eagle's medium
DMSO	Dimethylsulphoxide
dpm	Disintegrations per minute
DTT	Dithiothreitol
E. coli	*Escherichia coli*
EC_{50}	Median effective dose
EDTA	Ethylenediaminetetraacetic acid
ELISA	Enzyme-linked immunosorbent assay
ER	Endoplasmic reticulum
Eu	Europium ion
eYFP	enhanced Yellow fluorescent protein
eCFP	enhanced cyan fluorescent protein
FITC	Fluorescein isothiocyanate
GFP	Green fluorescent protein
GPCR	G protein coupled receptors
Gpp(NH)p	Guanylyl 5'-[by imido]diphosphate
GRK	G protein coupled receptor kinase
GTP	Guanosine 5'-triphosphate

h	hour
HEK293	Human Embryonic Kidney 293
HEPES	4-(2-Hydroxyethyl)-1-piperazine-N' 2-ethane-sulphonic acid
HTRF	Homogeneous Time-Resolved Fluorescence
IC_{50}	Median inhibitory dose
K_d	Equilibrium dissociation constant
KDa	Kilodaltons
Min	minute
myc	c-myc-epitope tag
NBCS	Newborn calf serum
NP40	nonidet P40 (polyoxyethylene (9)-*p*-*t*-octylphenol)
PAGE	Polyacrylamide Gel Electrophoresis
PCR	Polymerase chain reaction
PKA	Protein Kinase A
PKC	Protein Kinase C
PLA2	Phospholipase A2
PLC	Phospholipase C
SD	Standard deviation
SDS	Sodium dodecyl (lauryl) sulphate
SEM	Standard error of the mean
SMCC	Succinimidyl-trans-4-(maleimidylmethyl)cyclohexane-1-carboxylate
SNC80	(+)-4-[(αR)-α-((2S,5R)-4-Allyl-2,5-dimethyl-1-piperazinyl)-3-methoxybenzyl]-N,N-diethylbenzamide
TCA	Trichloroacetic acid
TEMED	N, N, N, N'-tetramethylethylenediamine
TM	Transmembrane segment of G protein coupled receptor
TRIS	Tris(hydroxymethyl)aminomethane
Tween20	polyoxyethylene sorbitan monolaurate
TX100	nonaethylene glycol octylphenol ether

CHAPTER 1

INTRODUCTION

CHAPTER 1 INTRODUCTION

1.1 Opioid receptors – a brief history

For centuries the pain relieving properties of the opium poppy *Papaver somniferum* have been recognised. The alkaloid drug morphine and its closely related analogue etorphine have been shown to be responsible for the pain relief. These drugs were shown to also have the undesirable qualities of dependency and tolerance which result from their repeated use. This led to the development of new drugs, which it was hoped would have the desired pain relief qualities without any undesirable properties. One drug that was discovered during this search was heroin, a diacetylated form of morphine that was originally thought to be a safer form of morphine. The most potent drug of pain relief to date remains to be morphine and despite its undesirable properties, it is still in much use today. Morphine and other alkaloid drugs activate opioid receptors. These are important in the regulation of anaesthesia and analgesia and therefore have been widely studied. Investigation of the mechanisms of tolerance and dependency has especially been studied with a view to developing new drugs that do not have these qualities. Tolerance to morphine is thought to arise, in part, from desensitization of these receptors.

Opioid receptors have been identified in the central nervous system (CNS) where they inhibit the release of neurotransmitters from dorsal root ganglion projections in the dorsal horn of the spinal cord and also in the peripheral nervous system (PNS). The proposal of opioid receptor sub-types resulted from differential pharmacology observed in the guinea pig ileum assay when compared to that of the mouse vas deferens. Subsequently, this variation in pharmacology was attributed to there being a higher density of δ-opioid receptors in the mouse vas deferens and the guinea pig ileum having a higher density of the μ-opioid receptor (Quock et al., 1999). Opioid receptor density in different brain regions varies widely (Quock et al., 1999) However, all three opioid receptor subtypes have been shown to be present in some neurones (Ji et al., 1995). Knock-out mice with the absence of a single opioid receptor

subtype are fertile with no marked anatomical deficit indicating that full activity of the endogenous opioid system is not critical for development (Kieffer, 1999). Opioids are involved in diverse biological phenomena including gut motility and the immune response which results from interaction with endocrine and immune systems. The adverse effects of opiates include respiratory depression, decreased gastro-intestinal motility and sedation.

Opiate binding sites were found in the mammalian brain in 1973 (Pert and Snyder 1973; Simon et al., 1973) and the naturally occurring opiate peptide ligands identified as enkephalins, dynorphins and endorphins by Bradbury et al. (1976), Cox et al. (1976), Goldstein et al. (1981), Hughes et al. (1975) and Pasternak et al. (1976). They were found to be derived from the larger pre-cursors, proenkephalin A (Noda et al., 1982), prodynorphin (Kakidani et al., 1982), and opiomelanocortin (Nakanishi et al., 1979). Pharmacological studies using different ligands demonstrated the presence of three opioid receptor subtypes named after their respective agonists μOR (for morphine), κOR (for ketacyclazone) and δOR (for [d]Ala^2, [d]Leu^5, enkephalin (DADLE)) (Chang and Cuatrecasas 1979; Lord et al., 1977). cDNAs encoding the μOR, δOR and κOR were isolated by Chen et al. (1993), Evans et al. (1992), Kieffer et al. (1992) and Yasuda et al. (1993). The availability of the cDNA for these receptors has allowed their study *in vitro* and has resulted in the identification of sub-type selective agonists, antagonists and inverse agonists. There is another receptor, ORL-1, which has been suggested to be another member of the opioid receptor family. However this receptor has its own specific ligand and does not exhibit significant binding of many opioid ligands identified to date. The ORL-1 receptor does have significant sequence similarities with the cloned opioid receptors and is reviewed along with them by Henderson and McKnight (1997).

1.2 G-protein coupled receptors

The opioid receptors have been classified as belonging to the large and varied family of G-protein coupled receptors (GPCRs) which, as for all cell-surface receptors, recognize specific extracellular signals, resulting in activation of intracellular effector molecules to generate an intracellular signal to elicit an

appropriate cellular response (Ji et al., 1998). GPCRs are the largest family of cell-surface receptors. They vary widely in their function and are involved in the control of many cellular processes including neurotransmission, cellular metabolism, secretion, cell differentiation and growth. A huge variety of ligands exist for these receptors, examples of which include, light, odorants, peptides and large glycoproteins. The importance of correct GPCR signalling is demonstrated in the many disease states that have been shown to result from a malfunctioning of their signalling. For example, mutant V2 vasopressin receptors cause X-linked nephrogenic diabetes insipidus. Other disease states resulting from defective GPCR signalling include cancer, diabetes and some neural disorders. Mutant receptors as well as naturally occurring polymorphic variations of receptors have been identified which either bind ligands incorrectly, are poorly trafficked to the cell surface, constitutively generate signals or are unable to signal. Some mutants, however, are beneficial. For example, a mutation in the chemokine receptor CCR5, which acts as a co-receptor for human immunodeficiency virus (HIV), prevents binding of HIV to the target cells thus limiting viral infection for those who are homozygous for this mutation (Liu et al., 1996).

The GPCR family is the single largest known gene family in the human genome and greater than 1% of the genes of the human genome have been shown to code for GPCRs. Because of this the Human Genome Sequencing programme (HGS) has generated a huge interest in these receptors as the database contains many sequences that are thought to code for seven transmembrane receptors with unknown function. The pharmaceutical industry are therefore looking at the necessary techniques that would allow these receptors to be studied, identifying appropriate ligands and subsequently their function. There is a huge potential for new therapeutic drugs for these receptors as discussed by Stadel et al. (1997).

1.2.1 GPCR structural features

The first GPCRs to be purified and characterized were rhodopsin (Nathans and Hogness, 1983) and the β_2AR (Dixon et al., 1986), since then a huge number of

GPCRs have been identified and many more predicted. GPCRs all have a similar structure consisting of an extracellular N-terminus with seven transmembrane domains that are linked by extracellular and intracellular loops and an intracellular C-terminal domain, see figure 1.1.

1.2.1.1 Extracellular N-terminus

The extracellular N-terminal domain varies in length from 7-595 amino acids (Ji et al., 1998) for different GPCRs. It is involved in the binding of large polypeptide ligands e.g. glucagon and glycoprotein hormones e.g. luteinizing hormone. The large extracellular N-terminus of family 3 GPCRs is involved in ligand binding and may also be involved in the dimerization of these receptors which is described in section 1.6.5. The N-terminal domain contains consensus sequences (Asp-X-Ser/Thr, where X is any amino acid except proline or aspartate) for N-linked glycosylation which is necessary to ensure correct trafficking of the GPCR to the plasma membrane.

1.2.1.2 Seven membrane spanning regions

GPCRs traverse the membrane seven times and are sometimes referred to as seven transmembrane (TM) receptors. The transmembrane regions are α helical in structure, although the α helices can extend outside the membrane. The residues within the transmembrane domains are generally hydrophobic, typically consisting of 20-27 amino acids that are entropically driven into the membrane. The transmembrane domains are numbered 1 to 7 and they are arranged in a counter-clockwise direction within the membrane when viewed from the extracellular surface. In general, transmembrane domains 1, 4 and 7 are more hydrophobic than 2, 3, 5 and 6. Proline residues are frequently found in the transmembrane domains, resulting in a kink in the helix backbone by 26°. The angle of the α helices influences how they interact with each other and with ligand molecules (Ji et al., 1998). Residues within the transmembrane domains are involved in ligand binding and receptor activation. The transmembrane domains form a rigid yet dynamic structure, which allows conformational changes to occur on ligand binding.

1.2.1.3 Ligand binding domains

There are 3 major families of GPCRs in mammals, the rhodopsin like (family 1), which is the largest and most studied family, the calcitonin like (family 2) and the metabotropic glutamate receptor (mGluR) like (family 3). These divisions are based on where ligands physically interact with the GPCR (Gether and Kobilka, 1998). The rhodopsin-like family is further divided into subfamilies. These are the 1a sub family which is activated by small molecular weight ligands e.g. catecholamines, that bind in a cavity formed by TM helices 3 to 6. The 1b subfamily which is activated by small peptides, including cytokine ligands and other peptides by interacting with the extracellular loops and N-terminal domain. The C-terminus of these peptides has been proposed to interact with the cavity within the transmembrane helices in a manner similar to that of the subfamily 1a. The 1c sub family are activated by glycoprotein hormones e.g. thyrotrophin stimulating hormone (TSH) which bind to the N-terminal region. Family 2 GPCRs include the calcitonin receptor that have ligand binding regions similar to that of type 1c although there is no sequence similarity between these and type 1c GPCRs. Family 3 GPCRs include the $GABA_B$ and glutamate receptors where the neurotransmitter ligands bind to the large extracellular N-terminal region (Bockaert and Pin, 1999).

Ligand interaction with receptors involves hydrogen bonds, ion pairs and hydrophobic contacts (Ji et al., 1998). Ligands have two main properties; affinity and efficacy. Affinity describes how well a drug binds to the receptor and efficacy describes the level of effect resulting from the ligand binding. Ligands range from agonists, which demonstrate positive efficacy, antagonists or neutral ligands, which demonstrate no efficacy and inverse agonists, which demonstrate a negative effect on efficacy. Ligands can demonstrate high affinity for a GPCR and have a neutral efficacy.

Ligand binding and receptor activation can be separated into two distinct mechanisms although these are difficult to separate. In the absence of ligand GPCRs are maintained in a certain conformation that changes upon ligand

binding. A high resolution structure of the bovine rhodopsin receptor was obtained recently by Palczewski et al. (2000) demonstrating the highly ordered structure of inactive receptor and the conformational changes on ligand activation. These conformational constraints are important in maintaining inactivity as a mutant β_2AR which demonstrates constitutive activity in the absence of any ligand was more unstable and demonstrated enhanced conformational flexibility than the wild-type receptor (Gether et al., 1997).

Ligand binding of biogenic amines has been studied in great detail, demonstrating the involvement of several key residues in TMs 3, 5 and 7 and the side chains of these residues in determining the specificity of agonist binding. The amine of the ligand pairs with an aspartate residue in TM 3 and the catechol ring interacts with residues in TM's 5 and 6. The interaction with TM 3 has been shown to be important for ligand binding, with residues in TM's 5 and 6 being important for receptor activation (Ji et al., 1998). Ligand activation has been demonstrated to involve a change in conformation in the TMs resulting in a change in orientation of TM 3 to TM 7 as was shown by Farrens et al. (1996), for the rhodopsin receptor and by Javitch et al. (1997), for the β_2AR receptor. This was confirmed recently by Ghanouni et al. (2001), for the β_2AR using fluorescent labelling of the receptor.

1.2.1.4 Conserved DRY (aspartate, arginine, tyrosine) sequence

There is a highly conserved DRY sequence in all family 1 GPCRs at the interface of TM 3 and intracellular loop 2 which is important for receptor activation. These residues are not conserved in other GPCR families. The conserved arginine has been hypothesised to be constrained in a hydrophilic pocket formed by conserved polar residues in TMs 1, 2 and 7. Receptor activation results in the protonation of the aspartate causing arginine to shift out of the polar pocket leading to cytoplasmic exposure of previously hidden sequences in the second and third intracellular loops. This has been indicated by computational studies and the generation of constitutively activated mutants by

mutation of the aspartate in the α_{1b} adrenergic receptor by Scheer et al. (1996) and the β_2AR by Wess (1997).

1.2.1.5 Extracellular loops

The extracellular loops vary in size although not to the same extent as the N-terminal region or the intracellular loops. They can be involved in ligand binding e.g. of peptide ligands to opioid receptors. The majority of family 1 receptors have two conserved cysteine residues in extracellular loops 1 and 2 that are thought to form a di-sulphide bond believed to be involved in maintaining the tertiary structure of the GPCR for ligand binding. There is some evidence that for opioid receptors this di-sulphide bond is broken upon ligand binding (Brandt et al., 1999).

1.2.1.6 Intracellular loops and intracellular C-terminal region

The intracellular loops of GPCRs vary in length from receptor to receptor, the largest variation being demonstrated by the third intracellular loop. Residues of the second and third intracellular loops have been shown by several groups to be involved in G-protein coupling especially the end of the 3rd intracellular loop near TM 6 (Böhm et al., 1997; Georgoussi et al., 1997; Merkouris et al., 1996). Sequences in the C-terminus are also involved in G-protein signalling. Phosphorylation sequences for G-protein coupled receptor kinases (GRKs) and second messenger activated kinases exist in both the third intracellular loop and the C-terminus. Receptor phosphorylation of the receptor occurs following activation by agonist and can result in receptor desensitization and internalization. This will be further described in section 1.4.5.

Palmitoylation is the reversible thioesterification by a palmitate group of one or more cysteine residues in the C-terminus. This results in the formation of a fourth intracellular loop. This has been shown for many GPCRs e.g. the β_2AR receptor (Ng et al., 1994). Palmitoylation occurs post-translationally and can affect both the ligand binding and G-protein interaction of GPCRs.

Figure 1.1 **Structure of a typical class 1 G-protein coupled receptor**

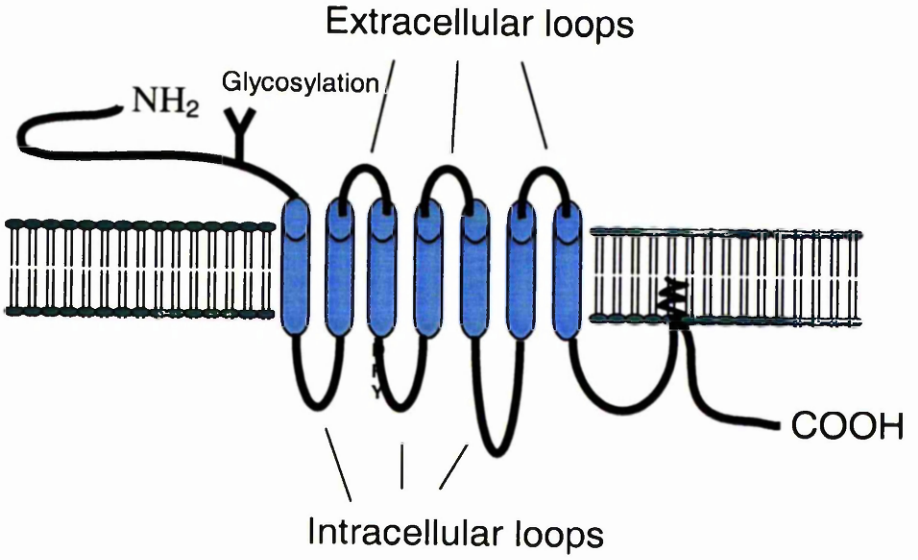

1.3 Opioid receptor signalling

The opioid receptors are all predominantly linked to pertussis sensitive Gαi/Gαo G-proteins and thus their activation results in the inhibition of adenylyl cyclase leading to a decrease in intracellular cAMP. Other effectors include Ca^{2+} and K^+ channels. The δOR has been shown to activate p42 and p44 mitogen-activated protein kinases on receptor activation (Burt et al., 1996). This activation has also been demonstrated for each of the opioid receptors (Fukuda et al., 1996). The structural features of the opioid receptors have been studied and shown to be consistent with GPCRs belonging to family 1. The ligand binding domains involve residues in the extracellular loops as well as the transmembrane domains. The three extracellular and intracellular loops vary in size between the μOR, κOR and δOR as does the intracellular C-terminus, which contains both palmitoylation and phosphorylation sites. (Guo et al., 2000; Wang et al., 1998; Kramer et al., 2000).

1.3.1 Opioid receptor sequence

The sequence of the human δOR is shown in figure 1.2.. 65-70% homology exists between the 3 opioid receptor types. The regions of highest similarity are those of the transmembrane regions and the intracellular loops and a small portion of the C-terminal tail near TM 7 domain. The regions with the most divergent residues are the second and third extracellular loops as well as the N- and C-terminal tails. Georgoussi et al. (1997) and Merkouris et al. (1996) identified at least two sites in the third intracellular loop and part of the carboxy terminal tail of the δOR as being important for G-protein coupling. δOR has been shown to activate different G-protein sub-sets in the presence of alkaloid compared to peptide opioid agonists (Allouche et al., 1999). This may be the result of different receptor conformations causing the activation of different sub-families of G-proteins.

Figure 1.2 figure of human δOR

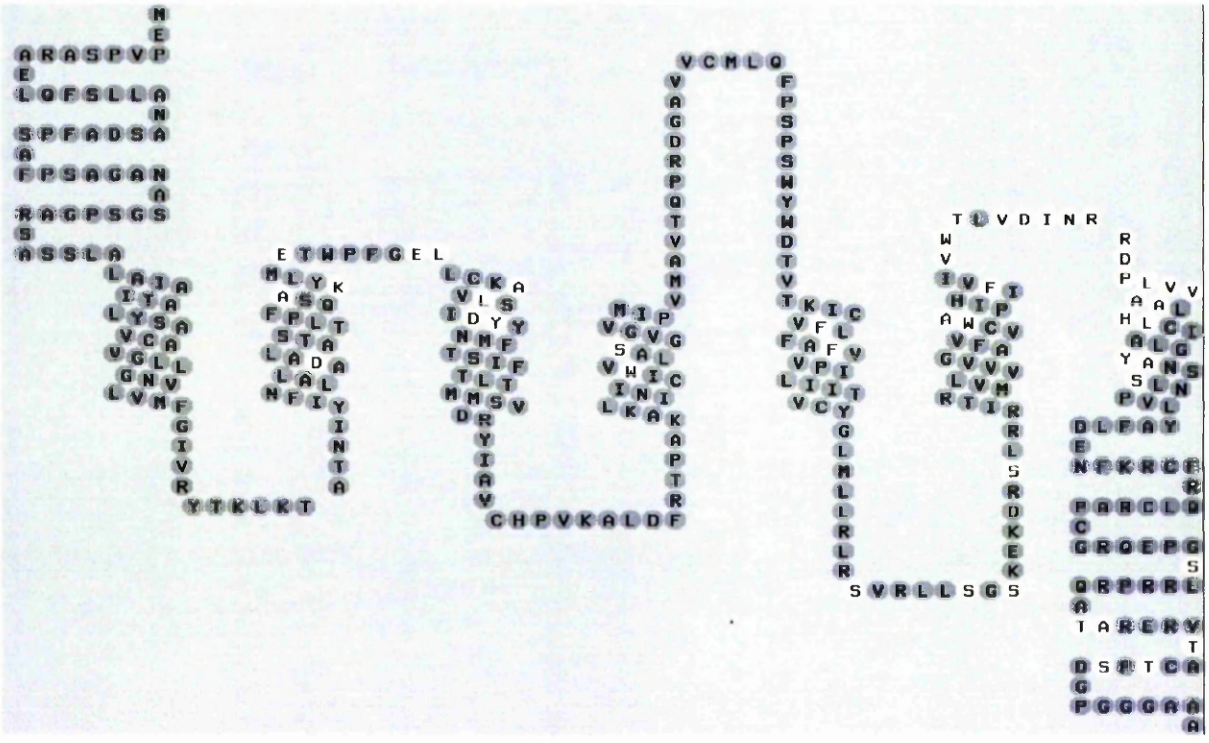

Figure was reproduced from the web site XXXX (www.gpcr.org/7tm/seq/), the white residues are those that are hyperlinked to a mutant database from that site.

(1) Laboratoire de Chimie Théorique de Nancy
U.A. CNRS 510
B.P. 239 - 54506 Vandoeuvre-les-Nancy CEDEX
France

(2) Sanofi Recherche
371, Rue du Pr. Blayac
34184 Montpellier CEDEX 4
France

1.3.2 Ligand binding of opioid receptors

The availability and use of many opioid ligands has led to proposals of several further receptor sub-types although no cDNAs encoding these extra sub-types have been identified. Several splice variants of μORs have been identified (Pan et al., 1999). A splice-variant of μOR, the MOR1b isoform has been identified. This differs by an 8 amino-acid deletion at the C-terminus, however, this does not alter the basic pharmacology of the receptor (Zimprich et al., 1995).

Investigations into ligand binding and the cloning of the opioid receptors has resulted in the isolation of several potent and selective opioid ligands which have been used to further study the pharmacology of these receptors. The use of chimeric receptors where regions of one receptor sub-type was replaced with that from another sub-type (Meng et al., 1995; Metzger and Ferguson 1995) and point mutations of the receptors has identified the ligand binding regions of the opioid receptors (Meng et al., 2000; Befort et al., 1996; Pepin et al., 1997). Ligand binding to each opioid receptor has also been performed by computer modelling (Pogozheva et al., 1998). The many studies on opioid receptor ligand binding and receptor activation have been reviewed (Law et al., 1999; Jordan et al., 2000). A summary of the findings are described here.

Investigations into the ligand binding domains of the opioid receptors led to the conclusion that opiate ligands are bivalent molecules where one part is responsible for signal transduction and the other responsible for selectivity of the ligand (Meng et al., 1995). The extracellular loops act to sterically inhibit binding of some drugs to confer selectivity (Metzger and Ferguson, 1995). Their work also showed that μOR selective ligands bound to a δOR where the sixth transmembrane domain and the third extracellular loop were replaced with that from the μOR. κOR and δOR chimeras demonstrated the importance of the TM domains 5-7 in δOR selectivity. Point mutations have been used to determine the critical residues for agonist and antagonist binding. Aromatic residues in the transmembrane domains at positions 129 and 308 (Befort et al., 1996), as well as residues at positions 284, 296, 297 (Valiquette et al., 1996) and 95 (Kong et

al., 1993) are necessary for binding of δOR selective ligands. To identify residues involved in receptor activation has been more difficult, however for high affinity binding the common feature is a protonated nitrogen. This suggests the ligand binding pocket of opioid receptors is similar to that of the biogenic amines described in section 1.2.1.3. where an aspartate or glutamate has to be present within the receptor as a counter-ion for the ligand. Claude et al. (1996) mutated a serine residue at position 177 and antagonist molecules now acted as full agonists. Befort et al. (1999) generated a constitutively active mutant of δOR via point mutations in transmembrane 3 and 7 demonstrating the importance of key residues in receptor activation. Meng et al. (2000) used point mutations of the δOR to identify residues in transmembrane domains that, when altered to the residues found in the ORL-1 receptor (Lys214 → Ala (TM5), Ile-277 → Val ; His278 →Gln ; Ile279 → Val (TM6), Ile304 → Thr (TM7)) demonstrated altered activation properties. These residues are thus involved in both ligand recognition and activation of the receptor.

Many GPCRs have been shown to have a di-sulphide bridge between cysteine residues in the 1st and 2nd extracellular loops, which is important in maintaining the correct receptor structure for ligand binding. This was also found to be true for opioid receptors as pre-treatment of membranes with the reducing agent dithiothreitol (DTT) prevented [^{3}H]diprenorphine binding leading to the conclusion that di-sulphide bonds are important for ligand binding to opioid receptors (Kamikubo, 1988). A study using point mutations of the 6 transmembrane cysteines of the δOR noted that these did not affect agonist or antagonist binding. However, mutagenesis of any of the two external cysteines abolished any agonist or antagonist binding (Ehrlich et al., 1998). DTT has been shown by Gioannini et al. (1989) to result in a decrease in receptor affinity for ligands without affecting receptor number.

1.4 GPCR signalling

Upon receptor activation by a corresponding ligand, a conformational change occurs within the receptor, facilitating its interaction with its G-protein. G-proteins are heterotrimeric proteins consisting of α, β and γ subunits. The β and γ sub

units are tightly associated and act as a dimer. In the absence of agonist, heterotrimeric G-proteins normally exist in an inactive, trimeric form consisting of the α, β and γ subunits. Receptor activation results in a decrease in the affinity of the Gα subunit for its bound GDP, which then dissociates and is replaced with GTP. Once GTP is bound, the α subunit assumes its activated conformation and dissociates from both the receptor and the βγ dimer. The βγ dimer promotes the association of the Gα subunit for its receptor possibly via isoprenylation of the Gγ subunit at its carboxy terminus, localising the Gβγ dimer to the plasma membrane (Higashijima et al., 1987). Both the Gα subunit and the βγ dimer have been shown to regulate the activity of effector molecules (Rosomer et al., 1996; Zhu et al., 1996). The fate of the α subunit of the heterotrimeric G-protein after activation is a matter of debate. One model shows that the α subunit can be de-palmitoylated upon activation and then released into the cytoplasm. Another possibility is that the α subunits cluster in sub-domains of the plasma membrane and are not released (Huang et al., 1999).

The Gα hydrolyses the GTP to GDP via its intrinsic GTPase activity and the αβγ trimer reforms. This GTPase activity is of great importance as it acts as a rate-limiting turn-off switch for signalling (Hamm, 1998). The GTPase activities of G proteins can vary enormously (Vaughan, 1998). The efficiency of the receptor G-protein interaction depends on the absolute number and density of each within the membrane. To overcome the problem of varying stoichiometry GPCR-Gα fusions have been produced to study receptor activation as demonstrated for the δOR by Moon et al. (2001). The use of GPCR-Gα fusion proteins has been reviewed by Seifert et al. (1999).

Molecular cloning has identified many types of each G-protein subunit. These include 20 Gα subunits, 6 Gβ subunits and 12 Gγ subunits (Hamm, 1998), which can then generate a large number of possible heterotrimer combinations, although there are preferred combinations of these subunits which generates a more limited number of physiologically relevant G-proteins (Hamm and Gilchrist, 1996).

1.4.1 G-protein sub-groups

The G-protein to which each receptor preferentially couples, confers the second messenger response which occurs upon agonist stimulation. G-proteins are named according to their α-subunits, which are divided into four sub families that regulate distinct effectors. Gαs activates adenylyl cyclase whereas Gαi inhibits adenylyl cyclase. Gαq activates phospholipase C-β and Gα12/Gα13 are involved in stimulation of Na^+/H^+ pumps, and have been shown to be involved in Rho mediated cytoskeletal effects (Offermanns et al., 1997). Each class of G-protein undergoes post-translational modifications e.g. myristoylation or palmitoylation. Palmitoylation is reversible, suggesting that the level of palmitoylation leads to variations in Gα membrane affinity and modulation of signalling. Palmitoylation, myristoylation and association with the βγ subunits all contribute to membrane attachment. Receptor cross talk can be shown to be linked to Gβγ exchange (Quitterer and Lohse, 1999) in some cases as activation of Gαi-coupled receptors often leads to enhancement of inositol phosphate signalling triggered by Gαq receptors.

Two bacterial toxins, namely cholera and pertussis toxins, activate and inactivate certain G-proteins respectively by catalysing ADP-ribosylation of key amino acids. Cholera toxin catalyses the ADP-ribosylation of an arginine residue that is a key contributor to the GTPase activity of the Gαs subunit of the G-protein. ADP-ribosylation by cholera toxin results in a continually active G-protein as the bound GTP is unable to be hydrolysed. Pertussis toxin ADP-ribosylates a cysteine residue which is four residues from the C-terminus of the Gαi- sub-family of G-proteins disrupting receptor-G-protein interaction. The effect of these toxins has been used to delineate the inhibition of adenylyl cyclase via Gαi from its stimulation via Gαs for the α2A adrenergic receptor (Milligan et al., 1991). These and other methods e.g. co-immunoprecipitation, have been developed to identify the G-protein involved in each receptor interaction.

1.4.2 Desensitization, down-regulation and sequestration

Desensitization is the loss of responsiveness of GPCRs to an external stimulus after repeated or continuous stimulation. This involves many cellular proteins and the processes involved have been elucidated for several GPCRs e.g. β_2AR (Zhang et al., 1996), vasopressin V2 receptor (Oakley et al., 1999) and the dopamine D2 receptor (Vickery and Von Zastrow, 1999). Desensitization is a multi-step process, first involving uncoupling of the receptor from the G-protein, causing the receptor function to be inhibited. Sequestration of the receptor into an intracellular compartment then occurs followed by possible down-regulation, if the stimulation is chronically present. Down-regulation involves a loss in receptor number due to degradation of the receptor protein and reduction of steady-state mRNA. Desensitization has been categorized as homologous (agonist-specific) or heterologous (agonist non-specific).

Homologous desensitization results from agonist activation of a specific receptor by G-protein receptor kinases (GRKs). Heterologous desensitization results from phosphorylation of receptors within a cell irrespective of the receptor being stimulated. In this case, receptor phosphorylation results from interaction with second messenger kinases e.g. protein kinase A and protein kinase C (Mullaney et al., 1995). Phosphorylation occurs on serine and threonine residues of the third intracellular loop and the C-terminal tail of GPCRs. The mammalian gonadotrophin-releasing hormone receptor lacks a C-terminal tail and is resistant to agonist-dependent phosphorylation and consequent desensitization (Willars et al., 1999).

1.4.3 Internalization

Soluble proteins called arrestins interact with receptors immediately after phosphorylation by GRKs, as phosphorylation increases the affinity of the receptor for the arrestin molecule. This interaction has been shown for several different receptor types with a wide diversity of agonists and classes of G-proteins. It is apparent that arrestin binding terminates signalling by halting receptor interaction with G-proteins (Barak et al., 1997; Law et al., 2000). β-

arrestin has been shown to function as an adapter protein that specifically targets GPCRs for dynamin-dependent endocytosis via clathrin-coated vesicles. (Zhang et al., 1996; Barak et al., 1997). The internalization process involves clathrin coated pits (Michaely et al., 1999) and the soluble protein dynamin which has GTPase activity and co-localises with clathrin. Dynamin contributes to the early stages of endocytosis by catalysing a GTP-dependent pinching off of endocytic vesicles from the plasma membrane. Other internalization mechanisms have been suggested e.g. the caveolae-mediated pathway or a novel non-clathrin-coated vesicle pathway as the clathrin coated pit mechanism is not the mechanism used by all receptors (Zhang et al., 1996). The D1 (postsynaptic) and D2 (presynaptic) dopamine GPCRs have been shown to internalize via distinct mechanisms which are dynamin dependent and independent and result in the receptors being delivered to different endocytotic vesicles (Vickery and von Zastrow, 1999).

1.4.4 Down-regulation

Down-regulation usually occurs after long term agonist exposure (Barritt and Gregory, 1997) where internalized receptors can be de-phosphorylated and re-cycle back to the membrane or transported to lysosomes and degraded leading to a loss in receptor number. Signal attenuation mechanisms also include removal of the agonist from the extracellular fluid via dilution, uptake by transporters or enzymatic degradation (Böhm et al., 1997). Downregulation may also result from reduced gene transcription and reduced *de novo* receptor synthesis (Li et al., 2000). For the β_2AR it has been shown that internalization is not essential for down-regulation to occur (Jockers et al., 1999).

1.4.5 Desensitization, internalization and phosphorylation of opioid receptors

The mechanisms of desensitization, internalization via clathrin-coated pits and down-regulation have all been described for opioid receptors as a result of several studies aimed at understanding tolerance and dependency of opiates. Key findings are discussed by Jordan et al. (2000) and Whistler et al. (1999). A

summary of the main features involved for δOR desensitization, sequestration and down-regulation will be described here.

Agonist induced phosphorylation of serine and threonine residues of the C-terminal tail and in the third intracellular loop is produced by GRKs but not protein kinase C (Pei et al., 1995). Kramer et al. (2000) have also demonstrated tyrosine phosphorylation on activation of δOR and the involvement of both β-ARK and β-arrestin in homologous desensitization of the δOR was demonstrated by Kovoor et al. (1997).

Phosphorylation is not the only process involved in desensitization as a mutant receptor, where serine 363 in the third intracellular loop was changed to alanine and therefore not phosphorylated, demonstrated unaltered desensitization compared to the wild type receptor (Kovoor et al., 1997). Only when clathrin-coated pit internalization was inhibited with 0.4M sucrose was the desensitization prevented.

Internalization has also been linked to the C-terminal tail as C-terminal deletions have resulted in impaired internalization. A δOR with a C-terminal deletion of 37 amino acids did not internalize on agonist activation whereas a 15 amino-acid C-terminal truncated receptor did. A C-terminally truncated mutant of δOR, in which the last 15 residues had been removed and with point mutations at the putative phosphorylation sites T358A, and S363G was used to show the importance of these residues in receptor phosphorylation upon agonist stimulation. GRKs were shown to be the prominent kinases responsible for this phosphorylation (Kieffer et al., 1999; Guo et al., 2000).

The processes of agonist-dependent activation and desensitization still occurred in a δOR with a 31 amino acid C-terminal deletion although this was sensitive to a protein kinase inhibitor indicating the involvement of phosphorylation at other positions other than the C-terminal tail in δOR desensitization (Wang et al., 1998). A functional δOR C-terminal truncation mutant (D344T) was not phosphorylated, and when expressed in CHO cells did not internalize, although

this mutant did internalize in HEK293 cells. This is the first example of a GPCR that doesn't require to be phosphorylated before it gets internalized (Murray et al., 1998).

The involvement of β-arrestin in the desensitization of δOR has been demonstrated by Cheng et al. (1998) and Kovoor et al. (1999) who showed the C-terminus to be important for a successful interaction with both the κOR and the δOR. Expression of constitutively active β-arrestin with a C-terminally truncated δOR restored the agonist-induced desensitization of that receptor (Kovoor et al., 1999). Point mutations between these two regions identified threonine 353 to be essential for down-regulation.

μOR receptor internalization has been demonstrated for most agonists e.g. Tyr-D-Ala-Gly-NMe-Phe-Gly-ol (DAMGO) or etorphine, however, the agonist morphine does not produce effective receptor internalization (Keith et al., 1996). For the δOR, full agonists induced receptor down-regulation, whereas partial agonists did not (Remmers et al., 1998).

The process of down-regulation may involve other components as indicated by Li et al. (2000) who showed the down-regulation of human κORs to involve rab5 and rab7 (involved in vesicle transport between intracellular compartments) as well as GRKs, arrestin and dynamin.

1.4.6 Pharmacology of δOR and μORs

It is possible that δOR may be a better clinical target than the μOR as its ligands provide greater relief from neuropathic pain, reduced respiratory depression, reduced constipation and a lower potential for developing dependency. Morphine has high affinity for both the μOR and the δOR although in μOR knock-out mice no morphine-induced analgesia was found (Matthes et al., 1996). δOR-selective agonists did not require functional μOR to mediate antinociception (Matthes et al., 1998). A transgenic μOR knock-out mouse has been used by Sora et al. (1997) to study μOR and δOR interactions. The results of various opioid knock-

out mice have been discussed by Kieffer (1999). Ligand dependent results were demonstrated where the δOR-selective agonist Tyr-DPen-Gly-Phe-DPen (DPDPE) gave a lower than expected antinociceptive effect in knock-out compared to control animals indicating that the presence of μOR may be necessary for the full effect of δOR ligands. This was not the case though for Deltorphin II and (+)-4-[(αR)-α-((2S,5R)-4-Allyl-2,5-dimethyl-1-piperazinyl)-3-methoxybenzyl]-N,N-diethylbenzamide (SNC80), which gave normal GPCR activation, indicating that the δOR was fully functional independently of the presence of the μOR. Sub-analgesic levels of δOR ligands have been shown to decrease the amount of morphine required for analgesia, which is an important finding in respect to dependency. It has also been demonstrated that the δOR does not have to be activated to potentiate μOR mediated analgesia. Evidence that activation of the δOR could potentiate the agonist response of the μOR was demonstrated by Vaught and Takemori (1979) where administration of leucine-enkephalin (moderately δOR selective) at a concentration unable to induce analgesia, was able to produce a rightward shift in the ED_{50} dose-response curve to morphine. More selective δOR ligands were also shown to have the same effect (Barrett and Vaught, 1982; Lee et al., 1980).

No synergy was detected between the δOR inverse agonist N,N-diallyl-Tyr-Aib-Aib-Phe-Leu (ICI 174,864) and morphine, suggesting that the δOR had to be activated for opioid receptor synergy to be observed (Heyman et al., 1989). The irreversible δOR antagonist [D-Ala2, Leu5, Cys6]enkephalin (DALCE) was observed to block δOR mediated antinociception but could not block the potentiation of the morphine effect on μOR (Jiang et al., 1990; Porreca et al., 1992). This led to the proposal that not all δOR were involved in morphine analgesia.

Pharmacological evidence of opioid receptor synergy has made opioid receptors an interesting target for GPCR dimerization studies as non sub-type selective ligands could also result in the pharmacologies observed. The discovery of sub-type selective ligands and the existence of opioid receptor dimers have been

utilized to elucidate the cause of the observed synergy. A mixed δOR antagonist/μOR agonist DIPP-NH2ψ was able to potentiate morphine-induced analgesia indicating that the δOR does not have to be activated to demonstrate this effect Schiller et al. (1999). Further evidence for μOR and δOR complexes was derived from evidence that DADLE bound with high and low affinity to δOR receptors non-complexed and complexed with μOR respectively. *In vivo* studies using compounds that are μOR antagonists / δOR agonists show a better therapeutic profile than the μOR only agonists (Wells et al., 2001; Jordan et al., 2000).

This pharmacology is consistent with potential receptor interactions which will be discussed in section 1.6.2. However, the pharmacological synergy, which has been described by Law and Loh (1999), may be the result of the effector pathways interacting synergistically and not the receptors themselves.

1.5 GPCR signalling diversity

GPCR signalling mechanisms are complex with many levels of control. Many signalling components and their substrates are anchored in the plasma membrane, which provides a unique mixture of proteins that can interact with each other. GPCRs interact with their extracellular ligands as well as intracellular effector molecules e.g. kinases and phosphatases, each of which have different sub-types, adding to the signalling complexity. The cytoskeleton provides compartmentalization and regional organization within cells and is involved in receptor movement from one compartment to another. Some neurotransmitter receptors have been shown to be targeted to specific membranes and anchored there by specific anchoring proteins e.g. in pre or postsynaptic membranes (Vickery and von Zastrow, 1999).

The stoichiometry of the individual signalling components within a cell can greatly affect signal generation resulting from GPCR activation within that cell. An agonist at a particular GPCR may have a different efficacy, depending on the level of G-proteins present within a cell as was demonstrated for the α_2-adrenergic receptor by Yang and Lanier (1999).

GPCR diversity also results, partly, via sub-types being encoded by differential gene splicing, resulting in different receptor mRNAs encoding for different receptor isoforms (Kilpatrick et al., 1999).

1.6 Dimerization of GPCRs - introduction

One mechanism by which receptor signalling can diversify is if the receptors physically interact with each other to alter their ligand binding or signalling properties. There is evidence for GPCR homo- and heterodimerization and the varying effects this may have on ligand binding, cell signalling and cellular trafficking (Bouvier, 2001; Salahpour et al., 2000; Milligan and Rees, 2000; Milligan, 2001; Marshall, 2001).

1.6.1 Growth factor dimerization

It is not so suprising that protein-protein interactions between GPCRs may result in another mechanism of cell-signalling control as dimerization has been widely accepted as a control mechanism for single transmembrane helix growth factor receptors.

Growth factor receptors are members of a large family of single transmembrane species involved in apoptosis and differentiation as well as cell-growth. These receptors are structurally similar in having an extracellular N-terminus, a single transmembrane domain and an intracellular C-terminus. Dimerization has been shown to be the process by which these receptors are switched on. Removal of the C-terminus of the epidermal growth factor (EGF) receptor results in a higher rate of dimerization on ligand activation indicating that the C-terminus hinders receptor dimerization (Tanner and Kyte, 1999). In the case of tumour necrosis factor (TNF) receptors ligand activation results in trimerization of the receptor (Heldin, 1995 and references therein).

1.6.2 GPCR homo and hetero-oligomerization

There is increasing evidence for the existence of receptor oligomers from experiments performed *in vitro*. Constitutive homodimerization of the thyrotrophin releasing hormone receptor has been described by Kroeger et al. (2001). Dimerization of the histamine H2 receptor has been demonstrated via immunoprecipitation and immunoblotting (Fukushima et al., 1997). Moreover, receptor homodimers have also been identified *in vivo* as in the case of the D3 dopamine receptor (Nimchinsky et al., 1997). Homodimers of muscarinic m3 receptors have also been shown in brain and heart tissue (Avissar et al., 1983). Photoaffinity labelling revealed dimers, which were shown to correspond to the low affinity state of the receptor, and tetramers corresponding to the high affinity state of the receptor.

Interaction between different signalling systems, which may be a result of the GPCRs physically interacting with each other has also been indicated by alterations in receptor pharmacology. Adenosine A1 receptors have been shown to heterodimerize with dopamine D1 receptors (Gines et al., 2000). The vasopressor angiotensin II receptor heterodimerizes with the vasodepressor bradykinin B2 receptor although these two hormone systems have also been shown to be inter connected by angiotensin-converting enzyme (Abdalla et al., 2000). The β_2AR has been shown to dimerize with δOR and κORs (Jordan et al., 2001). Somatostatin receptors (SSTR) have been shown to form ligand-induced homo and heterodimers with other members of the SSTR family (Rocheville et al., 2000a; Pfeiffer et al., 2001). The somatostatin receptor SSTR5 and the dopamine D2 receptor have been shown to form heterodimers. Somatostatin is involved in modulating dopamine-mediated control of motor activity and dopamine has been shown to activate SSTRs. These two receptors are co-localized in neuronal sub-groups. Interaction between the two receptors has been demonstrated via co-immunoprecipitation experiments and confirmed in live cells by photobleaching-fluorescence resonance energy transfer (pb-FRET) experiments (Rocheville et al., 2000b). The heterodimer showed a distinct pharmacology with higher ligand affinity for both dopamine and somatostatin

agonists. Synergy of agonist binding was demonstrated where the binding affinity of the second agonist was increased by the presence of the first agonist.

Franco et al. (2000) have reported evidence of heterodimerization between adenosine A_1 and dopamine D_1 receptors, where heterodimers between these receptors were found both *in vivo and in vitro*. μOR and δOR receptors have also been shown to form heterodimers resulting in a distinct pharmacology. The potency of highly selective agonists for the individual receptors was reduced whereas binding of partial agonists increased, suggesting the heterodimers have a novel binding pocket. Co-immunoprecipitation also indicated the presence of the heterodimers in cells (George et al., 2000; Gomes et al., 2000).

1.6.3 Domain swapping theory

Evidence that GPCRs can physically interact was demonstrated by expressing chimeric receptors that were split in the third intracellular loop. Muscarinic m2 and m3 receptor N-terminal and C-terminal fragments divided at the third intracellular loop could be expressed individually resulting in no ligand binding or signalling. Co-expression of the m3 N-terminal fragment and m3 C-terminal fragment resulted in ligand binding and activation of second messenger systems as did the co-expression of the m2 N-terminal fragment with the m2 C-terminal fragments (Maggio et al., 1993a). This led to the theory that GPCRs function as proteins with two interacting subunits consisting of TM 1-5 and TM 6-7.

Further investigations into GPCRs interaction within the membrane were performed with chimeric GPCRs with the N-terminal fragment of the α_{2c}-adrenergic receptor fused to C-terminal fragment of the muscarinic m3 receptor and vice versa. Individual expression of the chimeras resulted in no ligand binding or signal transduction from either receptor whereas co-expression of the chimeras resulted in binding of adrenergic and muscarinic ligands and signalling via activation of each receptor (Maggio et al., 1993b). For the adrenergic and muscarinic receptors to interact to form a functional receptor the chimeric proteins must have interacted in such a way to allow the formation of native adrenergic and muscarinic receptors.

Muscarinic m3 receptors have a large third intracellular loop in comparison with other GPCRs. Chimeric receptors between the α_{2c}-adrenergic and muscarinic m3 receptors identical to those described above but with a 196 amino-acid deletion in the third intracellular loop, no longer formed functional receptors when co-expressed (Maggio et al.,1996). This indicated that the length and flexibility of the third intracellular loop is required for correct receptor-receptor interactions to occur. Jakubik and Wess (1999) developed an ELISA assay to examine interactions between m3 truncations and m3 C-terminal fragments and demonstrated that there are 3 proline residues in transmembrane regions 5, 6 and 7 which are especially important for receptor assembly. Agonists and antagonists improved receptor assembly indicating that ligands anchor the two fragments together. Scarseli et al. (2000) reconstituted dopamine D2 receptors by co-expressing the N-terminal and C-terminal receptor fragments in the same cell. Further evidence of domain swapping was provided by Monnot et al. (1996) where reconstitution of the angiotensin II binding site occurred on co-expression of two deficient mutants. Computational studies have confirmed this domain swapping as a possible method for GPCR dimerization (Gouldson et al., 2000).

1.6.4 Lateral interaction and coiled-coil interactions

Domain swapping is not the only mechanism proposed for receptor-receptor interaction. Another mechanism is lateral interaction within the membrane which is the mechanism proposed for the V2 vasopressin receptor (Schulz et al., 2000). Co-expression of mutant receptors did not demonstrate functional recovery which would have been expected if domain swapping occurred. Disruption of cysteine residues on the 1st and 2nd extracellular loops by mutating the cysteine residues to alanine resulted in functional rescue of the receptor. Dopamine D2 receptors also appear to interact via lateral interaction as shown by co-expression of receptor point mutants (Lee et al., 2000a).

Coiled-coil conformation interaction is the mechanism by which the $GABA_B$ receptor isoforms have been proposed to interact, (Marshall et al., 1999; Margeta-Mitrovic et al., 2000) via the large C terminus of each receptor. Coiled-

coil interactions have been shown previously to be involved in a range of protein-protein interactions (Lupas, 1996).

1.6.5 Family 3 GPCR dimerization

Family 3 GPCRs are unique in structure as they have a large N-terminal extension that can be up to half the total size of the protein. These receptors have been shown to dimerize via di-sulphide bridges which occur in this N-terminal region. Mutants of the conserved cysteine residues of the calcium-sensing receptor (Fan et al., 1998) demonstrated effects on receptor expression at the cell surface, signal transduction, and dimerization. It was found that the majority of the mutant proteins were produced in an immature high mannose-linked glycosylated form and that only a few were fully mature with complex carbohydrates which allowed correct insertion in the membrane.

Another group of this family of GPCRs are the metabotropic glutamate receptors (mGluRs). The mGluR-5 dimerizes via the large N-terminal extension (Romano et al., 1996); again the dimerization was shown to be due to di-sulphide bonds. Crystal structures of the N-terminal extension of the mGluR-1 receptor have been produced in the presence and absence of glutamate. In each case the receptor exists in a di-sulphide (at cysteine 140) linked dimeric form (Kunishima et al., 2000). The importance of this cysteine in mGluR-1 dimerization was also shown by Ray and Hauschild (2000).

A lot of work has been performed recently on the $GABA_B$ receptor which also belongs to this family. Activation of this receptor results in inhibition of neuronal responses in the mammalian central nervous system. The $GABA_B$ receptor has a large N-terminal extension responsible for ligand binding but as there are no cysteine residues within it a di-sulphide linked homodimer would not be possible. Using a yeast-two hybrid screen with the C-terminal domain of $GABA_BR1$, the $GABA_BR2$ was identified (Kaupmann et al., 1998; White et al., 1998). The individual receptors identified did not have the ligand binding capabilities or signal transduction properties anticipated for the wild type $GABA_B$ receptor. Heterodimerization of these receptors has been shown to result in cell-surface

expression of the $GABA_BR1$, ligand binding properties of the wild type receptor and signalling events consistent with the wild-type receptor. This was the first time that heterodimerization of a GPCR has been shown to be essential for correct receptor trafficking and signalling. The consequences of these findings for how we think of GPCR signalling have been reviewed (Möhler and Fritschy, 1999; Marshall, 2001; Bouvier, 2001). A C-terminal motif arg-X-arg-(arg) which is responsible for the retention of the $GABA_BR1$ at the endoplasmic reticulum is thought to be masked by the $GABA_BR2$ receptor as the receptors interact via the C-terminal coil-coil sequences (Margeta-Mitrovic et al., 2000).

1.6.6 Domains involved in GPCR dimerization

Considerable effort has been made to elucidate the structural determinants of the dimer interface and as is often found in signal transduction systems there appear to be several different possibilities. C terminal truncation mutants of the δOR were found to be dimerization deficient (Cvejic and Devi, 1997), indicating the C-terminus as being important for the dimer interface. As discussed above, the large N-terminal extension of the family 3 GPCRs has been shown to be important for dimerization of these receptors. Wild-type histamine H2 receptors were shown to dimerize with a truncated receptor form lacking the C-terminus demonstrating that for this receptor the C-terminus is not important for dimerization (Fukushima et al., 1997). For β_2-AR the sixth transmembrane domain has been shown to be important. Hebert et al. (1996) showed that although peptides corresponding to the sixth transmembrane domain did not affect ligand binding they inhibited adenylyl cyclase activity upon agonist activation and dimerization of the receptors. Similarly, peptides corresponding to the 6^{th} and 7^{th} transmembrane domain of the D2 dopamine receptors (Ng et al., 1996) were shown to be inhibitors of dimerization. In contrast to this the dopamine D1 receptor has been shown to dimerize and peptides corresponding to the 6^{th} transmembrane domain inhibit dopamine binding and adenylyl cylase activity but there was no effect on dimerization (George et al., 1998). Vasopressin V2 receptors have been shown to interact within the TM domains. The first three transmembrane domains are required to allow interaction with the full length receptor (Schulz et al., 2000).

B2 bradykinin receptors showed no dependence on the sixth transmembrane domain for receptor dimerization but peptides corresponding to the N-terminus of the receptor inhibited dimerization (Abdalla et al., 1999). The different regions of GPCRs identified may not be the only regions that are necessary for receptor dimerization. The differences may be explained in part because the dopamine D_2 and β_2-ARs belong to family 1 subtype a whereas B2 bradykinin receptors, whilst belonging to family 1, are in sub-type b. For the B2 bradykinin receptor agonists have been shown to induce dimerization whereas antagonists do not. A peptide corresponding to the N-terminus of this receptor has been shown to reduce dimerization but peptides corresponding to the other extracellular loops had no effect on dimerization (Abdalla et al., 1999).

It is clear that GPCR dimerization is not a simple process involving the same region for each GPCR. Clearly further work will have to be performed in this area to elucidate what is involved in receptor dimerization. Peptide inhibitors of dimerization could be used as novel inhibitors of GPCR signalling.

The evidence presented thus far shows the presence of GPCR dimers but does not present any evidence as to why receptor dimerization is necessary. The presence of some mutant receptors has shed some light on how receptor – receptor interaction can affect cell signalling.

1.6.7 Dominant negative effects of dimerization

Co-expression of wild-type receptors with mutant or truncated receptors can result in dominant negative effects of the defective receptors on the ligand binding or signalling of the co-expressed wild-type receptors. The level of cell-surface expression of the wild-type receptor has also been shown to decrease upon co-expression with mutant receptors where signalling from the wild-type receptor is also reduced as it is retained in an intracellular position.

D3 dopamine receptors have been shown to be present in dimeric and tetrameric forms in brain. A C-terminally truncated mutant of the D3 receptor,

D3nf, is found to form heterodimers with the wild-type receptor and these receptor forms are found to be co-localised in cortical neurones. D3nf mutant receptors inhibit the cell-surface expression of the wild-type receptor as well as affecting ligand affinity (Nimchinsky et al., 1997). The presence of D3nf mutant receptors could be important biologically as there is increased expression of this form of the receptor in the brain tissue of patients suffering from schizophrenia (Karpa et al., 2000 and references therein) which may also result in decreased cell-surface expression of the wild-type receptor. Mutant dopamine D2 receptors have also been shown to reduce cell-surface expression of wild-type receptors when expressed in the same cells (Lee et al., 2000a).

Vasopressin V2 receptor truncation mutants have also been shown to be negative regulators of V2 activity by reducing cell-surface expression of the wild type receptor (Zhu and Wess, 1998) as well as reducing adenylyl cyclase activity and ligand binding. Dominant negative effects of mutant receptors may be useful as inhibitors of constitutively active receptors which can result in disease states. For example, missense mutations in the vasopressin V2 receptor have been linked to nephrogenic diabetes insipidus (Schulz et al., 2000) and the dopamine truncated receptor D3nf may be involved in schizophrenia (Karpa et al., 2000).

1.6.8 Dominant positive effect of dimerization

The converse of what is described above has also been shown where the wild-type receptor has a dominant positive effect on mutant receptors expressed. Hebert et al. (1998) showed that a palmitoylation deficient mutant β_2AR, when expressed with wild-type β_2AR resulted in cell surface expression of the mutant receptor and full adenylyl cyclase activity resulted. Expression of the mutant alone gave poor ligand binding and low functional activity. As this mutant is palmitoylation deficient the dimerization of these receptors is shown not to involve the palmitoylation state of the receptors. By using a phosphorylation deficient mutant phosphorylation was also shown not to be involved in dimerization.

1.6.9 Effect of ligands on GPCR dimerization

Several studies have been performed to try to elucidate the effect of ligands on GPCR dimerization and again the answer is not a simple one. The effect of agonist activation on receptor dimerization has varied from no effect, as shown for the muscarinic m3 receptor (Zheng and Wess, 1999) the Ca^{2+} sensing receptor (Bai et al., 1998), the V2 vasopressin receptor (Schultz et al., 2000), the δOR (McVey et al., 2001) and the κOR (Jordan and Devi, 1999), to promotion of receptor dimerization as demonstrated for the β_2AR (Hebert et al., 1996, Angers et al., 2000) and the B2 bradykinin receptor (Abdalla et al., 1999). A reduction in receptor dimerization on agonist activation has been reported for the δOR (Cvejic and Devi, 1997) where agonists, with the exception of morphine, resulted in monomerization of the receptor before its internalization. Specific receptor antagonists did not effect the ratio of monomer to dimer.

For the chemokine receptors the stimulatory effect of agonist on dimerization appears universal. The chemokine receptor CCR2 dimerizes leading to its activation. Dimerization is produced by its ligand, monocyte chemoattractant protein-1 or by a receptor specific antibody. Monomeric antibody Fab fragments do not lead to dimerization of the receptor (Rodriguez-Frade et al., 1999). Activation of the CXCR4 chemokine receptor requires agonist-induced receptor dimerization (Vila-Coro et al., 1999). Certain chemokine receptors are co-receptors for HIV, and receptor dimerization stimulated via an antibody raised to the extracellular domain of the CCR5 receptor impedes viral entry by inducing receptor dimerization. This occurs in the absence of chemokine, leading to activation and internalization of the receptor. There is a well studied chemokine CCR5 receptor polymorphism that renders homozygous individuals highly resistant to viral infection as the resultant mutant CCR5 receptor is not expressed on the cell surface thus impeding viral entry (Vila-Coro et al., 2000).

Further investigations will have to be performed to ascertain whether the differences in the effect of ligands on GPCR oligomerization for different receptors are real or are a function of how assays are performed.

1.6.10 Kinetics of ligand interaction with dimers

The presence of GPCR dimers and ligand binding to them may alter the expected kinetics of the ligand binding and receptor activation profile. Indeed the presence of D2 oligomers was indicated before any dimeric receptor species were identified. In various tissues there appeared to be co-operativity of ligand binding, where the binding at one site leads to an increased binding at the other site in the dimer. Further investigations led to the conclusion that oligomers were present, The potential effects of GPCR dimerization on ligand efficacy and affinity are discussed by Onaran and Gürdal (1999).

1.6.11 Function of GPCR dimerization

GPCR dimerization leading to activation has been described above for many receptors. The study by Mijares et al. (2000) who showed that dimeric anti-β_2AR antibodies acted as agonists whereas monomeric Fab fragments were antagonists provides more evidence for the dimer of the β_2AR being the active form.

Correct trafficking of the $GABA_B$ receptor to the cellular membrane has been demonstrated only when both the $GABA_BR2$ and the $GABA_BR1$ are co-expressed (Margeta-Mitrovic et al., 2000). Hetero-dimer formation between the β_2AR with opioid receptors has been shown to effect trafficking. β_2AR-κOR dimerization leads to inhibition of receptor internalization on agonist activation, whereas β_2AR –δOR dimerization does not inhibit agonist-induced internalization of either receptor (Jordan et al., 2001). Trafficking of mutant GPCRs to the cell-surface as a result of the addition of cell-permeable non-peptide antagonists has been demonstrated for eight out of fifteen mutant forms of the vasopressin V2 receptor. This was a result of the promotion of correct receptor folding which resulted in trafficking of the GPCR to the cell-surface (Morello et al., 2000). Schöneberg et al. (1996) demonstrated functional rescue of vasopressin V2 mutant receptors by co-expressing V2 receptor peptides which spanned the region of receptor that contained the mutation. Expression of several mutant forms of the vasopressin V2 receptor have been shown to cause nephrogenic

diabetes insipidus. Co-expression of these receptor peptides could lead to a possible treatment of this disease. Other mutant receptors which are poorly trafficked to the cell surface include mutant dopamine D2 receptors (Lee et al., 2000a) and the mutant D3nf receptors (Karpa et al., 2000). Intracellular retention has been shown in several cases to be the result of receptor dimerization within the endoplasmic reticulum (ER). Correct receptor folding and export from the ER were shown to be the key events for cell-surface expression of the δOR (Petäjä-Repo et al., 2000). The $GABA_BR1$ was retained intracellularly in the absence of $GABA_BR2$ via its c-terminal ER retention motif RXR(R) (Margeta-Mitrovic et al., 2000). CCR5 and the mutant CCR5Δ32 receptor dimerize in the ER (Benkirane et al., 1997) as do dimers of the vasopressin V2 receptors (Morello et al., 2000).

The consequence of dimerization of the protease activated receptor is unusual in that the protease activated receptor (PAR)3 acts as a co-factor for protease activated receptor 4 by presenting its agonist to the receptor. PAR4 resulted in thrombin activation when expressed alone but the EC_{50} for this was substantially decreased when the PAR3 receptor was co-expressed (Nakanishi-Matsui et al., 2000). Thrombin interacts with PAR3, which then gets cleaved, leaving thrombin in close proximity of the co-expressed PAR4 leading to its cleavage. PAR3 is therefore functioning only to allow PAR4 activation.

1.7 GPCR interaction with other proteins

There are many proteins that have now been identified which interact with GPCRs both intracellularly and extracellularly. These have been demonstrated to affect the signalling as well as trafficking of GPCRs within the cell. Milligan and White (2001) have reviewed these other interactions and described their effect on GPCR signalling. Although many such interactions are known their pharmacological significance has not yet been fully elucidated.

1.8 Dimerization - conclusions

There is a lot of evidence for GPCR dimerization although much of the evidence derived from studies performed *in vitro*. Although GPCR dimerization is an attractive concept to explain cross-talk between different signalling systems

more evidence will have to be provided for its functional significance *in vivo*. Functional rescue of mutant receptors is one area for which information on GPCR dimerization may be useful in developing new drugs. New technologies being developed which should allow receptor dimerization to be assessed in single cells should greatly improve our understanding of GPCR dimerization.

1.9 Properties of fluorescence

Fluorescent molecules are now widely used in biological assays and as I have used fluorescent molecules within this study a summary of fluorescent properties are described below. The phenomenon of fluorescence is depicted in figure 1.3 where a molecule is excited by light of a particular wavelength resulting in the energy of that molecule increasing. As the energy returns to the resting level there is an emission of light at a longer wavelength and therefore lower energy, which is termed fluorescence. Fluorescent molecules lose some energy as internal vibrational energy which results in the emitted light being of lower energy and hence at a longer wavelength. Each fluorescent molecule has its own particular absorption or excitation (absorption and excitation describe the same thing) and emission wavelengths i.e. the wavelength of light necessary to excite the fluorescent molecule is its excitation wavelength and the light emitted from this molecule will be at its emission wavelength. Fluorescent light is emitted in all directions though detectors are usually set at 90^{o} to the direction of the incident light. Non-fluorescent molecules lose energy as heat.

Figure 1.3 Energy changes on excitation of a fluorescent molecule

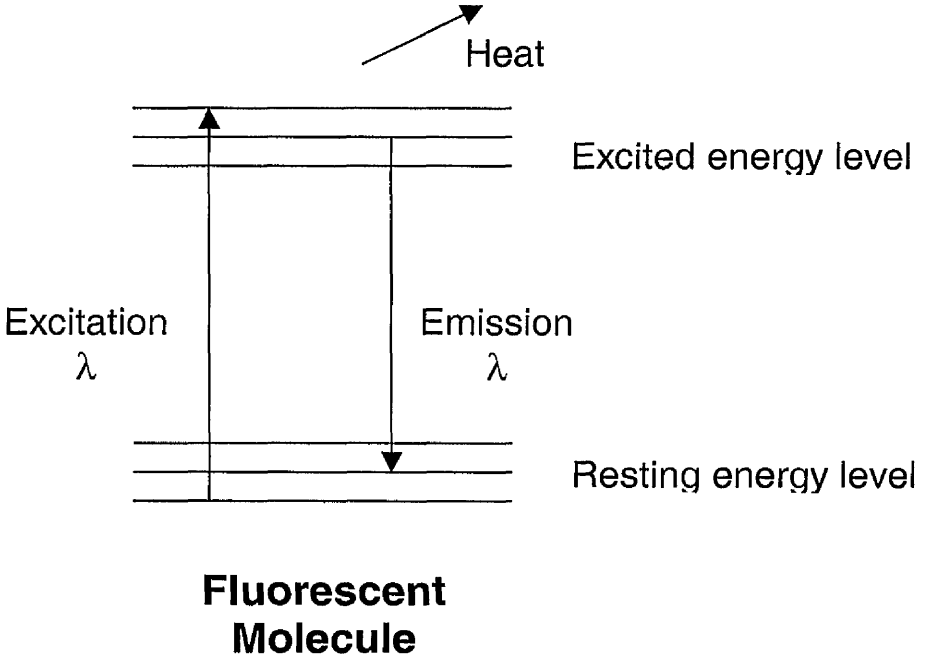

Fluorescent molecules are now being used in a variety of techniques to investigate molecular interactions and there are many properties that have to be considered when choosing a particular fluorophore for use in a specific assay format. These include:

Stokes shift, which is the wavelength distance between the absorption maxima and emission maxima. It is preferable for these to be far apart to ensure there is no direct interference of the excitation wavelength at the emission wavelength.

Quantum yield, which is a property of fluorescent molecules that refers to the amount of energy that is emitted, compared to that used to excite the fluorescent molecule. The maximal quantum yield is 1. (Fluorescein has a quantum yield of 0.6).

Extinction co-efficient is a calculated value from the absorbance; it is the amount of light at a given wavelength that is absorbed by the fluorochrome. The

molar extinction co-efficient is defined as the optical density of a one-molar solution of the fluorochrome through a one cm light path. To be useful in biological assays fluorescent molecules have to have an extinction co-efficient of tens of thousands (Fluorescein 70,000. Cy5 200,000). To calculate the concentration of a fluorescent compound the absorbance should be measured at a particular wavelength and the concentration calculated from the extinction co-efficient.

Strongly fluorescent molecules have a high extinction co-efficient and a quantum yield close to one to allow the development of highly sensitive fluorescence based assays.

Quantum efficiency is the product of quantum yield and the extinction co-efficient.

Fluorescent lifetime is the length of time the fluorescent molecule takes to decay back to its resting level. If the length of time for which the sample is excited is longer than the fluorescent lifetime of the fluorophore, the sample can undergo many excitation and decay cycles. The lifetime of the fluorescence molecule is important especially for time-resolved fluorescence resonance energy transfer (TR-FRET), which will be discussed in more detail later. Fluorescent lifetimes also have to be considered when designing fluorescence anisotropy assays (Pope et al., 1999).

The reduction of fluorescence emission can arise in several ways including:
Photobleaching is the result of photodestruction of the fluorochrome as the excited state of a fluorophore is more chemically reactive than when it is in the ground state, giving decreased fluorescence. Different fluorophores have different susceptibility to photobleaching and the light intensity of the incident light, the length of time of illumination and the chemical environment affect the amount of photobleaching.

Quenching, which means a diminishing of the signal emitted due to the environment of the fluorophore. Quenching results from the energy that would

have been emitted as light of a particular wavelength being absorbed or transferred to another molecule.

Light scattering, which results from the light from the excitation source "bouncing off" other molecules in solution resulting in a range of wavelengths which may interfere with the true emission reading. Light scattering is particularly relevant in solutions of high turbidity.

1.10 Fluorescent Assays

The use of fluorescent probes in the study of receptor interaction has increased recently as there are obvious advantages in using fluorescent ligands i.e. reduction in cost, increased safety over using radiolabelled ligands, as well as the ability to use live cell preparations.

Fluorescent labelling of ligands has previously been limited to the availability of suitable commercially available dyes where the fluorescent moiety has not altered the binding affinity for the receptors. As fluorescently labelled selective agonists become available for receptors, the ability to look at whole cell binding using a confocal microscope with appropriate quantitative software becomes possible. There are several different fluorescent assay formats that are used in the study of GPCRs including direct fluorescent intensity of the fluorescent molecule.

1.10.1 Fluorescence anisotropy

Fluorescence anisotropy is another assay that has been used to assay ligand binding to GPCRs (Pope et al., 1999). In this case there needs to be no separation of bound from free ligand as small fluorescent ligand molecules have little or no polarisation signal when rotating free in solution. A large polarisation signal is observed when bound to the receptor within a membrane.

1.10.2 Fluorescence Resonance Energy Transfer

Fluorescent resonance energy transfer (FRET) involves the non-radiative energy transfer between two molecules. This is a non-destructive quantifiable technique, which involves the use of two fluorescently labelled molecules whose excitation and emission spectra overlap i.e. the emitted light from one fluorophore excites the second fluorophore (figure 1.4). By measuring the output from the second fluorophore the amount of energy transfer can be calculated. For FRET to be able to take place the fluorescent moieties must be close together (10-100Å range) (Pope et al., 1999), therefore this technique measures molecular interactions by either the occurrence of FRET or its disruption. FRET has previously been used to produce a fluorescent indicator for Ca^{2+} (Romoser et al., 1997, Miyawaki et al., 1997). It may be possible to use FRET to examine the interaction of receptors with G-proteins, arrestins and kinases. A related technique termed bioluminescence resonance energy transfer (BRET) has been used to demonstrate homodimerization of the β_2AR receptor (Angers et al., 2000). FRET and BRET are discussed further in Chapters 4 and 5.

Figure 1.4 **A) Energy diagram of fluorescence resonance energy transfer between fluorescent donor and acceptor molecules**

A)

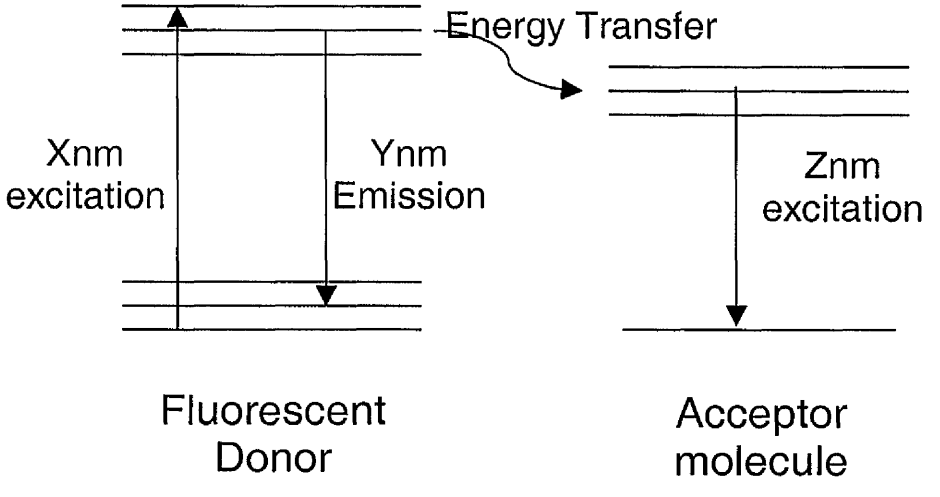

Figure 1.4 B) Schematic representation of spectral overlap required for fluorescence resonance energy transfer

B)

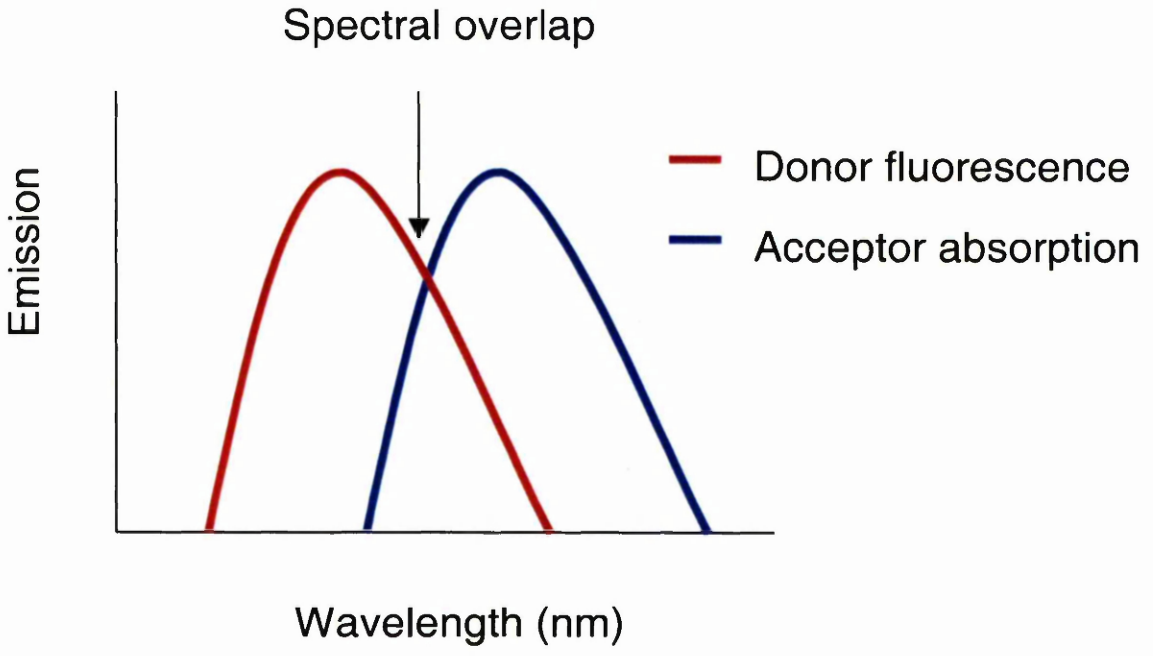

1.10.3 Fluorescence Correlation Spectroscopy

To follow the kinetics of agonist association and dissociation, the sensitive technique known as Fluorescence Correlation Spectroscopy (FCS) can be used. This can be performed in an extremely small (femtolitre) volume and looks at the interactions of single molecules in solution and can be performed in individual cells, in real time (Eigen and Rigler, 1994). This technique employs a confocal microscope and measures the time for a fluorescent moiety to traverse the illuminated area. A highly sensitive single-photon detection device registers photons of fluorescent light.

Kinetics can also be performed using fluorescence correlation spectroscopy (FCS) which involves the measurement of molecular size by analysis of the diffusion time across the laser focus. This highly sensitive technique can

measure single molecules and in femtolitre volumes. FCS has been used to measure binding for GPCRs achieving similar Kd values to that obtained from radiolabel ligand binding assays (Auer et al., 1998). Fluorescence Incidence Distribution Analysis (FIDA), is a related technique which has been adapted for confocal microscopy studies (Kask et al., 1999). Fluorescence correlation microscopy (FCM) combines the FCS technique with fluorescence imaging and has been used to localise a GFP-tagged epidermal growth factor receptor (EGFR) within live cells (Brock et al., 1999).

1.10.4 Fluorescence Recovery After Photobleaching

Fluorescence Recovery After Photobleaching (FRAP) is another technique which has been used to study receptor interactions. This involves exposing a small area of cell membrane to a brief high intensity laser pulse to photolyse a fraction of the labelled protein. This results in a rapid decrease in the monitored fluorescence intensity. The recovery is shown by the rate of the diffusion of the non-photolysed protein into the previously bleached area. Again this technique uses confocal microscopy and is performed on whole cells (Barak et al., 1997).

1.11 Green Fluorescent Protein (GFP)

The use of fluorescence in biology has been greatly influenced by the discovery of Green Fluorescent Protein (GFP). This is a 27kDa protein produced by the jellyfish *Aequorea victoria* where it is the acceptor of non-radiative energy transferred from aequorin. The fluorescent properties of GFP include a large quantum yield and extinction co-efficient, the product of which results in the intrinsic brightness of the fluorophore. Many variants of GFP have now been produced with altered properties to allow its use in biological systems, which include its stability at 37°C, enhanced brightness at neutral pH and varying excitation and emission maxima (Tsien, 1998). GFP is strongly fluorescent and requires no co-factor as it is the correct folding of the protein that results in the formation of its chromophore (Tsien, 1998). GFP has been widely used in biology by fusing the GFP to the N or C-terminus of the protein of interest. It has

been used to detect gene expression (Gervaix et al., 1997) and to track enzymes (Fejes-Toth et al., 1996).

Having a fluorescent receptor protein overcomes the problems associated with selectively labelling a receptor molecule with fluorescent dyes. There are no problems with calculating labelling stoichiometry, or worries about labelling at essential residues generating a mis-functional protein. GFP has been coupled to the C-terminus of many different GPCRs allowing cellular trafficking to be studied by following the fluorescence. Barak et al. (1997), Kallal et al. (1998) and Tarasova et al. (1997) demonstrated the trafficking of the cholecystokinin receptor type A (CCKAR) and that agonists induced internalization and antagonists inhibited spontaneous internalization of the receptor. Confocal microscopy was used to follow the trafficking in live cells demonstrating that the internalized receptor was present in endosomes before re-cycling back to the cell-surface. Other molecules involved in GPCR trafficking have been labelled with GFP. Barak et al. (1997) used a GFP tagged β-arrestin-2 molecule to follow its translocation to the cell-surface after activation and subsequent phosphorylation of the β_2AR or the dopamine D1A receptors. This GFP tagged β-arrestin may be suitable for identification of agonists that activate orphan receptors. A further study of the substance P receptor which is a GPCR was performed using GFP fusions of protein kinase C, GRK2 and β-arrestin-2 (Barak et al., 1999).

1.11.1 FRET with GFP

Many new GFP variants have been produced which can be used in energy transfer assays or direct fluorescence in cells which have been reviewed by Billinton and Knight (2001). GFP mutants can be used in FRET as there are several variants with the necessary overlapping excitation and emission maxima. Rosomer et al. (1997) and Miyawaki et al. (1997) both describe an internal Ca^{2+} indicator that was designed using a calmodulin binding sequence with GFP variants at either end. The GFP variants used have overlapping excitation and emission spectra, Blue or Cyan FP as fluorescent donors with Green or Yellow FP as acceptor molecules. Upon Ca^{2+} binding there is a change in direction and

distance between the two GFP variants, which results in energy transfer between them when excited with the appropriate wavelength of light.

A study of the physiological role of the A kinase anchoring proteins with FRET allowed investigation of the specificity in signalling events controlled by compartmentalization and clustering of the signalling enzymes with their activators (Ruehr et al., 1999). A decrease in FRET signal was observed microscopically detecting synaptic excitation that resulted in an increase in post-synaptic Ca^{2+} with activation of the Ca^{2+} activated protease calpain. The substrate for the protease included a μ-calpain binding site; flanked by eYFP and eCFP which was present in the post-synaptic neurones. This protease substrate was attached to the postsynaptic dendrites via a PDZ domain present in the eCFP (Vanderklish et al., 1999).

1.12 Other fluorescent proteins

Other naturally occurring fluorescent molecules are being identified and tested for use in a similar manner to GFP, including DsRed, which is a 28kDa protein, expressed in a coral of the *Discosoma* species, described by Baird et al. (2000). DsRed has the advantage of emission at a longer wavelength greater than any of the mutant GFP molecules produced, making it possible to use DsRed in the presence of other fluorescent molecules to either study independently or using FRET. Further studies on this or other fluorescent protein molecules are likely to result in a brightly fluorescent protein molecule with longer wavelength emission than GFP and biological stability.

1.13 Research objectives

Currently, the evidence for GPCR homo and heterodimerization is increasing although some intriguing differences have been noted e.g. in the effect of agonist on the dimerization of GPCRs.

The primary aim of this study is to investigate δOR homo and heterodimerization with other GPCRs. The pharmacology available for opioid receptors indicates complicated signalling mechanisms in which several different GPCR signalling

systems are involved. Opioid receptor pharmacology indicates several opioid receptor sub types and as no cDNAs for these sub-types has been identified it is intriguing to speculate that homo and heterodimerization reactions between opioid receptors are responsible for this pharmacology.

The techniques involved to look at GPCR dimerization have involved disruption of the cells expressing the GPCRs of interest. Initially this study also involves disruption of the cells and subsequent co-imunoprecipitation of differentially tagged GPCRs.

A large portion of this work involves the development of a robust intact cell assay with a large signal to noise ratio for the study of δOR homo and heterodimerization which can be applied to other GPCRs.

CHAPTER 2

Materials

And

Methods

CHAPTER 2 MATERIALS AND METHODS

2.1 Materials

All reagents used in this study were of analytical or similar grade and were purchased from the following suppliers:

2.1.1 General Reagents

Alexis Corporation Ltd., Bingham, Nottingham, U.K.

DTT

Amersham Pharmacia biotech., Buckinghamshire, U.K.

Rainbow molecular weight markers
FluoLink™ Mab Cy3 labelling kit

BDH

glycine, Na_2HPO_4

Boerhinger Mannheim U.K. Ltd., Lewes, East Sussex, U.K.

Restriction enzymes, complete™,EDTA-free Protease Inhibitor Cocktail tablets and DNA molecular weight markers X (0.07-12.2kbp).

Calbiochem-Novabiochem Ltd., Beeston, Nottingham, U.K.

Geneticin (G418)

Fisher Scientific Equipment, Loughborough, U.K.

Acetic acid, DMSO, EDTA, HEPES, hydrochloric acid, KCl, KH_2PO_4, K_2HPO_4, $MgCl_2$, NaCl, Na_2CO_3, $NaHCO_3$, NaH_2PO_4, sucrose, SDS, trichloroacetic acid.

FMC Bioproducts, Rockland, USA

Agarose

Fuji Photo Film Co. Ltd., Tokyo, Japan

X-ray film

Genosys, Cambridge, U.K.

Oligonucleotides

Gibco BRL Life Technologies Inc, Paisley, U.K.

Lipofectamine™, TRIS, 1kb DNA ladder, oligonucleotides

Invitrogen, San Diego, CA, U.S.A

pcDNA3, pcDNA3(-)

Merck Ltd., Pole, Dorset, U.K.

Agar, NaOH

Novex , Germany
7% Tris-acetate polyacylamide gels

Nunc, IL., U.S.A.

Black 96 and 384 well plates

Oxoid Ltd., Hampshire, U.K.

Tryptone, yeast extract

Premier Beverages, Stafford, U.K.

Marvel

Promega Ltd., Southampton U.K.

Restriction enzymes, DNA purification kits - Wizard™ Minipreps and Wizard™ Maxipreps systems

Prozyme® INC., European distributor Europa Bioproducts Ltd., Cambridgeshire, UK.

Phycolink™ SMCC-cross-linked Allophycocyanin

Qiagen Ltd., West Sussex, U.K.

QIAquick Gel Extraction Kit

RBI® Research Biochemicals International Natick MA, USA

ICI-174,864

Sigma Chemical Company., Poole, Dorset, U.K.

Alumina (activity grade 1), ampicillin, DOWEX AG50 W-X4 (200-400 mesh), forskolin, imidazole, mineral oil, protein-G sepharose, TEMED, thimerosal,

Stratagene Ltd., Cambridge, U.K.

PfuTurbo™ DNA polymerase

Whatman International Ltd., Maidstone, U.K.

GF/C Glassfibre filters

2.1.2 Radiochemicals

Amersham Pharmacia biotech., Buckinghamshire, U.K.

[^{3}H]adenine (specific activity: 20 Ci/mmol)

[^{3}H]CGP-12177 (specific activity:41 Ci/mmol)

[^{3}H]dihydroalprenalol (specific activity: 75Ci/mmol)

[^{3}H]diprenorphine (specific activity: 66Ci/mmol)

Du Pont NEN Ltd., Stevenage, Hertfordshire, U.K.

[γ^{32}P]GTP (specific activity: 30 Ci/mmol)

[^{3}H]naltrindole (specific activity: 20Ci mmol)

[^{3}H]DADLE (specific actlvity: 50Ci/mmol)

2.1.3 Tissue Culture

American Tissue Culture Collection, Rockville, U.S.A.

Human Embryonic Kidney (HEK293) cells

Costar Scientific Corporation, Buckinghamshire, U.K.

Dishes 10cm and 6cm diameter, Flasks 25cm^2 and 75cm^2, Plates 6, 12 and 24 wells, Disposable cell scraper

Gibco Life Technologies Inc, Paisley, U.K.

Glutamine (200mM), Newborn calf serum, $NaHCO_3$ (7.5% $^{w}/_{v}$), Optimem-1 medium

Sarstedt, Numbrecht, Germany

Cryovials

Sigma Chamical company, Poole, Dorset, U.K.

Dulbecco's Modified Eagle's Medium (DMEM)

Sterilln Bibby Ltd., Stone, Staffordshire, U.K.

Pipettes 5ml, 10ml and 25ml.

2.1.4 Standard Buffers

Phosphate Buffered Saline (PBS)

Na_2HPO_4	8.1mM
K_2HPO_4	1.5mM
NaCl	140mM
KCl	2.7mM

pH adjusted to 7.3
This was usually made up as a 10x stock and diluted when required

Phosphate Buffered Saline with Tween (PBS/T)

As for PBS but with Tween20 added (0.1% $^{w}/_{v}$)

Tris-EDTA Buffer (TE)

Tris/HCl	10mM
EDTA	0.1mM

pH adjusted to 7.5

SDS-Page Sample Buffer

DTT	50mM
SDS	1.7%
Tris/HCl (pH6.8)	58mM
Bromophenol Blue	0.002%
Glycerol	6%

This was stored in aliquots at –20°C until required.

2.1.5 Antisera

Anti- Flag antibody (M5)

Mouse monoclonal antibody that binds to N-terminal Flag proteins.

Purchased from Sigma Chemical company, Poole, Dorset, U.K.

Anti-myc antibody (A-14)

Rabbit polyclonal antibody that binds to N-terminal c-myc proteins.

Purchased from Santa Cruz™ biotechnology, Inc., CA, U.S.A.

Anti-myc 9E10-FITC antibody

Mouse monoclonal antibody labelled with Fluorescein Isothiocyanate (FITC).

Purchased from Santa Cruz™ biotechnology,Inc.,CA, U.S.A.

Anti-myc-EuK antibody

Mouse monoclonal 9E10 antibody raised against the 408-439 sequence of human c-myc protein, labelled with Europium cryptate ions.

Purchased from Packard Bioscience Ltd., Berkshire, U.K.

M2-XL665 anti- Flag antibody

Mouse monoclonal antibody that binds to N-terminal methionine- Flag proteins. labelled with allophycocyanin.

Purchased from Packard Bioscience Ltd., Berkshire, U.K.

LANCE Eu-iabelled W1024-anti-myc antibody

Mouse monoclonal antibody which has been fluorescently labelled with Eu^{3+}.

Purchased from Wallac oy, Turku, Finland

Anti-GFP antibody

Sheep antibody raised against GFP, produced by the Scottish Antibody Production Unit, Lanarkshire, U.K.

Anti-mouse IgG

Goat polyclonal antibody conjugated with horseradish peroxidase, purchased from Amersham Pharmacia biotech., Buckinghamshire, U.K.

Anti-rabbit IgG

Donkey polyclonal antibody conjugated with horseradish peroxidase, purchased from Amersham Pharmacia biotech., Buckinghamshire, U.K.

Anti-Sheep IgG

Donkey polyclonal antibody conjucated with horseradish peroxidase, purchased from Jackson Immunoresearch. PA., U.S.A.

2.2 Cell Culture

All tissue culture manipulations were performed in a Laminar Flow Hood designed for this purpose. Aseptic techniques were used with all manipulations of cells or preparation of plastics. Liquid waste was added to antiseptic before discarding. Solid waste was removed and autoclaved before being disposed.

2.2.1 Routine Cell Culture

Human Embryonic Kidney cells (HEK293) were grown in DMEM, supplemented with 10% Newborn Calf Serum and 2mM L-Glutamine. The cells were grown as a monolayer on tissue culture treated plastic plates, dishes or flasks. Cells were incubated in cell culture incubators (Jencons Nuaire) at 37°C in a humidified atmosphere with 95% air / 5%CO_2.

Cells were split when confluent by removing the medium followed by the addition of 1ml of trypsin solution (0.1% $^{W}/_{V}$ trypsin, 0.025% $^{W}/_{V}$ EDTA and 10mM Glucose). When the cells were detached 9ml of DMEM was then added to prevent further trypsinisation. The cells were then re-suspended in this medium and seeded into new flasks, plates or dishes containing DMEM.

2.2.2 Transient Transfections

Lipofectamine™ reagent (Gibco Life Technologies) was used to transfect the cells with the appropriate cDNA according to the manufacturers' instructions. Briefly, DNA was diluted to 0.1mg/ml with sterile water before the addition of Optimem. cDNA / Optimem for a 10cm^2 dish being 600µl containing 8µg of DNA. To this an equal volume of Lipofectamine™ reagent which had also been diluted

with Optimem was added, with there being 20µl of Optimem being added for a 10cm^2 dish. The DNA / lipofectamine mixture was left for 30 - 45min at room temperature before the addition of 4.8ml Optimem (for a 10cm^2 dish), all of the mixture was then added drop-wise to the dish of cells which contained cells of approximately 80% confluency rinsed with Optimem. The dishes were then placed back in the tissue culture incubators for 4 h before the addition of 6ml of DMEM. The cells were placed back in the incubators overnight before the entire medium on the dishes was replaced with fresh DMEM. Cells were routinely harvested 48 h after transfection.

2.2.3 Generation and maintenance of stable cell lines

Human Embryonic Kidney 293 cells were transfected using the method described in 2.2.2. 48 h after transfection, DMEM containing 1mg/ml Geneticin (G-418) was added to select for antibiotic resistant clones. This medium was changed every 3 days and as non-resistant cells started to die discrete colonies of resistant clones were observed. Each clone was "picked" using a pipette, the cells and some medium were withdrawn and placed in an individual well of a 24 well dish and allowed to grow. As the clones grew they were subsequently transferred to 6 well dishes, 25cm^2 flasks and 75cm^2 flasks. The clones were then split into 3 x 75cm^2 flasks, one each for harvesting, freezing down and maintaining growth.

2.2.4 Preservation of cell lines

Stable cell lines were preserved at a low passage, the cells were grown to confluency before trypsinisation to remove them from the flask. The cells were then centrifuged for 5min at 3000 rpm in a bench top centrifuge. The pellet was then resuspended in 1ml of NBCS with 7.5% DMSO (as a cryoprotectant). The cells were then transferred into 1.5ml cryovials. These were frozen slowly in a -80°C freezer by wrapping the vials in cotton wool first. Long term storage was in liquid nitrogen tanks.

These cells were resuscitated for use by thawing the cryovial at room temperature, before addition of the cells to 9ml of pre-warmed DMEM. The cells were then spun in a bench top centrifuge for 5min at 3000 rpm. The medium was removed and the cells resuspended in a further 10ml of DMEM, this removes the DMSO from the cells. The cell suspension was then added to a 75cm^2 flask and routine cell-culture continued.

2.2.5 Cell harvesting

Cells were harvested by removing the medium and washing the cells with 2 x 6ml of ice-cold PBS. A disposable cell scraper was then used to remove the cells from the surface of the flask or dish in a small volume of PBS. The cell suspension was then centrifuged for 5min at 3000 rpm on a bench top centrifuge at 4°C. The PBS was removed and the cell pellets stored at -80°C before membrane preparation.

2.3 Molecular biology

Molecular biology manipulations were performed with materials which had been autoclaved, on a bench which had been swabbed with 70% alcohol. Disposable gloves were worn at all times to prevent contamination of the DNA.

2.3.1 Reagents for Molecular Biology

Gel loading buffer (6x)

Bromophenol Blue (2%)	1.25ml
Sucrose	4g

These were dissolved in autoclaved water to give a final volume of 10ml. The buffer was stored in aliquots at -20°C.

TAE buffer

Tris-acetate	40mM
EDTA	1mM

This was prepared as a 50x stock solution by adding 242g of Tris / HCl, 57.1ml of glacial acetic acid and 100ml of 10mM EDTA (pH8) to deionised water in a final volume of 1 litre. This was diluted in deionised water when required.

Luria Bertani (LB) broth

Bacto-tryptone	10g
Bacto-yeast extract	5g
NaCl	10g

These were dissolved in 1 litre of deionised water and sterilised by autoclaving.

LB ampicillin agar plates

This has the same composition as the LB with the addition of bacto-agar (1.5% $^{w}/_{v}$). This was left to cool before ampicillin was added to a final concentration of 50μg/ml. The liquid agar was then poured into 10cm diameter petri dishes and allowed to solidify at room temperature before storing at 4°C.

2.3.2 Transformation

This is the transfer of DNA into *E.coli*, which allows multiple copies of the DNA to be produced as the bacteria replicate. DH5α was the strain of *E.coli* used for

transformation along with the vector pcDNA3.1(-), allowing a high copy number of the plasmid to be produced per bacteria.

Preparation of competent bacteria

E.Coli must first be "made competent" to allow the entry of foreign DNA. This involved treating the bacteria with various chemicals.

Solution 1

Potassium acetate	3ml
$RbCl_2$ (1M)	10ml
$CaCl_2$ (1M)	1ml
$MnCl_2$ (1M)	5ml
Glycerol (80% $^{v}/_{v}$)	18.75ml

The final volume was made up to 100ml with deionised water and the pH adjusted to 5.8 with 100mM acetic acid. This was then filter-sterilised and stored at 4°C.

Solution 2

MOPS (100mM; pH6.5)	4ml
$CaCl_2$ (1M)	3ml
$RbCl_2$ (1M)	0.4ml
Glycerol (80% $^{v}/_{v}$)	7.5ml

The final volume was made up to 40ml with deionised water and the pH adjusted to 6.5 with HCl before filter sterilization, this was stored at 4°C.

A confluent 5ml culture of *E.Coli* DH5α cells, which had been grown overnight in LB broth was added to 250ml of sterile LB broth and incubated with shaking at 37°C, for 4-5 h. When the optical density at 550nm was 0.48 the bacteria were pelleted by centrifugation at 3000 rpm, at 4°C for 5min. The bacteria were suspended in 100ml of solution 1 and incubated on ice for 5min. The bacteria were pelleted as before then resuspended in 15ml of solution 2 and incubated on ice for 15min. The DH5α bacteria were now suitable for transformation or were stored at -80°C in aliquots until required.

Transformation of DNA

10-50ng of each plasmid DNA was incubated with 50μl of competent bacteria in a sterile tube for 15min on ice. The DNA / bacteria mix was then subjected to heat shock at 42°C for 90 s before being plunged back into ice for a further 2min. 450μl of LB broth was added and the bacteria allowed to recover in a shaking incubator at 37°C for 45 min. 200μl of this mixture was then plated onto a LB ampicillin agar plate which was left on the bench for a short time to allow the agar to absorb the liquid before an overnight incubation at 30°C. Colonies picked from the plate can be cultured further in LB broth for DNA extraction. The plate was kept at 4°C for up to one month.

Transformed *E.Coli* LB broth cultures were also maintained as glycerol stocks by mixing 1 volume of culture with 1 volume of glycerol in a sterile eppendorf tube, and stored at -80°C. Cells kept as glycerol stocks are viable for up to 2 years.

2.3.3 DNA Preparation

DNA was purified using Promega Wizard™ Miniprep and Maxiprep kits according to the manufacturer's instructions.

2.3.4 Polymerase chain reaction (PCR)

PCR mix

Component		volume
Template DNA	(0.1μg/μl)	2μl
Primer 1	(25 pmol/μl)	1μl
Primer 2	(25 pmol/μl)	1μl
Deoxynucleotides triphosphate	(2.5mM)	5μl
Pfu polymerase buffer (10x)		5μl

The volume was made up to 50μl with autoclaved water, the mix was added to thin-walled PCR tubes, one drop of mineral oil was added on top. The mixture was heated to 95°C for 10min, to denature the double stranded DNA and allow the primers to bind, before the addition of 0.5ml of Pfu turbo enzyme and the PCR cycles initiated in a Hybaid OmniGene temperature cycler.

PCR cycles

Denaturation	Annealing	Extension	Cycles
95°C; 1min	60°C; 1min*	72°C; 4min	35
95°C; 1min	60°C; 1min*	72°C; 10min	1

* The annealing temperature was determined empirically and was set at 55, 60 or 65°C.

After the PCR cycles the aqueous lower layer was removed and transferred into another sterile tube.

2.3.5 Agarose gel electrophoresis

Gel loading buffer (6x) was added in the ratio of 1:5 with the DNA, which had been diluted with autoclaved water. Agarose gel was prepared by the addition of 1% agarose in 40ml of TAE buffer and heating in the microwave oven until the agarose was dissolved. 5μl of ethidium bromide (10mg/ml) was mixed with the liquid agarose before pouring into the chamber of the electrophoresis kit (Gibco Horizon 58 with Model 200 power pack). The appropriate combs were inserted to form the wells in the gel. After the gel had set, TAE buffer was added to cover the gel. The DNA in the gel loading buffer was loaded into the wells and the electrophoresis started. The gel was examined under UV light and an electronic image printed.

2.3.6 DNA purification from Agarose Gel

Purification of DNA fragments from agarose gel was performed using the QIAquick Gel Extraction kit (Qiagen, West Sussex, U.K.).

2.3.7 DNA sequencing

Sequencing of DNA was performed at the Protein and Nucleic Acid Chemistry Laboratory (PNACL) of Leicester University. An ABI Bigdye-terminator ready reaction kit was used for the PCR reaction, while a Perkin Elmer ABI 377 DNA sequencer was used for the electrophoresis and analysis of sequences.

2.3.8 Construction of Flag-δOR and c-myc-δOR

The DNA for human δ opioid receptor (hδOR) in the plasmid pcDNA4 was a kind gift from Glaxo Pharmaceuticals.

The set of PCR oligonucleotide primers used for the construction of Flag-δOR were

Sense oligonucleotide 5' -
AAAAAAGGGCCC**GCCACC**ATGGACTACAAGGACGACGATGATAAGGAACC
GGCCCCCTCCGCC-3'

This primer introduced an *Apa*I site (underlined) followed by the Flag epitope tag at the 5' end. The Kozak sequence is in bold.

Antisense oligonucleotide 5' – TGCTCTAGATCAGGCGGCAGCGCC-3'

This primer added an *Xba*I site (underlined) at the 3' end followed by a stop codon.

The set of PCR oligonucleotide primers used for the construction of c-myc-δOR were

Sense oligonucleotide 5' –
AAAAAAGGGCCC**GCCACC**ATGGAACAAAAACTTATTTCTGAAGAAGATCTG
GAACCGGCCCCCTCCGCC-3'

This primer introduced an *Apa*I site (underlined) followed by the c-myc epitope tag at the 5' end. The Kozak sequence is in bold.

Antisense oligonucleotide 5' – TGCTCTAGATCAGGCGGCAGCGCC-3'.
This primer added an *Xba*I site (underlined) at the 3' end followed by a stop codon.

The PCR amplified fragments were purified by agarose gel (1% $^{v}/_{v}$) electrophoresis followed by gel extraction. The fragments were digested with *Apa*I and *Xba*I before ligating to pcDNA3.1(-) (Stratagene) using these restriction sites. Both DNA constructs were fully sequenced.

2.3.9 Construction of Flag-δOR-GFP and c-myc-δOR-GFP

The Flag-δOR and c-myc-δOR cDNA was used as a template to which the GFP sequence was fused to the C-terminus. This necessitated the removal of the stop codon in the receptor cDNA and the introduction of a new restriction site so that the 5' end of the GFP cDNA could be ligated in frame with the 3' end of the FlagδOR and the c-myc-δOR. *Xba*I was chosen as the linker as a primer to generate the GFP with a 5' *Xba*I site was available.

PCR of the GFP cDNA was performed using the following primers:

Sense oligonucleotide 5' –CTAGTCTAGAAGTAAAGGAGAAGAACTTTTCAC-3'

The underlined bases refer to the restriction site for *Xba*I therefore this primer provides the generation of GFP with a 5' *Xba*I site.

Antisense oligonucleotide 5'-TGCTCTAGATTATTTGTATAGTTCATCCATGCC-3'

The underlined bases refer to the restriction site for *Xba*I therefore this primer provides the generation of GFP with a 3' XbaI site.

The sense primer used previously to generate a 5' *Xba*I site on the receptor was used again here, the following primer was used to remove the stop codon, replacing it with an *Xba*I site.

Antisense oligonucleotide 5' – TGCTCTAGATCAGGCGGCAGCGCC-3'

The underlined bases refer to the restriction site for *Xba*I, therefore this primer provides the generation of an *Xba*I restiction site and the removal of the stop codon of the δOR.

The PCR fragments were purified by gel electrophoreses and extraction. Restriction enzymes *Apa*I and *Xba*I were used to digest the receptor fragment and *Xba*I was used to digest the GFP fragment which was then ligated to pcDNA3.1(-) using the *Apa*I and *Xba*I restriction sites. As the GFP generated contained *Xba*I sites at both the 5' and 3' end the cDNA isolated from the successfully ligated clones was digested with *Apa*I and *Eco*RV restriction enzymes, followed by gel electrophoresis and clones containing the GFP in the correct orientation were identified.

2.4 Assays

2.4.1 Cell membrane radioligand binding

The expression of the δOR in stable cell lines and in transiently transfected cells was assessed by [^{3}H]diprenorphine or [^{3}H]naltrindole binding studies. These were performed in triplicate in borosilicate glass tubes, containing the following mix:

Membrane protein (0.75mg/ml)	20μl
Assay buffer (50mM Tris/HCl, pH7.5, 5mM $MgCl_2$, 1mM EDTA)	140μl
[^{3}H]diprenorphine or [^{3}H]naltrindole (15nM or 50nM)	20μl
Naloxone (3mM) or assay buffer	20μl
Total volume	**200μl**

The reaction mix was incubated at 25°C for 45min. Binding was stopped by the addition of 2.5ml of ice-cold wash buffer (50mM Tris/HCl pH7.5, 0.25mM EDTA), followed by vacuum filtration through GF/C filters to remove the free radioligand from the membrane. The filters were washed 3 times with ice-cold wash buffer, and air-dried before adding to 5ml of liquid scintillant. The vials were counted after an overnight incubation in a Beckman LS6500 scintillation counter using the ^{3}H counting channel. The specific binding was calculated by subtracting the counts in the presence of the competing antagonist naloxone from the total counts. Receptor expression level was expressed as fmol/mg, using the specific activity of the radiolabels ([^{3}H]diprenorphine, 128.8 dpm/fmol or [^{3}H]naltrindole, 73.3 dpm/fmol).

The binding affinity of the receptors was assayed similarly using increasing concentrations of [^{3}H]naltrindole.

2.4.2 Intact cell radioligand binding

Intact cell binding was performed using two different methods, the first method being similar to that described above for the membrane binding with the addition of 2 x 10^5 cells in place of the membranes. In this case the assay buffer was Krebs Ringers Hepes (KRH) buffer.

KRH buffer

NaCl	20mM
KCl	5mM
$MgSO_4$	1.2mM
$CaCl_2$	1.2mM
Hepes	20mM
Na_2HPO_4	1.2mM
Glucose	10mM
Bovine Serum Albumin	0.1%

The pH was 7.4.

This assay was also performed in the presence of 3nM anti-c-myc-Eu^{3+} and 15nM anti-Flag-APC antibodies, the assay buffer used was 50% Newborn calf serum / PBS and the incubation time was 2 h at room temperature. The

radioligands used to determine the receptor expression levels were [^{3}H]naltrindole (73dpm/fmol), [^{3}H]DADLE (123dpm/fmol), [^{3}H]dihydroalprenolol (136dpm/fmol) and [^{3}H]CGP 12177 (91dpm/fmol).

The second method of intact cell binding was performed using cells that were attached onto the surface of 12 well dishes. The antagonist [^{3}H]naltrindole was used in this case and the assay mix was as described above with the assay buffer being the (KRH) buffer. On each 12 well plate 1 well was not used in the binding assay but the cells were detached from the surface of the well and counted. The mean value obtained for the cells per well was used, with the specific activity of [^{3}H]naltrindole (73.3dpm/fmol) and Avogadro's number to calculate the receptor number per cell.

2.4.3 Adenylate cyclase catalytic activity

The catalytic activity of adenylate cyclase was assayed in accordance with Wong (1994) based on the use of [^{3}H]adenine. Cells were split into 24 well dishes 24 h before the addition of [^{3}H]adenine (0.5μCi per well) in DMEM for an overnight incubation.

The cells were then washed in DMEM, 2mM L-glutamine, 20mM HEPES (pH7.4) containing IBMX, which is a non-selective inhibitor of phosphodiesterases. DADLE was added in this medium in the presence of 50μM forskolin, at 37°C for 30min. The reaction was stopped by the addition of 0.5ml of stop solution (5%TCA, 1mM ATP, 1mM cAMP). The plates were either stored at -20°C or incubated at 4°C before separating the nucleotides.

Separation of the cAMP from the other adenine nucleotides is based essentially on the method of Salomon et al. (1974). The dowex and alumina columns were set up according to Farndale et al. (1991). Columns were constructed from 5ml syringes with a glass wool plug to prevent loss of the resin. Racks containing the columns were aligned over each other while the assay took place. Before each use the columns were primed as follows: the dowex columns were washed with

several volumes of water, 2 volumes of HCl (1M) followed by 5 further volumes of water. The alumina columns were washed with 5 volumes of imidazole (0.1M). The column bed volumes were at least 1ml of the respective resin.

Separation of the [^{3}H]cAMP from the other labelled components ([^{3}H]ATP, [^{3}H]ADP, [^{3}H]AMP, [^{3}H]adenine) begins with the dowex column, which is negatively charged and although no components bind to the dowex the cAMP is selectively retained which allows the other components to be removed by washing the dowex with water (Farndale et al., 1991). The alumina column binds cAMP with low affinity and this is competed off using imidazole.

The 0.5ml stop solution sample was added to the dowex column, followed by the addition of 3ml of deionised water. The eluant was collected in scintillation vials to which 5ml of scintillation fluid had previously been added. This contains predominantly the adenine nucleotides with the exception of [^{3}H]cAMP. The dowex columns were then placed on top of the alumina columns and 10ml of deionised water added to the dowex columns. This passed through the dowex and onto the alumina, including the [^{3}H]cAMP. The dowex columns were then removed and the alumina columns washed with 10ml of imidazole (0.1M). The eluate was collected into scintillation vials containing 9ml of liquid scintillant. Both sets of vials were counted in the Beckman scintillation counter using the [^{3}H] channel. Results were expressed as the ratio of [^{3}H]cAMP to total [^{3}H]adenine nucleotides (x100) which was then expressed as a percentage inhibition of the forskolin stimulation in the absence of any agonist.

2.4.4 High affinity GTPase activity assays

High affinity GTPase assay was performed essentially as described in Gierschik et al. (1994). An assay mix for 100 tubes was prepared as follows:

	Volume (µl)	Final concentration
Creatine Phosphate (0.4M)	250	20mM
Creatine Phosphokinase (2.5U/ml)	200	0.1U/ml
ATP (0.04M; pH7.5)	250	2mM
App(NH)p	25	0.2mM
Ouabain (0.01M)	1000	2mM
NaCl (4M)	250	200mM
$MgCl_2$ (1M)	50	10mM
DTT (0.1M)	200	4mM
EDTA (0.02M; pH7.5)	50	0.2mM
Tris/HCl (2M; pH7.5)	200	80mM
GTP (0.1mM)	50	1µM
[γ^{32}P]GTP 5µCi		50nCi

The volume was then made up to 5000µl by the addition of deionised water.

The assay mix was left on ice until it was added to the assay tubes.

1.5ml eppendorf tubes were used, containing:

Membrane protein (0.5mg/ml)	20μl
Agonist or water or GTP*	10μl
Deionised water	20μl
Assay mix	50μl
Total volume	**100μl**

*Each sample was assayed in the presence of each of these components. The addition of water estimates the basal activity, addition of agonist gives the stimulated activity and the GTP (100μM final) gives the non-specific activity.

The assay tubes were set up in triplicate and were incubated at 37°C for 20min before the addition of 900μl of an ice-cold charcoal solution (5% activated charcoal in 10mM H_3PO_4) to each tube, which terminates the reaction. The tubes were then spun at 3000rpm for 5min in a bench top centrifuge at 4°C. The supernatant contains the free Pi and 500μl of this was removed and transferred into scintillation vials for Cerenkov radiation counting in a Beckman counter. High affinity GTP hydrolysis rate (pmol/min/mg) was obtained by subtracting the counts from GTP (100μM final) control tubes, taking into consideration the specific activity of the [γ^{32}P]GTP, the concentration of unlabelled GTP in the assay (0.5μM), the membrane protein concentration and the incubation time. Results were presented as the percentage increase of the high affinity GTPase activity by agonist, over basal.

2.4.5 Time-resolved fluorescence resonance energy transfer (TR-FRET) assays

Heterogeneous TR-FRET assay

Cells were transiently transfected at 80-90% confluency in $6cm^2$ dishes. A total of 3μg of DNA per dish was transfected using Lipofectamine™ reagent (Gibco Life Technologies).

The cells were harvested in PBS 48 h after transfection and a sample diluted in PBS/0.5mM EDTA before counting using a haemocytometer. $5x10^5$ cells were incubated with 3nM anti-c-myc-Eu^{3+} antibody and 15nM anti-Flag-APC antibody (unless otherwise stated) for 2 h at room temperature in a 100μl volume. Mixing of samples was performed during the incubation on a rotating wheel. The incubation was performed in 50% Newborn calf serum / PBS. After the incubation the cells were washed with 2 x 1ml of PBS and re-suspended in 30ml PBS before being transferred to a well of a black 384 plate (Nunc). The TR-FRET measurement was performed using a Victor or a victor^2 fluorescence plate reader. The TR-FRET signal being measured after a 50μs delay following excitation of the sample at 320nM for the victor^2 and 340nm for the Victor fluorescence plate reader. Data were collected for 200μs with a cycle time of 1s at both 615nm and 665nm, the emission maxima of Europium and APC respectively.

Homogeneous TR-FRET assay

1-8 x 10^5 cells were incubated in a total volume of 100μl containing 50% Newborn calf serum / PBS and varying concentrations of anti-c-myc-Eu^{3+} and anti- Flag -APC in a 96 well, black maxisorb plate (Nunc). TR-FRET signals were read at 30min intervals for up to 3 h. The TR-FRET measurement was performed in a Victor^2, with a 50μs delay after excitation of the sample at 320nM. Data were collected for 200μs with a cycle time of 1s at both 615nm and 665nm.

Between readings the plate was kept in the dark, at room temperature, with mixing on an orbital plate shaker.

2.5 Other Protocols

2.5.1 Preparation of cell membranes

Plasma membrane containing samples were prepared from frozen cell pastes, which had been stored at -80°C. The cell pellets were resuspended in TE buffer and then ruptured by homogenisation with a hand held Teflon-on-glass homogeniser, followed by passing the sample through a 25 gauge needle 10x. Any non-ruptured cells and cell nuclei were removed by centrifugation at 1200rpm for 10min on a bench top centrifuge at 4°C. The supernatant fraction was removed and further centrifuged at 75,000 rpm for 30min in a Beckman Optima TLX Ultracentrifuge (Palo Alto, CA) with a TLA 100.2 rotor, to pellet the plasma-membranes. The membranes were resuspended in TE and the protein concentration determined after the membranes were passed through a 25 gauge needle 10x to ensure they were in a homogeneous mixture. The membranes were aliquoted and stored at -80°C until required.

2.5.2 Labelling anti-Flag (M5) antibody with cross-linked Allophycocyanin (APC)

1.5mg of anti-Flag (M5) antibody was reduced by the addition of 25µl of 1M DTT and incubating at room temperature for 30min. The reduced antibody was then desalted into 20mM Na_3PO_4, pH 7.5, using a Superdex 200 gel filtration column (Pharmacia) at a flow rate of 1.5ml / min using an FPLC system (Pharmacia). The protein was eluted in 9ml, to this 10µM of SMCC x1 APC was added and the reaction incubated overnight at 4°C during which the SMCC-APC reacts with the free sulfhydryl groups (-SH) generated by the reduction of the protein with DTT. Any unreacted sulphydryl groups on the antibody were blocked by the addition of 100µM N-ethyl maleimide one h at 4°C. Labelled antibody was

separated from unlabelled antibody by gel filtration on a Superdex 200 column, run at 1.5ml / min with in PBS, 0.05% Tween20. The elution profile showed a good separation of the labelled antibody from the free SMCC-APC. The concentration and the labelling ratio were determined by the absorbance at 650nm and 280nm and calculating the concentrations of APC and protein using their respective extinction co-efficients.

2.5.3 Electrophoresis of polyacrylamide gels

Approximately 10μg of protein was loaded per lane of a 15 well 2-20% PAGE gel or 7% Tris-actetate gel (Novex). For the immunoprecipitates 8μl of the total 60μl was run per lane. Tris-acetate running buffer (50mM Tris base, 50mM Tricine, 0.1% SDS, pH8.24) was used for the NuPage Tris-Acetate gels. The samples were then run until the dye front was at the end of the gel, with running conditions of 200 constant volts, which took approximately one hour.

2.5.4 Protein transfer onto membrane

The proteins were then transferred to nitrocellulose using electroblotting. The nitrocellulose was placed next to the gel ensuring there were no air bubbles between them, this was then sandwiched between two pieces of filter paper which had been soaked in transfer buffer, again ensuring no air bubbles were present. This was placed with the nitrocellulose on the anode side of the gel transfer apparatus. The transfer tank was then filed with blotting buffer (20% methanol, 25mM Tris and 192mM Glycine). The protein transfer conditions were 30 constant volts for 1 h.

2.5.5 Incubation with antibodies

Following the transfer of the protein to the nitrocellulose the nitrocellulose was then blocked for one hour with 5% Marvel in PBS/0.1%Tween20. The nitrocellulose was then washed at room temperature for 30min with 3 changes of PBS/ 0.1% Tween20. The nitrocellulose was then incubated for at least 1 hour at room temperature (or overnight at 4°C), with the appropriate primary antibody diluted in 1% Marvel in PBS/ 0.1% Tween20. The nitrocellulose was then washed for 30min at room temperature with PBS/ 0.1% Tween20 for 1 hour to remove any unbound primary antibody with at least 3 changes of PBS/ 0.1% Tween20. The incubation with the peroxidase labelled secondary antibody (diluted 1:4000 in 1%Marvel in PBS/0.1%Tween20), for one hour at room temperature. The excess secondary antibody was removed by washing the nitrocellulose with at least 3 changes of PBS/ 0.1% Tween20. During each wash or antibody incubation step the blot was agitated on an orbital shaker.

1° antibody	dilution	2° antibody	dilution
Anti-Flag (M5)	1:2000	Anti-mouse	1:5,000
Anti-c-myc (9E10)	1:1000	Anti-rabbit	1:10,000
Anti-GFP	1:20,000	Anti-sheep	1:10,000
Anti-β_2AR	1:1000	Anti-rabbit	1:10,000

2.5.6 Enhanced chemi-luminescence

Detection of the bound peroxidase labelled secondary antibody attached to the blot was achieved using an enhanced chemi-luminescence (ECL) kit from Pierce. The nitrocellulose was washed x 3 with PBS/ 0.1% Tween20 before placing on a plastic sheet and covering with a 1:1 mixture of the solutions of the kit, this was incubated for 5min at room temperature before blotting off the excess solution and placing the nitrocellulose between two plastic sheets. A

signal was obtained when a piece of X-ray film was placed over the nitrocellulose for a length of time in the dark room. The film was then developed in an X-omat developer (Kodak).

2.5.7 Immunoprecipitation

To prepare cell lysates suitable for immunoprecipitation, transfected HEK293 cells were washed 3x with PBS before harvesting and resuspending in 1x RIPA buffer (unless otherwise stated). The cell suspensions were then placed on a rotating wheel in eppendorfs for one h at 4°C. The 2 x RIPA buffer was made as a stock and stored at 4°C until required. On the day of the cell lysis the 1x RIPA buffer was prepared. The composition of the buffers was as follows:

2 x RIPA buffer

component	concentration
Hepes pH7.5	100mM
NaCl	300mM
TX100	2% ($^{W}/_{V}$)
Na-deoxycholate	1% ($^{W}/_{V}$)
SDS	0.2% ($^{W}/_{V}$)

1x RIPA buffer

	Volume	Final concentration
2x RIPA	25ml	1x
NaF (0.5M)	1ml	10mM
EDTA(0.5M; pH 8)	0.5ml	5mM
Na phosphate (0.1M)	5ml	10mM
ethylene glycol	2.5ml	5%
protease inhibitor cocktail (25x)	800µl	1x
H_20	15.2ml	
Total volume	**50ml**	

Immunoprecipitation

Any unlysed cells and large cell debris were removed by centrifugation on a bench top centrifuge at 13,000 rpm for 10min at 4°C. The supernatant was then taken and the protein concentration determined using the BCA assay. This supernatant was referred to as the cell lysate.

500µg of protein of each sample was removed and the volume made to 800µl with 1x RIPA buffer. To this 20µl of protein-G sepharose resin, (40µl of a 1:1 solution of resin : RIPA) which had been equilibrated in RIPA, was added. The assay tubes were then place this back on the rotating wheel at 4°C for one h, this was to remove any proteins that bound to the protein-G sepharose non-specifically.

The protein-G sepharose was pelleted with a 15 s spin in a bench top centrifuge, the cell lysate was removed and added to a fresh eppendorf containing a further

20µl of protein-G sepharose which had been pre-equilibrated with the antibody to be used for the immuno-precipitation. 2µg of A14 anti-myc anti-body or anti-β_2AR antibody or 8.6µg of anti-Flag (M5) antibody was used per sample. The cell lysate / antibody / protein-G sepharose mixture was incubated overnight at 4°C on a rotating wheel.

The resin was pelleted with a 15 s spin in a bench top centrifuge and the supernatant was then removed and discarded. The protein-G sepharose was then washed 3 x 1ml of RIPA buffer before the addition of 60µl of reducing sample buffer. The resin was agitated every 15 min to help the dissociation of the proteins from the protein-G sepharose. After 1 h at room temperature the sample was heated to 85°C for 4min before running on 7% Tris-acetate gels. 8µl of the immunorecipitate was loaded into each well of the 15 well gels.

The other buffers used to generate cell lysates before immunoprecipitation were as follows:-

1% TX100 buffer

component	concentration
Tris-Cl pH7.4	50mM
NaCl	300mM
TX-100	1% ($^{w}/_{v}$)
Glycerol	10% ($^{w}/_{v}$)
$MgCl_2$	1.5mM
$CaCl_2$	1mM

1% NP40 buffer

component	concentration
Tris-Cl pH8	50mM
NaCl	120mM
NaF	20mM
Na-pyrophosphate	10mM
EDTA	1mM
EGTA	5mM
NP40	1% ($^{v}/_{v}$)

0.5 % CHAPS buffer

component	concentration
Tris-Cl pH7.4	50mM
NaCl	300mM
CHAPS	0.5% ($^{w}/_{v}$)
Glycerol	10% ($^{w}/_{v}$)
$MgCl_2$	1.5mM
$CaCl_2$	1mM

2%SDS buffer

component	concentration
Tris-Cl pH8	50mM
2% SDS	2% ($^{w}/_{v}$)
NaCl	300mM

Tween20 buffer

component	concentration
Tris-Cl pH7.4	50mM
NaCl	300mM
Tween20	1% ($^{w}/_{v}$)
Glycerol	10% ($^{w}/_{v}$)
$MgCl_2$	1.5mM
$CaCl_2$	1mM

2.5.8 Confocal Imaging

HEK293 cells which had been stably transfected with Flag-δOR-GFP were plated onto sterile glass coverslips 24 h before examination using a Zeiss Axiovert 100 laser scanning confocal microscope with a Zeiss Plan-apo 63 x 1.4 NA oil immersion objective. Experiments were performed in a coverslip chamber in Krebs Ringers Hepes (KRH) buffer (pH7.4) at 37°C. Cells were excited at a wavelength of 488nm and detected with a 515 - 540nm band pass filter. Images were taken at various time-points following the addition of 1μM DADLE.

CHAPTER 3

Investigation of homo and heterodimerization of epitope tagged δORs using co-immunoprecipitation

CHAPTER 3

An investigation of homo and heterodimerization of epitope tagged δORs using co-immunoprecipitation

3.1 Introduction

By using SDS-PAGE, western blotting techniques and co-immunoprecipitation, GPCR monomers, dimers and oligomers in membranes of both native tissue and of heterologous cells transfected with GPCRs have been identified. Examples include the adenosine A1 receptor, which has been identified as homodimers in pig brain cortical membranes as well as from rat tissues and as heterodimers with the dopamine D1 receptor in co-transfected heterologous cells and in neuronal primary cultures (Franco et al., 2000). The dopamine D3 receptor forms dimers and tetramers in both brain and in transfected cells (Nimchinsky et al., 1997) as does the muscarinic m3 receptor in various brain regions as demonstrated by Avissar et al. (1983) using a photoaffinity agent.

SDS-PAGE, a technique described by Laemmli (1970), has been used to separate proteins according to their molecular mass. Generally proteins are resolved to their respective monomers however, some non-covalent interactions between proteins still remain allowing identification of higher molecular weight forms. The involvement of di-sulphide bonds in protein-protein interaction can be demonstrated by the addition of a reducing agent, usually dithiothreitol or 2-mercaptoethanol. A differential pattern of GPCR bands in the presence and absence of reducing agent indicates the importance of di-sulphide interaction between receptors for the κOR homodimers (Jordan and Devi, 1999) and the muscarinic m3 homodimers (Zeng and Wess, 1999). The family 3 receptors metabotropic glutamate receptor-1 (Romano et al., 1996) and the Ca^{2+} receptor (Fan et al., 1998) demonstrate the di-sulphide interaction to be vital for their dimerization.

Di-sulphide bonds are not the only interaction responsible for GPCR dimerization as several studies have also shown the presence of dimeric and multimeric receptor species in the presence of reducing agents. Hebert et al. (1996) demonstrated β_2AR homodimerization under non-reducing conditions but also stated that inclusion of reducing agents did not lead to monomerization of this receptor. The same was true for the dopamine D3 receptors from brain and in transfected cells (Nimchinsky et al., 1997).

Other possible protein-protein interactions are not easily determined by SDS-PAGE as shown by the somatostatin SST2A-SST3 heterodimers which were resistant to reducing agents but sensitive to high detergent concentrations. This suggests that dimerization involves non-covalent hydrophobic interactions between the receptors. Again this is not always the case as Hebert et al. (1996) stated that β_2AR homodimers were stable at high (10%) concentrations of SDS. Protein dimers that are resistant to SDS are not only limited to GPCRs as other proteins e.g. the α and β subunits of the major histocompatibility complex form an SDS-resistant dimer (Caplan et al., 2000).

As non-covalent interactions can be disrupted using SDS-PAGE the initial use of chemical cross-linkers to stabilize dimeric or oligomeric interactions present has been widely used. These cross-linkers are small molecules that will covalently interact with two molecules in close proximity. Hydrophilic cross-linkers exist e.g. 3,3'-Dithiobis[sulfosuccinimidyl propionate], (DTSSP), which are membrane impermeable and cross-link via cell-surface residues only. Hydrophobic cross-linkers e.g. Dithiobis[succinimidyl propionate], (DSP), can cross the lipid bilayer and cross-link via internal residues or with residues within the membrane itself. Cross-linkers can be useful to identify interactions between proteins and the different type of cross-linkers can indicate where these interactions take place although care has to be taken to ensure that the cross-linking is only between two interacting molecules and that spurious results do not occur (Fancy and Kodadek,1999).

Chemical cross-linking has been employed to confirm the presence of β_2AR (Hebert et al., 1996), δOR (Cvejic and Devi, 1997), dopamine D2 (Ng et al., 1996) and chemokine receptor CXCR4 homodimers (Vila-coro et al., 1999) as well as δOR-κOR heterodimers (Jordan and Devi, 1997). Chemokine receptor CCR2 dimerization on activation by its ligand was stabilized by chemical cross-linking (Rodríguez-Frade et al., 1999) as was the chemokine receptor CCR5 dimerization induced by its agonist (Vila-Coro et al., 2000).

Co-immunoprecipitation is useful in the identification of GPCR homodimers which cannot be identified by investigation of their respective pharmacology. The use of specific antibodies for the individual receptors permitted identification of heterodimeric complexes between the wild-type dopamine D3 receptor and a mutant form of the receptor (D3nf), (Nimchinsky et al., 1997). As it is not possible to use specific antibodies to distinguish the respective partners in homodimeric receptors, co-expression of differentially tagged receptors has been used therefore to identify homodimers. This technique has been used to identfy δOR homodimers (Cvejic and Devi, 1997), β_2AR homodimers (Hebert et al., 1996) and SST2A and SST3 homodimers as well as heterodimers (Pfeiffer et al., 2001).

For ease of immunodetection and detection of homodimer and heterodimer species using co-immunoprecipitation the human δOR was Flag- or c-myc-epitope tagged on the N-terminus by PCR. To assess the internalization of the Flag-δOR receptor, GFP was fused to its C-terminus. Radiolabelled antagonist binding and high affinity GTPase assays were used to monitor expression and activation of these receptors following transient transfection. Cell lines that stably express the Flag-δOR and Flag-δOR-GFP were established and intact cell adenylyl cyclase assays used to determine their signalling capacity. Co-immunoprecipitation of Flag and c-myc-tagged receptors was used to investigate homodimerization. A variety of conditions were used to elucidate the specificity of interaction co-immunoprecipitation of the c-myc-tagged δOR with other Flag-tagged GPCRs.

3.2 Results

Construction and expression of human δOR with an N-terminal Flag or c-myc tag and N-terminally Flag tagged δOR with a C-terminal GFP.

A PCR strategy was used to incorporate the Flag epitope (Asp-Tyr-Lys-Asp-Asp-Asp-Asp-Lys) or the c-myc epitope (Glu-Gln-Lys-Leu-Ile-Ser-Glu-Glu-Asp-Leu) at the N-terminus of the human δOR as described in section 2.3.4. A schematic representation of these constructs is shown in figure 3.1. Transient transfection of 10μg of each construct into HEK293 cells resulted in expression levels of 887 ± 262 fmol/mg and 731 ± 143 fmol/mg for the Flag-δOR and the c-myc-δOR respectively (figure 3.2). Wild type δOR resulted in an expression level of 3095 ± 1470 fmol/mg after transient transfection of 10μg of DNA into HEK293 cells.

Incorporation of a modified form of GFP from *Aequorea victoria* with enhanced autofluorescence properties (Zernicka-Goetz et al., 1997) onto the C-terminus of the cDNAs of both the Flag and c-myc-tagged forms of the human δOR was also performed using a PCR-based strategy (section 2.3.4). These fusion proteins encode single open reading frames in which the C-terminus of the δOR was linked directly to the N-terminus of the GFP after removal of the stop codon of the receptor (figure 3.1). Transient transfection of 10μg of each DNA was performed in HEK293 cells and resulted in expression levels of 530 ± 240 and 469 ± 234 fmol/mg for the Flag-δOR-GFP and the c-myc-δOR-GFP respectively (figure 3.2).

Signalling capacity of N-terminally tagged δOR receptors with and without a C-terminal GFP

The signalling capacity of transiently expressed receptors was assessed by measurement of agonist stimulated high affinity GTPase activity. The level of GTPase activity over basal is shown in figure 3.3. Flag-δOR and c-myc-δOR demonstrated 17.5% ± 6.8% and 35.6% ± 8% increase respectively in GTPase

activity over basal. Flag-δOR-GFP and c-myc-δOR-GFP showed 7.6% ± 6.1% and 9.6% ± 7% agonist induced increase in GTPase activity over the basal respectively. Wild type δOR gave an increase over basal GTPase activity of 51% ± 6.

Production of HEK293 clones which stably express Flag-δOR or Flag-δOR-GFP and assessment of their expression and functionality

HEK293 cells were stably transfected with Flag-δOR or Flag-δOR-GFP and receptor expression level was assessed using [^{3}H]naltrindole binding at a single concentration (5nM) of the radiolabelled antagonist in intact cells. The receptor expression level of the clones was assessed and is shown in figure 3.4. The signalling capacity of the clones stably expressing the receptors was measured in the presence of 1μM of the δOR agonist DADLE. Direct stimulation of the adenylyl cyclase was achieved by including 50μM forskolin in the assay mix, which stimulated the adenylyl cyclase activity resulting in elevated cAMP levels. Inhibition of the cAMP levels was evident as the receptor was functioning via a Gαi-family G-protein. The inhibition of the adenylyl cyclase activity for the stable clones tested is shown in figure 3.5.

Clone F28 expressing Flag-δOR and clone FG6 expressing the Flag-δOR-GFP were chosen and used in further work. Antagonist saturation binding studies were performed on clone F28 cells with up to 8nM [^{3}H]naltrindole (figure 3.6A). The data were transformed and plotted as a Scatchard plot (figure 3.6 B). A dissociation constant (K_d) of 1.38 ± 0.47 nM for the Flag-δOR was calculated and the maximum receptor level obtained (Bmax) for Flag-δOR was 20.36 ± 3.87 pmol/mg protein.

The signalling capacity of the stable clones was further assessed using a dose-response to DADLE and its effect on the forskolin stimulated levels of cAMP (figure 3.7). The EC_{50} for the Flag-δOR and Flag-δOR-GFP was 0.02nM ± 0.009 and 0.02nM ± 0.011 respectively. This demonstrated that the addition of the GFP to the C terminus of the receptor did not eliminate its ability to inhibit adenylyl

cyclase, as there was no statistically significant difference in the EC_{50}'s observed ($p > 0.05$).

Internalisation of the Flag-δOR-GFP was followed in real time using confocal microscopy, after the addition of 100nM DADLE, to live cells. A punctate pattern of GFP fluorescence was observed within the cells 5 min after agonist stimulation (figure 3.8). This agrees with the internalisation rate observed by Chu et al. (1997) where the $t_{½}$ was shown to be <10 minutes. This demonstrated that the addition of GFP at the C terminus of this receptor did not prevent internalisation of the receptor.

Immunodetection of Flag and c-myc-tagged δOR with and without GFP

Immunodetection of Flag-δOR and c-myc-δOR with and without the C-terminal GFP was performed and shown in figures 3.9A and B respectively. Membranes of transiently transfected HEK293 cells were resolved using SDS-PAGE and electro-blotted onto nitrocellulose before immunoblotting with anti-Flag and anti-c-myc-antibodies respectively. δOR receptor migrated at 60 kDa with another band running at 35kDa. δOR-GFP migrated at 100 kDa with another band at 60kDa. Higher molecular weight species that may represent dimers and oligomers of the receptors were also observed (figures 3.9A and B).

Constitutive δOR homodimers are detected by co-immunoprecipitation

Following transient expression of either form of the receptor in HEK293 cells these could be immunoprecipitated with appropriate anti-c-myc (figure 3.10A) or anti-Flag antibodies (figure 3.10B). No immunoprecipitation was observed, however, when the antibody/epitope-tagged GPCR combinations were reversed, confirming the specificity of immunoprecipitation (Figure 3.10A and 3.10B).

Immunoblotting of SDS-PAGE resolved membrane fractions expressing the c-myc-tagged δ-opioid receptor with the anti-c-myc antibody resulted in detection of a 60 kDa polypeptide (figure 3.10A). Such a polypeptide was not detected by

the anti-c-myc antibody in membranes expressing the Flag-tagged form of the receptor (figure 3.10A) which confirmed the specificity of immunodetection with the anti-c-myc antibody. Similarly the anti-Flag antibody specifically recognised the Flag-δOR when expressed in membrane fractions (figure 3.10B). Co-expression of the c-myc and the Flag epitope-tagged forms of the δOR, followed by immunoprecipitation with the anti-Flag antibody and immunoblotting with the anti-c-myc antibody also resulted in detection of the 60 kDa c-myc-tagged δ opioid receptor (Figure 3.10A). Equivalent results were obtained when the protocol was reversed and immunoprecipitation of cells co-expressing the two epitope-tagged forms of the δopioid receptor was performed with the anti-c-myc antibody followed by immunoblotting with the anti-Flag antibody (figure 3.10B). However, expression of either the c-myc or Flag-tagged δOR alone failed to result in detection of the 60 kDa polypeptide using either of these two protocols (Figures 3.10A and 3.10B). Such results confirm previous data on the ability to detect homo-oligomers of co-expressed but differentially tagged forms the δ-opioid receptor (Cvejic and Devi, 1997).

Separate expression of the c-myc and the Flag epitope-tagged forms of the δ-opioid receptor followed by physical mixing of cell lysates prior to immunoprecipitation with either antibody also failed to result in co-immunoprecipitation of the two forms of the receptor (figure 3.10c). Immunoprecipitation of δOR resulted in the detection of co-transfected c-myc-δOR with GFP fused at its C-terminus (figure 3.10c).

Effect of ligands on co-immunoprecipitation of the δOR

Cvejic and Devi (1997) demonstrated via cross-linking, that agonists decreased the level of δOR homodimerization whereas antagonists had no effect. An attempt to repeat these results was unsuccessful as after cross-linking with DSP the receptors did not resolve on SDS-PAGE or Tris-Borate gels (data not shown).

The effect of ligands was then investigated using the co-immunoprecipitation technique described above in the absence of cross-linkers, in the presence of ligand. HEK293 cells transiently transfected with c-myc-δOR and Flag-δOR were incubated with a final concentration of 100nM of either the agonist DADLE (figure 3.11) or the antagonist naltrindole (figure 3.12) before production of the cell lysates prior to immunoprecipitation. Immunodetection was performed with anti-c-myc antibody after immunoprecipitation with anti-Flag antibody (figures 3.11 and 3.12). No effect of either ligand was demonstrated on the monomeric and potential dimeric δORs identified.

Heterodimerization between δOR and other GPCRs can be detected by co-immunoprecipitation

Heterodimerization between δOR and other GPCRs was investigated using the co-immunoprecipitation technique described above. Immunoprecipition was performed with anti-Flag antibody and immunodetection with anti-c-myc antibody (figure 3.14, lanes 1-5). Immunoprecipitation with anti-c-myc antibody and detection with anti-Flag antibody (figure 3.13, lanes 7-11) was also performed. In each case, equal amounts of DNA for each construct were transiently transfected into the HEK293 cells. The Flag-tagged receptors co-transfected were the IP prostanoid receptor-GFP (figure 3.13, lanes 5 and 11), the IP prostanoid receptor (figure 3.13, lanes 4 and 10), the β_1AR-GFP (lanes 3 and 9) and the β_2AR-GFP (lanes 2 and 8). Co-immunoprecipitation between c-myc-δOR and Flag-β_1AR-GFP, c-myc-δOR and Flag-β_2AR-GFP and between c-myc-δOR and Flag-IP prostanoid receptor-GFP (figure 3.13) was observed. Co-immunoprecipitation of c-myc-δOR with Flag-IP prostanoid receptor was not observed (figure 3.13). Immunoprecipitation with anti-c-myc antibody and detection with anti-Flag antibody revealed potential dimeric forms of Flag-δOR receptor (figure 3.13).

Constitutive heterodimerization between the δOR and the closely related μOR was established on transient transfection of HEK293 cells with c-myc-δOR and Flag-μOR prior to co-immunoprecipitation experiments. Immunoprecipitation was

performed with anti-Flag antibody and immunodetection with anti-c-myc-antibody. Monomeric and potential dimeric forms of the c-myc-δOR were identified (figure 3.14). George et al., (2000) and Gomes et al., (2000) have since confirmed the interaction between these two opioid receptor subtypes.

When the c-myc-tagged δ-opioid receptor was co-expressed along with the human β_2-adrenoceptor, co-immunoprecipitation experiments akin to those described above but now using combinations of the anti-c-myc antibody and an anti-β_2-adrenoceptor antibody, were able to provide evidence for the presence of hetero-interactions between these two GPCRs (figure 3.15). Immunoprecipitation of the β_2-adrenoceptor resulted in the presence of the c-myc-tagged δ-opioid receptor in the precipitated sample, which could be detected by immunoblotting following resolution of the sample by SDS-PAGE. A second polypeptide with mobility consistent with a dimer containing the c-myc-tagged δ-opioid receptor was also detected (figure 3.15). Neither of these bands was detected when the human β_2-adrenoceptor was expressed in the absence of the c-myc-tagged δ-opioid receptor and then immunoprecipitated (figure 3.15). Equivalent results were obtained when the c-myc-tagged δ-opioid receptor was co-expressed with a form of the β_2-adrenoceptor that had been C-terminally tagged with enhanced yellow fluorescent protein (eYFP) or with a form of the β_2-adrenoceptor tagged at the N-terminus with the Flag epitope and at the C-terminus with green fluorescent protein (GFP) (figure 3.15). Immunoprecipitation of either of these modified forms of the β_2-adrenoceptor resulted in co-precipitation of the c-myc-tagged δ-opioid receptor and detection of both monomeric and potential dimeric species. These rather unexpected observations led us to consider whether such co-immunoprecipitation approaches following transient transfection of cells might produce artefactual results following solubilization of GPCRs from the membrane environment, a concept which was investigated further.

Co-immunoprecipitation of human δOR with β_2AR

The solubilization conditions used to release the receptors from the membrane environment were investigated to ensure the lysis conditions used were not responsible for the homo and hetero-interactions found. Co-immunoprecipitation of the c-myc-δOR with Flag-δOR or with the Flag-β_2AR-GFP was performed on cell lysates that had been prepared using a range of solubilization buffers. Constitutive δOR homodimerization was indicated by immunoprecipitatation of the Flag-δOR, immunodetecting with anti-c-myc-antibody as well as immunoprecipitation with anti-c-myc-antibody with detection by anti-Flag antibody (figure 3.16A and B). Constitutive heterodimerization of c-myc-δOR with Flag-β_2AR-GFP was indicated under the same combination of immunoprecipitation and imunodetection conditions (figure 3.16A and B). The solubilization buffers which gave successful co-immunoprecipitations contained either 1% TX100, 1% NP40 or 0.5% CHAPS. The solubilization buffer containing 1% Tween20 did not indicate the presence of any homo or heterodimers. 2% SDS showed heterodimerization of δOR with Flag-β_2AR-GFP when immunoprecipitating with anti-c-myc antibody and detecting with anti-Flag antibody (Figure 3.16A, lane 3). The 2% SDS solubilization buffer did not indicate corresponding heterodimerization when immunodetection was with anti-c-myc antibody after immunoprecipitation with anti-Flag antibody (figure 3.16B, lane 3) The 2% SDS containing solubilization buffer did not indicate the presence of any δOR homodimers (figures 3.16A and B). The CHAPS containing solubilization buffer was able to indicate homodimers of δORs. Heterodimerization between the c-myc-δOR and Flag-β_2AR-GFP (figure 3.16A) was also indicated. However, heterodimerization between c-myc-δOR and Flag-β_2AR-GFP when immunoprecipitated with anti-Flag antibody did not reveal any c-myc-δOR (Figure 3.16B).

Figure 3.1 Schematic representation of Flag-δOR, c-myc-δOR, Flag-δOR-GFP and c-myc-δOR-GFP

Homologous primers allowed the introduction of A) Flag and B) c-myc epitopes at the N-terminus of the δOR preceeded by an *Apa*I restriction site and an *Xba*I site at the C-terminus to permit sub-cloning into pcDNA3.1(-). GFP was amplified using PCR to introduce an *Xba*I site at either end permitting ligation to the C-terminus of the receptor constructs C). The orientation of the resulting DNA was determined by digestion of these constructs with *Xba*I and *Eco*R1.

A

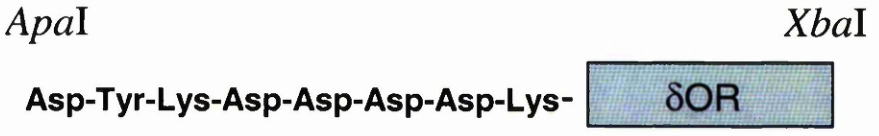

B

C

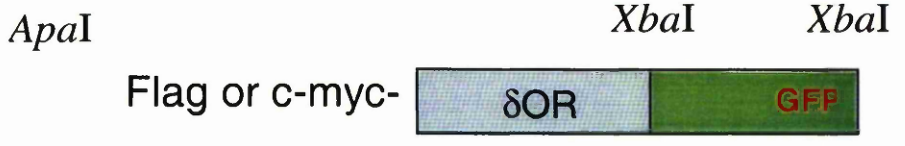

Figure 3.2 Estimation of δOR expression levels in membranes of HEK293 cells after transient transfection using a single concentration of [^{3}H]diprenorphine

The specific binding of [^{3}H]diprenorphine to membranes of HEK293 cells which had either been mock transfected or transiently transfected with δORs was assessed. Non-specific binding was determined in the presence of 300μM naloxone. The specific [^{3}H]diprenorphine binding was obtained by subtraction of the non-specific binding from the total binding. The specific binding was expressed as fmol of [^{3}H]diprenorphine bound per mg membrane protein. [^{3}H]diprenorphine specific binding presented are the mean ± S.E.M. of three independent experiments performed in triplicate.

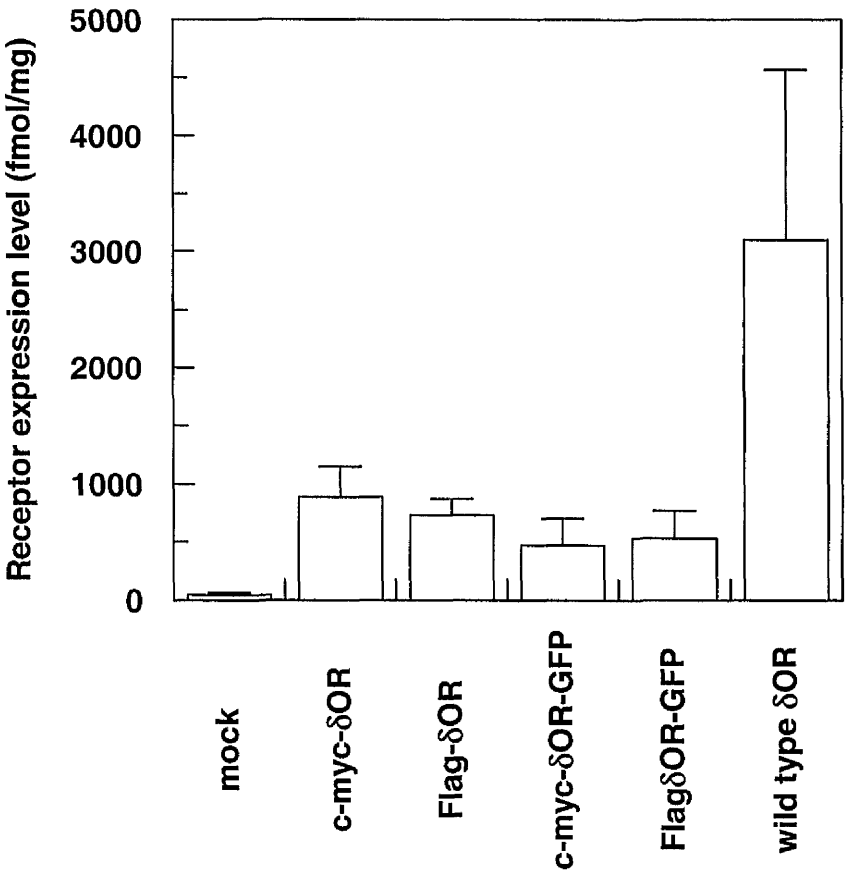

Figure 3.3 High affinity GTPase activity of transiently transfected δOR constructs.

The DADLE-stimulated (1μM) high affinity GTPase activity of membranes of HEK293 cells, which had been either mock transfected or transiently transfected with δOR constructs was assessed. Basal, non-specific and DADLE-stimulated GTPase were calculated. The percentage increase over basal is shown and is the mean ± S.E.M. for 5 independent experiments performed in triplicate.

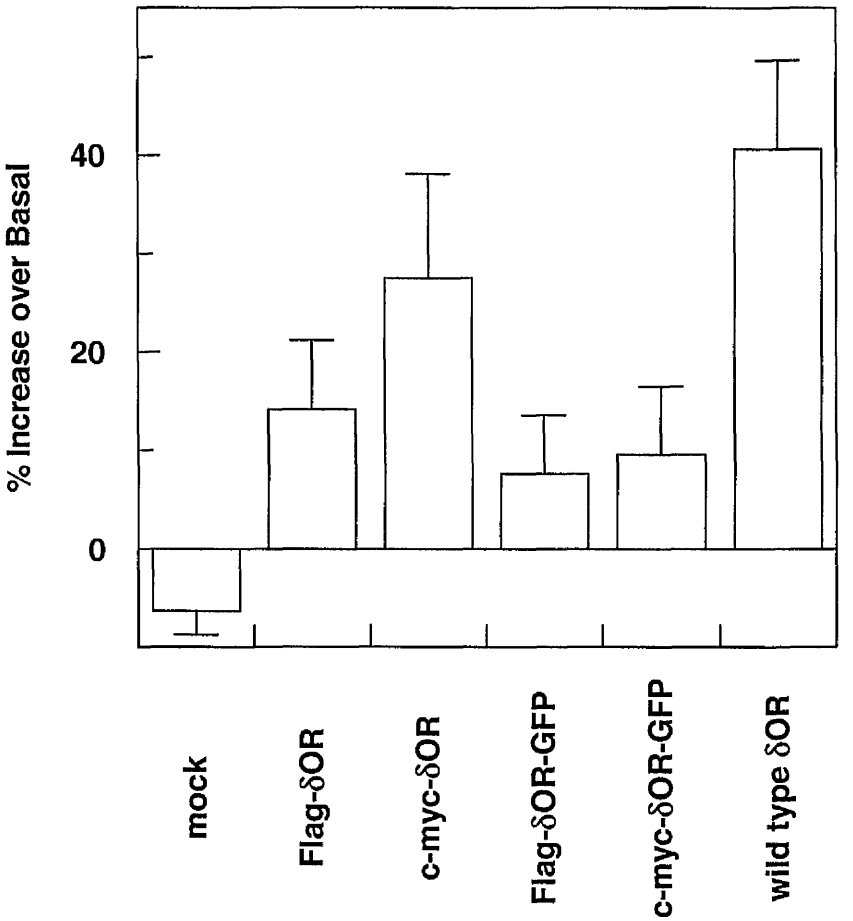

Figure 3.4 Intact cell [^{3}H]naltrindole binding on stable cell lines expressing Flag-δOR or Flag-δOR-GFP.

Whole cell binding experiments were performed on the stable clones expressing Flag-δOR or Flag-δOR-GFP. The specific [^{3}H]naltrindole binding was assessed by subtracting the non-specific binding (determined in the presence of 300μM naloxone) from the total binding. The specific binding is expressed as receptor number per cell x 1000). This graph is a typical representation of two independent experiments performed in triplicate.

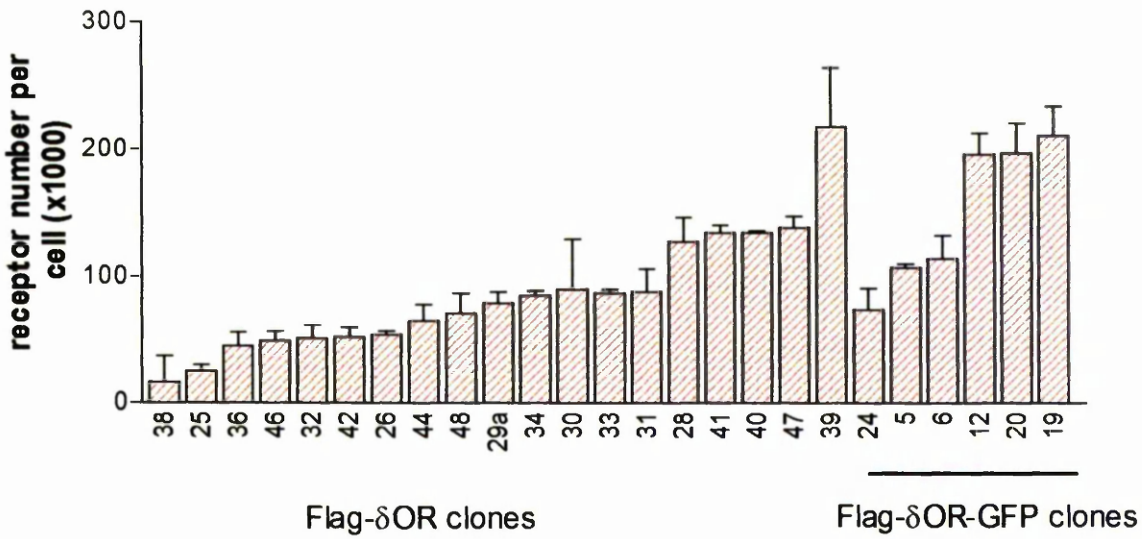

Figure 3.5 Intact cell adenylyl cyclase activity of δOR stable cell lines in the presence of 1μM DADLE and 50μM forskolin

Stable clones expressing Flag-δOR or Flag-δOR-GFP were assessed for their ability to inhibit adenylyl cyclase activity after stimulation by 1μM DADLE. The inhibition was measured in the presence of 50μM forskolin, which stimulates adenylyl cyclase resulting in increased levels of cAMP. The data are the percentage decrease of the forskolin stimulation. This graph is a typical representation of two independent experiments performed in triplicate.

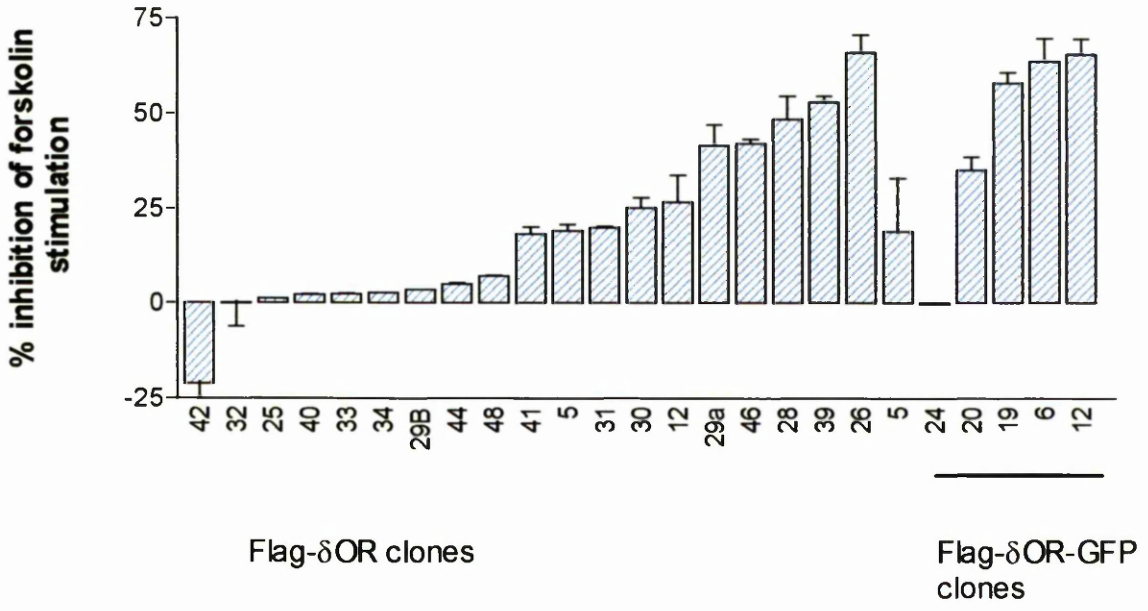

Figure 3.6 Determination of K_d and B_{max} of stable clone F28 expressing Flag-δOR in HEK293 cells

A) Saturation binding performed on membranes of clone F28 cells, with increasing concentrations of [^{3}H]naltrindole. Non-specific binding was determined at each data point in the presence of 300μM naloxone. B) Transformation of the specific binding data to generate a Scatchard plot. The data shown here are a representative experiment, which was performed on two individual occasions.

A)

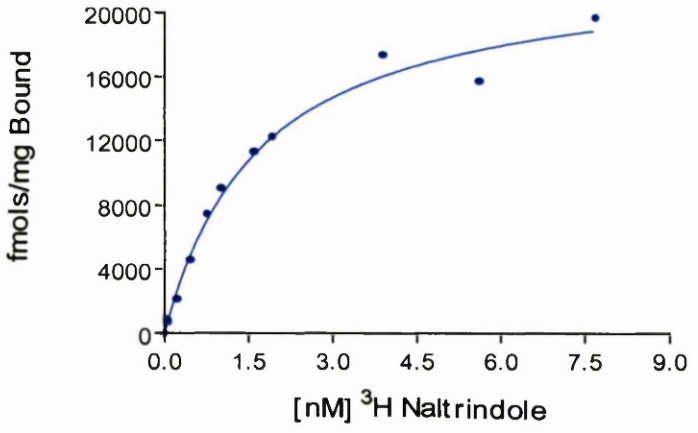

B)

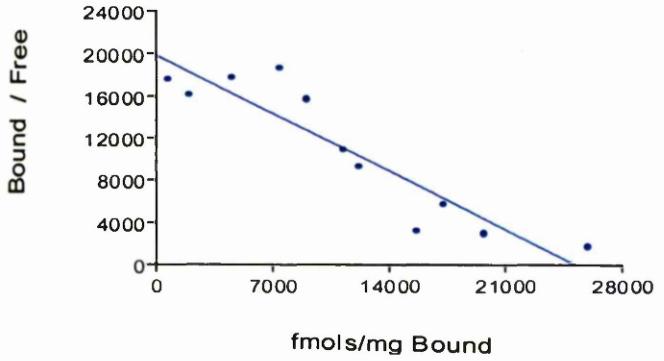

Figure 3.7 Adenylyl cyclase activity dose response to DADLE in stable cell lines after stimulation of the cells with forskolin.

HEK293 cells which were stably transfected with Flag-δOR (clone 28) or Flag-δOR-GFP (clone 6) were assessed for their ability to inhibit forskolin stimulated adenylyl cyclase activity in the presence of increasing concentrations of DADLE. The results are presented as the percentage of the forskolin stimulation. IC_{50} was determined as 0.02nM ± 0.009 for Flag-δOR and 0.02nM ± 0.011 for Flag-δOR-GFP. Data are the mean ± S.E.M. of three independent experiments performed in triplicate. Statistical analysis has shown there to be no significant difference between these IC50's ($p > 0.05$)

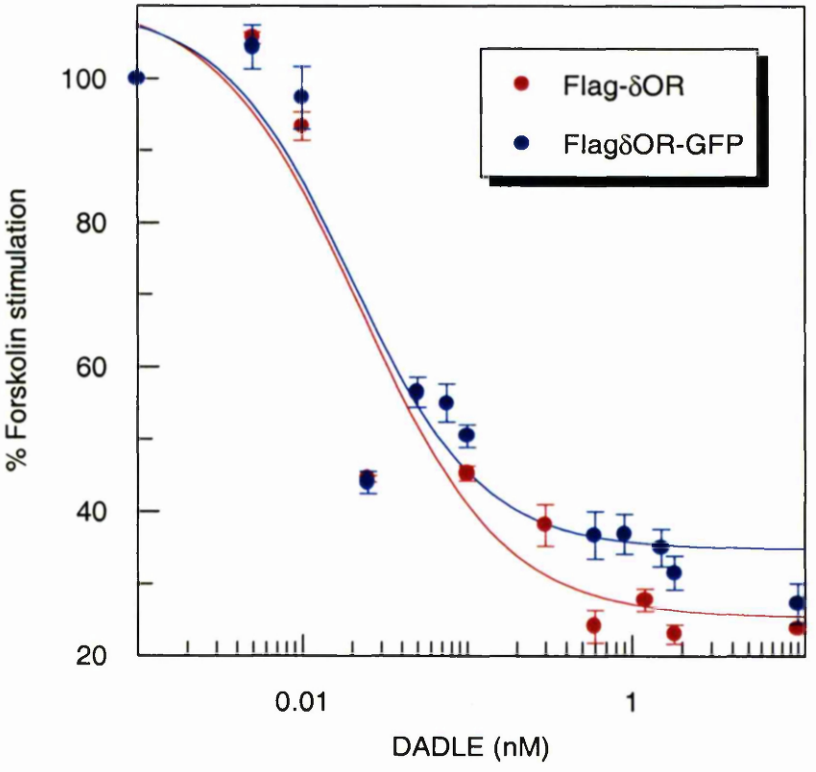

Figure 3.8 Internalisation of Flag-δOR-GFP in real time after stimulation with 100nM DADLE

Clone FG6 cells were plated onto glass coverslips 24 hours before examination using a Zeiss Axiovert 100 laser scanning confocal microscope with a Zeiss Plan-apo 63 x 1.4 NA oil immersion objective. Experiments were performed in a coverslip chamber in Krebs Ringers Hepes (KRH) buffer (pH7.4) at 37°C. Cells were excited at a wavelength of 488nm and detected with a 515-540nm band pass filter. Images were taken at A) 0, B) 5, C) 10 and D) 30min following the addition of 100nM DADLE. The pictures shown are a representative sample of the experiment performed at least three times.

A)

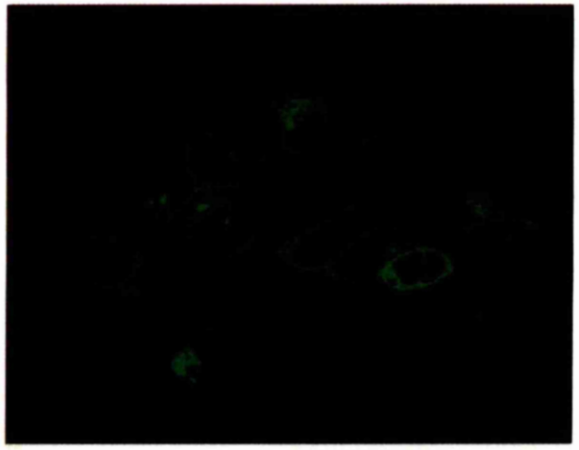

C)

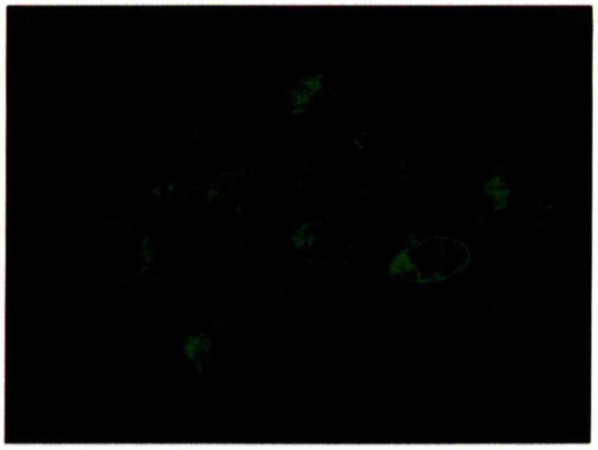

B)

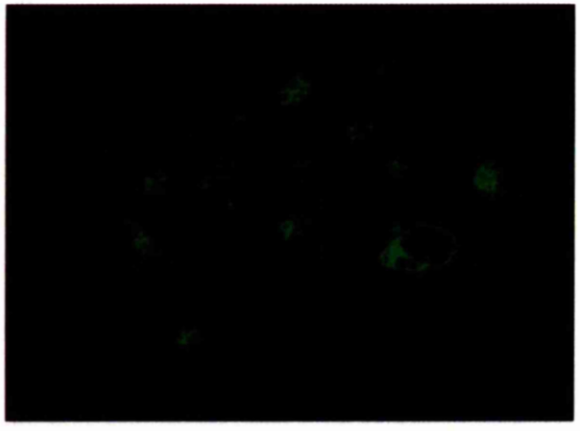

D)

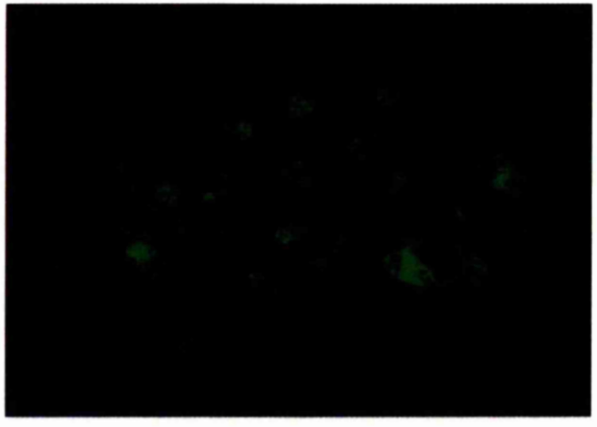

Figure 3.9 Immunodetection of transiently transfected N-terminally epitope tagged δORs

SDS-PAGE resolved membrane proteins of HEK293 cells transiently transfected with N-terminally tagged δORs were electro-eluted onto nitrocellulose before immunodetection with A) anti-Flag and B) anti-c-myc antibodies. Flag-δOR and c-myc-δOR bands were evident at 60kDa with another band evident at 35 kDa. Flag-δOR-GFP and c-myc-δOR-GFP were evident at 100Kda with another band running at 55kDa.

3.9 A)

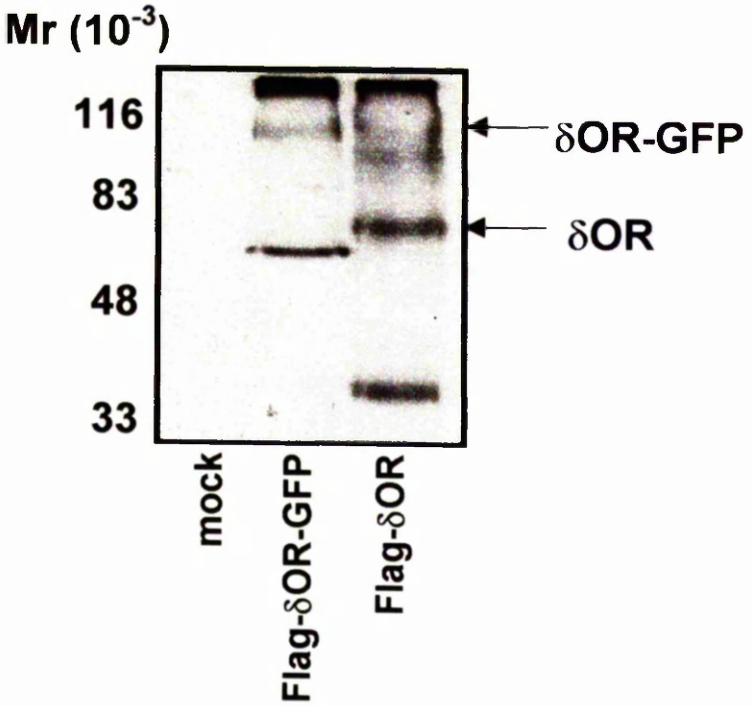
Mr (10^{-3})
116
83
48
33
δOR-GFP
δOR
mock
Flag-δOR-GFP
Flag-δOR

3.9 B)

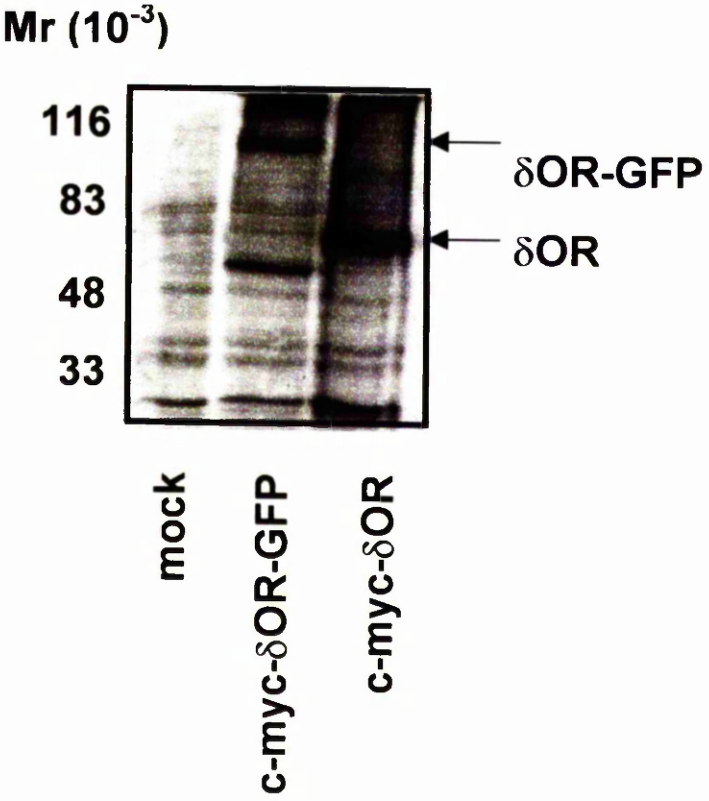
Mr (10^{-3})
116
83
48
33
δOR-GFP
δOR
mock
c-myc-δOR-GFP
c-myc-δOR

Figure 3.10 Detection of constitutive δOR homodimers by co-immunoprecipitation.

500μg of cell lysate from HEK293 cells transfected with both Flag-δOR and c-myc-δOR (lane 3 in A and B, lane 1 in C). Flag-δOR only (lane A4 and B1) or c-myc-δOR only (lane A5 and B2). In figure C, lane 2 Flag-δOR and c-myc-δOR-GFP receptors were co-expressed. In figure c, lane 3 a mixture of cell lysates from cells transfected with either Flag-δOR or c-myc-δOR.

In A and C immunoprecipitation was performed with anti-Flag antibody and immunodetection with anti-c-myc-antibody, in B immunoprecipitation was with anti-c-myc-antibody and immunodetection with anti-Flag antibody.

Cell membranes of HEK293 cells transiently transfected with c-myc-δOR (lanes A1 and B4) or Flag-δOR (lane A2 and B5). Immunodetection was performed with anti-c-myc-antibody. The blot shown here is representative of experiments which were performed at least three times.

3.10 A)

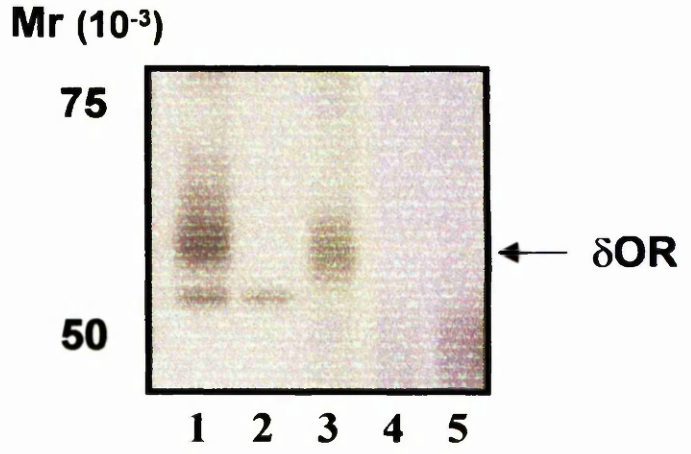

3.10 B)

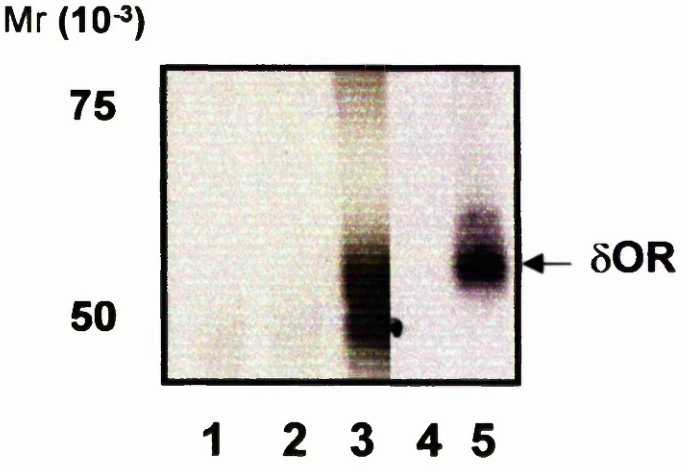

3.10 C)

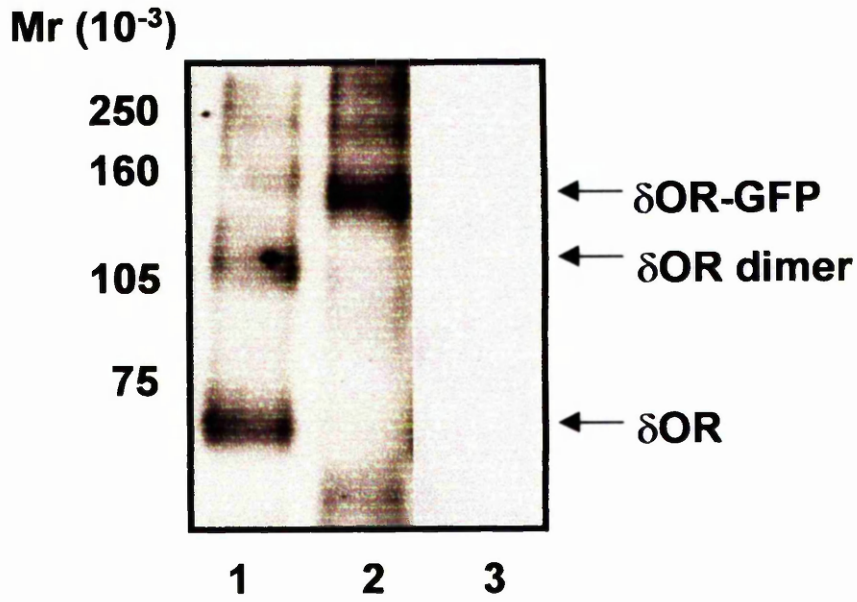

Figure 3.11 Lack of effect of DADLE on constitutive homodimerization of δORs, detected by co-immunoprecipitation

HEK293 cells transiently transfected with both Flag-δOR and c-myc-δOR were incubated in the presence of 100nM DADLE for the times indicated, 500μg of cell lysate was then immunoprecipitated with anti-Flag antibody, followed by immunodetection with anti-c-myc antibody. The data presented here are a representative immunoblot of experiments that were performed three times.

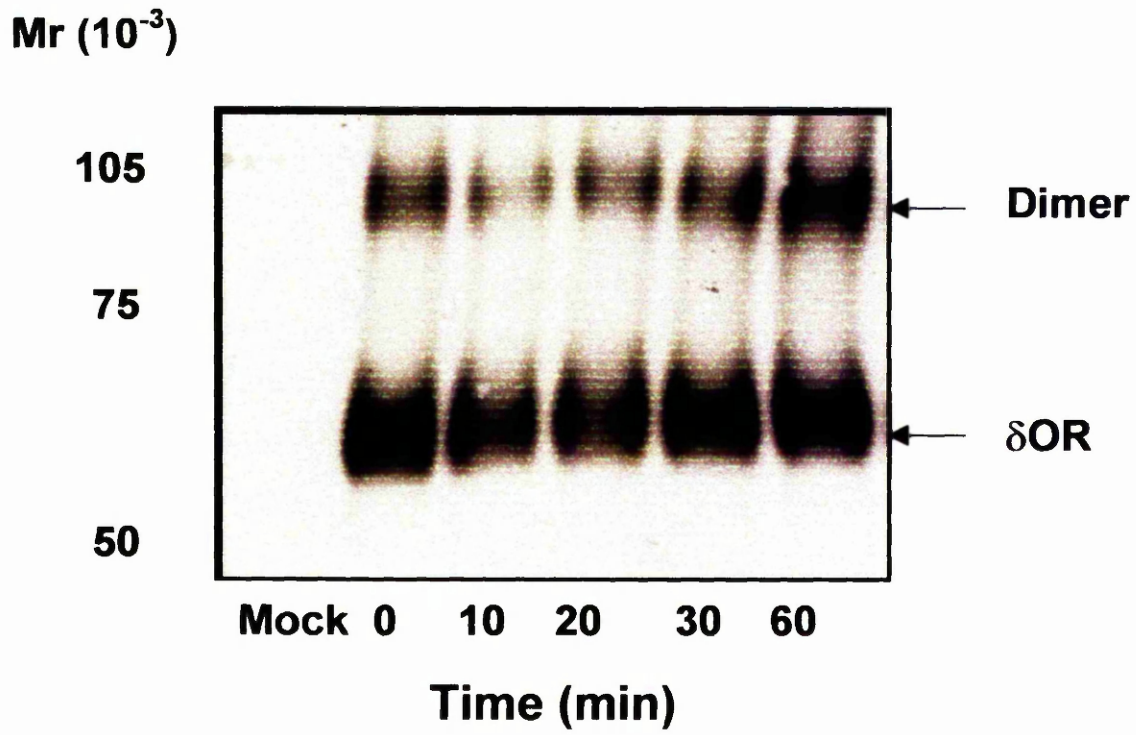

Figure 3.12 Lack of effect of naltrindole on constitutive homodimerization of δORs, detected by co-immunoprecipitation

HEK293 cells transiently transfected with both Flag-δOR and c-myc-δOR were incubated in the presence of 100nM naltrindole for the times indicated, 500μg of cell lysate was then immunoprecipitated with anti-Flag antibody, followed by immunodetection with anti-c-myc-antibody. Molecular weight markers were run in lane M. The data presented here are a representative immunoblot of experiments that were performed three times.

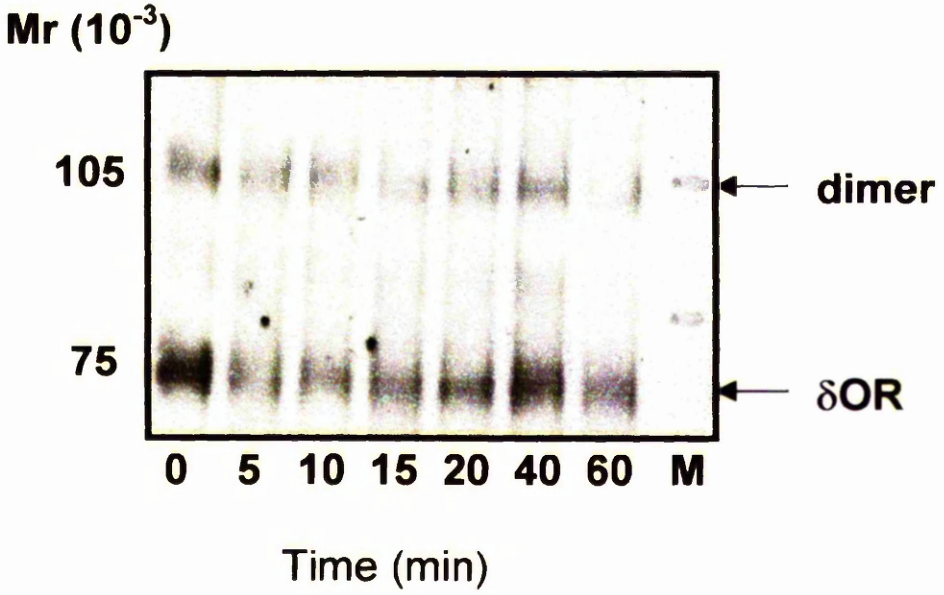

Figure 3.13 Evidence of constitutive heterodimers of δORs with other GPCRs using co-immunoprecipitation

Co-immunoprecipitation of 500μg of cell lysates of HEK293 cells transiently transfected with c-myc-δOR and the following, Flag-δOR (lanes 1 and 7), Flag-β_2-AR-GFP (lanes 2 and 8) Flag-β_1AR-GFP (lanes 3 and 9), Flag-IP prostanoid receptor (lanes 4 and 10) or Flag-IP prostanoid receptor-GFP (lanes 5 and 11). Samples in lanes 1 – 5 were immunoprecipitated with anti-Flag antibody and immunodetection was with anti-c-myc antibody. Samples in lanes 7-11 were immunoprecipitated with anti-c-myc-δOR and blotted with anti-Flag antibody Molecular weight markers were run in lane 6. The data shown here are a representative blot of the experiment which was performed at least three times.

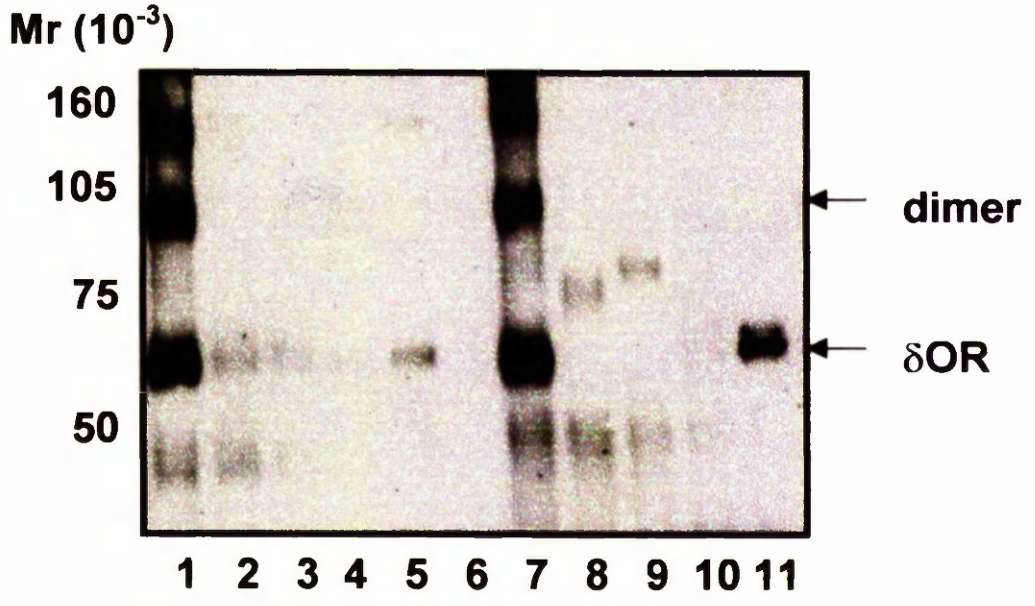

Figure 3.14 Constitutive heterodimerization between δOR and μORs, detected by co-immunoprecipitation

Immunoprecipitation of 500μg cell lysates of HEK293 cells transiently expressing both Flag-δOR and c-myc-δOR (lane 1), Flag-μOR only (lane 2), Flag-μOR and c-myc-δOR (lane 4), was performed with anti-Flag-antibody and immunodetection with anti-c-myc antibody. In lane 3 HEK293 cells stably expressing Flag-δOR (F28) were transiently transfected with c-myc-δOR, immunoprecipitation was performed with anti-Flag antibody and immunodetection with anti-c-myc antibody. Immunoprecipitation of Flag-μOR resulted in the co-immunoprecipitation of the c-myc-δOR. The data shown are a representative blot of experiments performed at least three times.

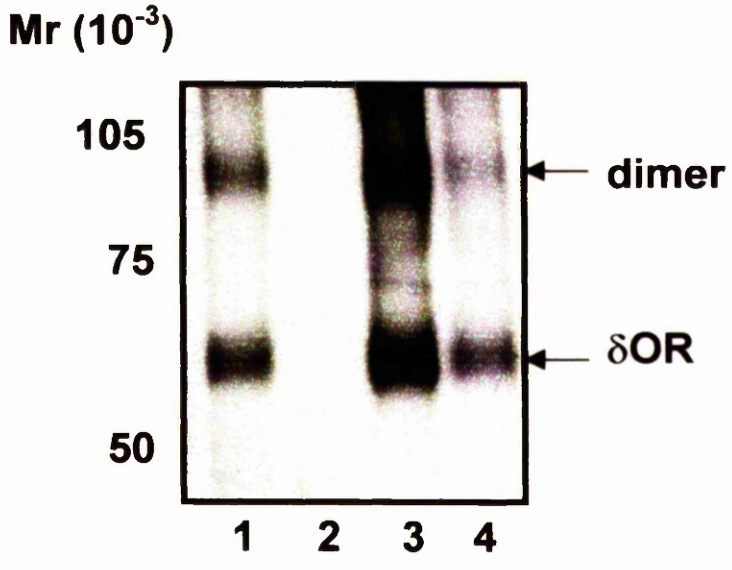

Figure 3.15 Constitutive heterodimers between δORs and β_2ARs are detected by co-immunoprecipitation

Immunoprecipitation of 500μg cell lysates of HEK293 cells transiently expressing the c-myc-δOR (lanes 1, 3 and 4) in combination with wild type β_2-AR (lane 1), Flag-β_2-AR-GFP (lane 3) or β_2-AR-eYFP (lane 4). In (lane 2) the wild type β_2-AR was expressed alone. Immunoprecipitation was performed with an anti-β_2-adrenoceptor antibody, and immunodetection with anti c-myc antibody. The non-specific band present in all lanes represents detection of the anti-β_2-AR antibody. The data shown are a representative blot of experiments performed at least three times.

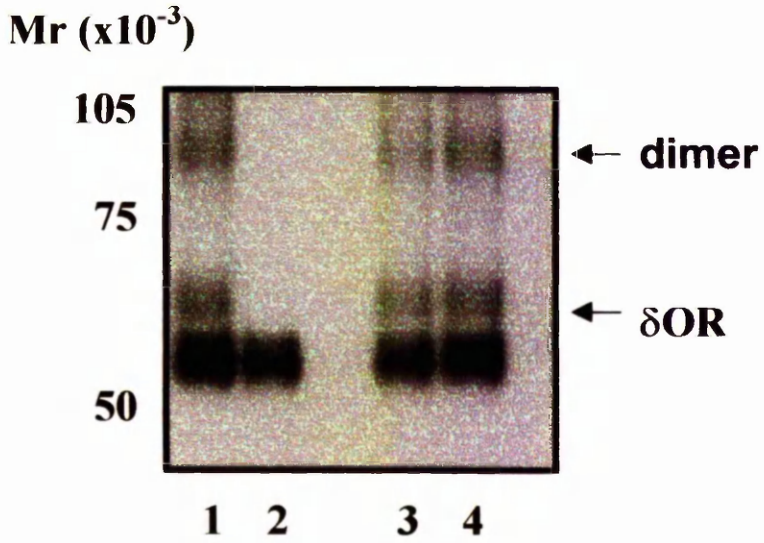

Figure 3.16 Constitutive heterodimerization between δOR and β_2AR-GFP is evident under various lysis conditions

Cell lysates of HEK293 cells transiently transfected with c-myc-δOR and Flag-δOR or with c-myc-δOR and Flag-β_2AR-GFP were produced with lysis buffers (described fully in section 2.5.7) containing the following detergents 1) 1% TX100, 0.5% Na-deoxycholate, 2) 1% Tween20, 3) 2% SDS, 4) 0.5% CHAPS 5) 1% NP40, 6) 1% TX-100. 500μg of each cell lysate was immunoprecipitated with either A) anti-c-myc antibody or B) anti-Flag-antibody. Immunodetection was performed with A) anti-Flag antibody or B) anti-c-myc antibody. The blot shown is representative of experiments which were performed at least three times.

3.16 A)

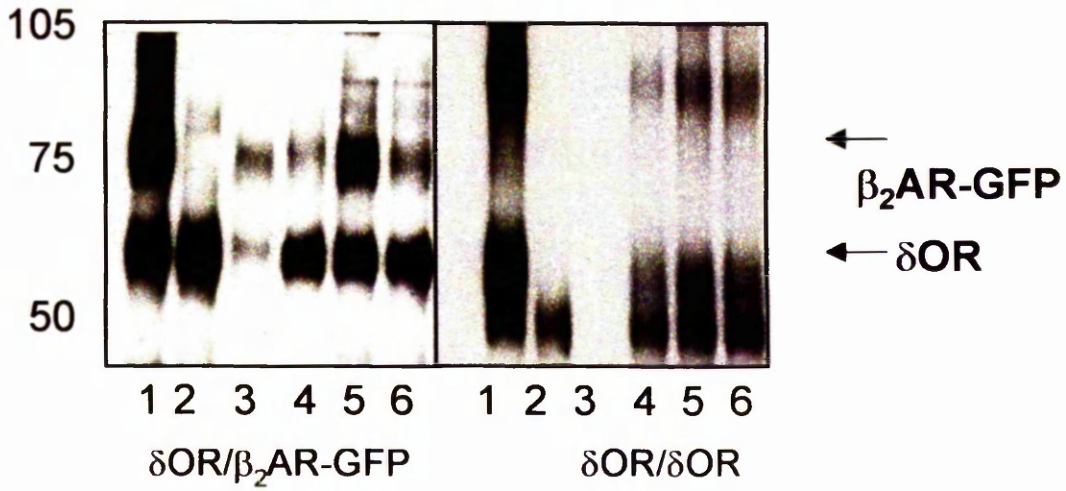
Mr (10-3)
105
75
50
1 2 3 4 5 6 1 2 3 4 5 6
δOR/β2AR-GFP
δOR/δOR
β2AR-GFP
δOR

3.16 B)

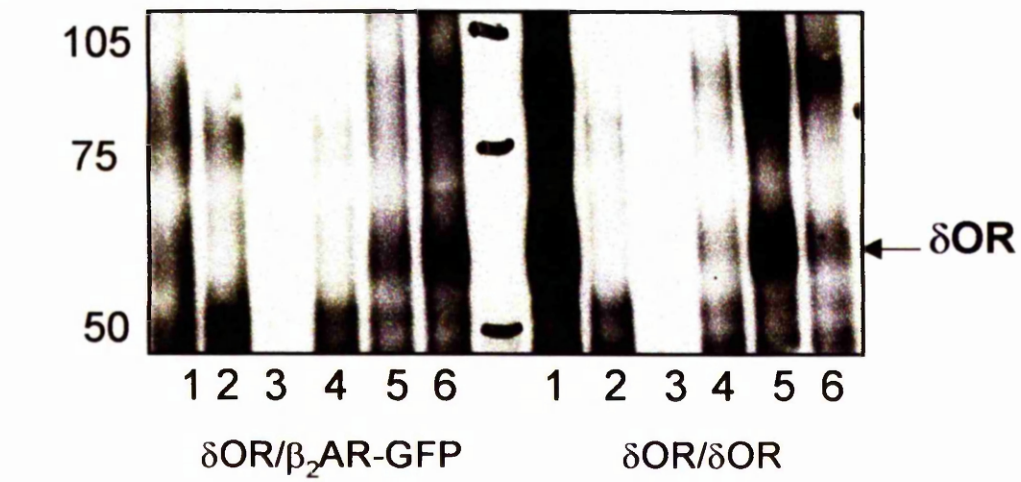
Mr (10-3)
105
75
50
1 2 3 4 5 6 1 2 3 4 5 6
δOR/β2AR-GFP
δOR/δOR
δOR

3.3 Discussion

The use of epitope tags allows proteins of interest to be identified easily, using commercially available antibodies without the need of the lengthy process of antibody generation for each protein to be studied. As epitope tags consist of a short sequence of amino acids they have only a limited potential to disrupt the activity of the protein to which they have been added. For GPCRs epitope tags have been widely used without detrimental effects to GPCR ligand binding or cell signalling. However, when using epitope tags care has to be taken to ensure that is the case.

The human δOR with N-terminal Flag or c-myc epitope tags (described in figure 3.1) were constructed and used within this study. N-terminal epitope–tagging of GPCRs has previously been utilized, along with co-immunoprecipitation to demonstrate homodimeric δORs (Cvejic and Devi, 1997) and β_2ARs (Hebert et al., 1996, Hebert et al., 1998). Heterodimeric δOR or κOR with β_2ARs have also been demonstrated using N-terminal epitope tags (Jordan et al., 2001), as have heterodimers between somatostatin receptor subtypes (Pfeiffer et al., 2001).

Transient expression of these constructs was assessed using a single concentration [^{3}H]diprenorphine binding assay which is shown in figure 3.2. The expression level of the tagged constructs was found to be lower than that for the receptor alone.

The δ-opioid receptor on stimulation can activate the pertussis toxin sensitive G-proteins, Gαi and Gαo. The high affinity GTPase activity via activation of these G-proteins was examined to ensure that the addition of the N-terminal tag did prevent receptor functionality. The activity of the transiently expressed receptors is shown in figure 3.3. DADLE stimulated high affinity GTPase activity in cells transfected with the tagged receptors although the level of stimulation was lower than that observed for the wild-type receptor. The high affinity GTPase activity of the GFP-fusion constructs was particularly poor, therefore stable cell lines were set up to confirm that the receptor constructs were indeed functional and that the

low level of high affinity GTPase measured was, in part, due to the low receptor expression level.

Immunoblots confirmed the transient expression of each receptor species in HEK 293 cells (figure 3.9). The predicted molecular masses from the amino-acid sequence for the δ-OR and the δ-OR-GFP are 41 and 69 kDa respectively. Detection of Flag-δOR with anti-Flag demonstrated bands at 35kDa and 60kDa (figures 3.9A) as well as unresolved material at the top of the gel which may be aggregated, or oligomeric receptor species. The membranes containing δOR-GFP showed bands at 55 and 100kDa (figure 3.9A). The anti-c-myc detection of the corresponding c-myc-tagged constructs gave similar bands (figure 3.9B). The 60 kDa species likely represents the glycosylated monomeric Flag and c-myc-tagged δOR with the other bands likely to represent multimeric and aggregated receptor species. In each immunoblot of membranes transfected with δOR alone there was a contaminating band running at approximately 35kDa and at 55Kda in the immunoblot of membranes transfected with δOR-GFP. The nature of this polypeptide was not established although may be non-glycosylated receptor.

Intact cell [^{3}H]naltrindole binding studies on the Flag-δOR and Flag-δOR-GFP stable cell lines were performed (figure 3.4) and single point adenylyl cyclase assays (figure 3.5) demonstrated the receptor expression level of the clones and confirmed their signalling capacity. The Kd determined from Scatchard plot of [^{3}H]naltrindole binding demonstrated its expected high affinity for the δOR. The inhibition of the adenylyl cyclase on stimulation with DADLE was in agreement to that found by Merkouris et al. (1997). DADLE gave a slightly lower amount of inhibition for the GFP-labelled receptor, although the IC_{50} (0.02nM ± 0.011) was equivalent to that found for the Flag-δOR (0.02 ± 0.009 nM) as shown by statistical analysis ($p > 0.05$).

Several stable clones of Flag-δOR-GFP were identified as having the receptor mainly at the plasma membrane, as shown for clone FG6 in figure 3.8. The fusion of GFP to the C-terminus of GPCRs has been shown in several instances

not to affect ligand binding, effector action or trafficking of GPCRs (Tarasova et al., 1997, Drmota et al., 1998, McLean et al., 1999).

This Flag-δOR-GFP stable cell line was used to demonstrate agonist-activated internalisation of the receptor in real time, using confocal microscopy. Flag-δOR-GFP was internalized to intracellular vesicles upon stimulation with agonist DADLE. Internalization was evident within 5 minutes of agonist stimulation. This agrees with the internalization rate observed by Chu et al. (1997) where the $t_{½}$ was shown to be <10 minutes thus demonstrating that the addition of GFP at the receptor C-terminus did not affect its rate of internalisation. The presence of some internal receptor at time zero was not unexpected as Petäjä-Repo et al. (2000) demonstrated that a large proportion of transiently expressed δOR was retained within the ER.

The aim of this project was to study possible homo and heterodimerization of δORs. Cvejic and Devi (1997) demonstrated that the mouse δOR could form homodimers when transfected into a heterogeneous cell line. Initial experiments using co-immunoprecipitation to confirm these results were successful, as differentially tagged δORs could immunoprecipitate each other when expressed in the same cell (figure 3.10). Both monomeric receptor was identified as well as a potential dimeric receptor species migrating at 120kDa. In the co-immunoprecipitation experiments described here the immunoprecipitates were resuspended in sample buffer containing 50mM DTT and heated to 85°C before loading onto SDS-PAGE gels. This indicates that disulphide bonds alone are not responsible for the homo and heterodimeric interactions observed as potential dimeric species are detected after such treatment. However, it should be noted that disulphide bonds have been shown to be responsible for maintaining κOR homodimers, as well as δOR:κOR heterodimers (Jordan and Devi 1999). δOR:μOR heterodimers have also been shown to be disrupted by reducing agents (Gomes et al., 2000).

Ligand modulation of homo and heterodimerization has been studied for several GPCRs. The effects have varied from promoting dimerization of the β_2AR

(Hebert et al., 1996, Angers et al., 2000), no effect on dimerization as described for the muscarinic m3 receptor (Zeng and Wess, 1999) and the δOR (McVey et al., 2001) or reduction of δOR dimerization (Cvejic and Devi, 1997). This lack of consensus may arise, in part, from the different methods employed to study GPCR dimerization or may reflect true variation of GPCR dimerization. In this study, no effects of the agonist DADLE or the antagonist naltrindole were observed in co-immunoprecipitation studies. The variations in band intensity observed in figures 3.11 and 3.12 are likely to be due to variations in loading of the gel sample as they are not consistent with the time of incubation with the ligand. This is in contrast to the effect of ligands found by Cvejic and Devi (1997) where agonists showed a time and concentration-dependence for reduction of the level of receptor dimerization and a consequent increase in the monomeric component. The technique used to demonstrate this effect was also co-immunoprecipitation, but after cross-linking of the receptors with the hydrophobic cross-linker DSP. In this study replication of their data was not successful as SDS-PAGE of the immunoprecipitated samples after cross-linking resulted in a high molecular weight mass aggregate which did not resolve into the gel (data not shown).

Co-immunoprecipitation of δOR with other receptors

To examine the specificity of the δOR interaction, and initially as potential negative controls for the homodimerization experiments, co-immunoprecipitation of δOR was performed with other co-expressed GPCRs.

Immunoprecipitation of the c-myc-δOR with anti-c-myc antibody resulted in co-immunoprecipitation of each of a range of co-expressed Flag-tagged GPCRs. No co-immunoprecipitation was observed with the Flag-IP prostanoid receptor (figure 3.13). Correspondingly immunoprecipitation of Flag-IP prostanoid receptor did not result in the co-immunoprecipitation of the c-myc-δOR (figure 3.13). Each of the other Flag-tagged receptors were able to co-immunoprecipitate the c-myc-δOR to some extent although the time required to

detect an appropriate ECL signal was greater when the Flag-β_1AR-GFP (lane 2) and the Flag-β_2AR-GFP (lane 3) were co-expressed.

The varying levels of co-immunoprecipitated receptor may result from different expression levels of the individual receptors or as a result of differing affinities of the antibodies for the receptors at either the immunoprecipitation or immunodetection steps. It is possible that the lack of co-immunoprecipitation of Flag-IP prostanoid receptor with the c-myc-δOR could be due to poor receptor expression or possibly the lack of a C-terminal GFP. Flag-IP prostanoid receptor-GFP did result in co-immunoprecipitation with the c-myc-δOR therefore it may be possible that the C-terminal GFP is resulting in aggregation of the co-transfected receptors.

No direct receptor:receptor interaction has been demonstrated in the literature between the δOR and β_1AR or IP prostanoid receptors although the opiate and adrenergic signalling systems have been shown to interact (Ammer and Schulz, 1997, Stone et al., 1997). At which level of the signalling mechanisms interaction occurs is not clear. Interestingly, the prostanoid receptor EP3 has been shown to be involved in morphine tolerance (Nakagawa et al., 2000) as has the calcitonin gene-related peptide receptor (Powell et al., 2000). The opioid receptor system has also been shown to interact pharmacologically the cannabinoid receptor systems (Manzanares et al., 1999).

Clearly opiate signalling mechanisms are not simple as pharmacological interaction with several other GPCR signalling systems has been observed. Further investigation is needed to determine if the pharmacological interaction is a result of receptor:receptor interaction.

Co-expression of c-myc-δOR and Flag-μOR and immunoprecipitation of the lysate with anti-Flag (M5) antibody allowed the immunodetection of the c-myc-δOR, indicating that the δOR and μOR receptors can form constitutive homodimers (figure 3.14). δOR:μOR heterodimers could in part be responsible for the observed opiate subtype pharmacology for which no individual receptor

cDNA has been identified. As the μOR used has no C-terminal GFP this co-immnoprecipitaion could not be attributed to GFP-induced receptor aggregation. George et al. (2000) and Gomes et al. (2000) have since confirmed the existence of δOR:μOR heterodimers.

To investigate the constitutive heterodimerization of GPCRs further the wild type β_2AR, Flag-β_2AR-GFP, and β_2AR-eYFP were co-transfected with c-myc-δOR. Immunoprecipitation of the β_2-adrenoceptor with anti-β_2AR resulted in the presence of the c-myc-tagged δ-opioid receptor in the precipitated sample that could be detected by immunoblotting following resolution of the sample by SDS-PAGE. Equivalent results were obtained when the c-myc-tagged δOR was co-expressed with a form of the β_2-adrenoceptor-eYFP or with Flag-β_2AR-GFP (figure 3.15).

A second polypeptide with mobility consistent with a dimer containing the c-myc-tagged δOR was also detected (figure 3.15). Neither of these bands was detected when the human β_2-adrenoceptor was expressed in the absence of the c-myc-tagged δ-opioid receptor and then immunoprecipitated (figure 3.15). Immunoprecipitation of either of these modified forms of the β_2-adrenoceptor resulted in co-precipitation of the c-myc-tagged δ-opioid receptor and detection of both monomeric and potential dimeric species.

These rather unexpected observations led us to consider whether such co-immunoprecipitation approaches following transient transfection of cells may produce artefactual results following solubilization of GPCRs from the membrane environment. However it should be noted that Jordan et al. (2001) have since published data demonstrating the existence of cell-surface hetero-dimers between the mouse δOR and the human β_2AR as well as the rat κOR with the human β_2AR which alters the trafficking properties of the co-expressed receptors.

There is also the possiblity that heterodimeric interactions observed may result from a mass action effect resulting from overexpression of receptors. It must be

acknowledged, therefore, that the interactions demonstrated may not be evident at lower expression levels or *in vivo*.

The possibility of these results being artefactual was thus further investigated using different detergents to solubilize the receptors from the membranes. Those used included the zwitterionic detergent CHAPS, the non-ionic detergents Trition X100, NP40, Tween20 and the ionic detergent SDS.

After transient transfection of c-myc-δOR and Flag-β_2AR-GFP and solubilization in buffer containing the various detergents, co-immunoprecipitation was performed with the anti-Flag or anti-c-myc antibodies. Immunodetection of the precipitated samples, shown in figure 3.16 demonstrated that lysates produced with buffers containing 2% SDS or 1% Tween20 were unsuitable for subsequent co-immunoprecipitation of either receptor. SDS has denaturing properties and samples lysed in this buffer were extremely viscous and therefore difficult to load onto the SDS-PAGE gel which may explain the lack of any protein bands. The 2% SDS containing solubilization buffer did however indicate heterodimerization between c-myc-δOR and Flag-β_2AR-GFP on immunoprecipitation with anti-Flag antibody and immunodetection with anti-Flag antibody (Figure 3.16A, lane 3), indicating that the SDS containing buffer may be solubilizing the proteins from the membrane. Tween20 is an ionic detergent, which as previously been shown to solubilize membrane proteins (Chambers and Rickwood, 1993) The buffers containing TX100, CHAPS and NP40 did result in solubilization and subsequent co-immunoprecipitation of both receptors. (figures 3.16A and 3.16B). The result with CHAPS was not completely consistent even on repeating the experiment several times. In figure figure 3.16A, in lanes 4 both the δOR and the β_2AR-GFP receptors are evident but this is not the case in figure 3.16B where in lane 4 the c-myc-δOR is identified on co-expression with Flag-δOR but not on co-expression with Flag-β_2AR-GFP. Successful co-immunoprecipitation was observed indicating the presence of both δOR homodimers and δOR:β_2AR-GFP heterodimers using the anti-c-myc antibody for immunoprecipitation and immunodetection by anti-Flag antibody (figure 3.16A), and vice versa (figure 3.16B)

As the detergents used have been shown to be suitable for solubilization of membrane proteins (Chambers and Rickwood, 1993) and differ in both micelle size and aggregation number it is less likely that the results obtained are artefactually introduced during detergent solubilization of the hydrophobic GPCR proteins. However, the inconsistent results obtained with the solubilization buffers containing CHAPS and SDS indicate the necessity for careful controls with these experiments.

Co-immunoprecipitation is a useful technique to demonstrate interactions between differentially tagged proteins. Careful controls have to be include to ensure the interactions demonstrated are not artefacts to the conditions used, especially when investigating interactions of the extremely hydrophobic GPCRs. It may be possible to use the C-terminal δOR-GFP fusion to examine receptor dimerization via FRET with a corresponding δOR-Blue fluorescent protein (BFP) fusion as the enhanced GFP used in this study has good spectral overlap with BFP (Billinton and Knight, 2001). Development of such an assay to determine GPCR homo and heterodimerization that can be performed on live cells would be extremely advantageous to this study. The work performed to develop of such an assay is described in chapters 4 and 5.

CHAPTER 4

Development of a time-resolved fluorescence resonance energy transfer assay to determine GPCR dimerization in live cells

CHAPTER 4

Development of a time-resolved fluorescence resonance energy transfer assay to determine GPCR dimerization in live cells

4.1 Introduction

When two molecules are in close proximity and have appropriate excitation and emission maxima, non-radiative energy transfer can occur, resulting in excitation of the acceptor molecule. This process is known as fluorescence resonance energy transfer (FRET) and has been used for a variety of purposes, including the measurement of enzyme activity (Zhang et al.,1999, Fattori et al., 2000), immunodetection (Oswald et al., 2000) and analytical chemistry (Blomberg et al., 1999). Structural changes within macromolecules have also been measured using FRET, which is possible as the data are obtained in real time (Heyduk and Heyduk, 1997). Various fluorescently labelled biological components have been used in energy transfer assays including protein, DNA and RNA molecules. Assay formats include the use of intrinsic probes where, for example, the DNA or protein molecule itself is labelled with one or both fluorescent moieties. For some protein molecules, the fluorescence from internal tryptophan residues is utilised to measure a FRET signal with an external fluorescent acceptor molecule, which interacts with the protein. This is the approach used by Remmers (1998) who set up a homogeneous FRET assay for the detection and quantitation of G-proteins using an environmentally sensitive N-methyl-3'-O-anthranoyl (mant) guanine nucleotide analogue. The fluorescence increases as this mant guanine nucleotide binds to G-protein molecules, partly as a result of energy transfer from the tryptophan residues in the G-protein to the mant guanine nucleotide.

As there are few intrinsic probes suitable for energy transfer available the majority of FRET assays have been developed with the use of extrinsic fluorescent probes which are covalently attached to the molecule to be studied. Care has to be taken though, to ensure that the label itself does not alter the properties of the molecule being studied. Extrinsic labelling with fluorescent molecules has been successfully performed on DNA, as Heyduk and Heyduk (1997) demonstrated an energy transfer signal with a 15bp double-stranded DNA molecule labelled at one end with a europium chelate and the acceptor label, Cy5, at the other.

Another method of fluorescently labelling molecules for FRET is via fluorescent antibodies. This does not require the protein or oligonucleotide to be purified before covalently labelling with its fluorophore. Suitably labelled specific antibodies, however, are not always available and may have to be produced specifically for the assay. Generic reagents have, however, been used successfully by Pope et al. (1999) in a ligand binding assay where a biotinylated ligand, which is fluorescently labelled via a streptavidin-APC molecule, binds to a receptor fusion protein-Fc to which protein-A-Eu^{3+} has labelled. Others have been unsuccessful with the use of such generic reagents (Stenroos et al., 1998). Specific antibodies labelled with fluorescent molecules have been used in several examples including antibodies labelled with FITC and Cy3 where the resultant energy transfer is not time-resolved (Damjanovich et al., 1997). Binding of an Eu^{3+}-chelate labelled interleukin 2 (IL2) was measured in a time-resolved manner in the presence of an anti-IL2 receptor α chain antibody labelled with Cy5 (Stenroos et al., 1998). A homogeneous TR-FRET assay, using terbium and tetramethylrhodamine labelled antibodies to measure the concentration of the β subunit of human chorionic gonadotropin in serum, was described by Blomberg et al., (1999) where the antibodies used recognised different epitopes of the same protein.

FRET assays can be performed in a homogeneous format, which does not involve any separation of bound from free label. The main advantage over the heterogeneous assay is that no separation of the bound from the free label is

required, providing a quick and simple assay format suitable for high throughput drug screening (Pope et al., 1999). The homogeneous assay format has allowed the development of assays, which use crude protein preparations where previously purified protein had to be used (Blomberg et al., 1999). Many of the assays described above have been in a homogeneous format. A comparison of a homogeneous assay format with terbium and tetramethylrhodamine was performed by Blomberg et al., (1999) comparing it to a heterogeneous Eu^{3+} separation assay. Although the homogeneous assay was not as sensitive the desired results were achieved.

FRET assays have been used successfully to look at the protein:protein interaction of receptor subunits. The IL-2 receptor is a multi subunit cytokine receptor found at the plasma membrane of cells. The pre-assembly of the subunits of the IL-2 receptor was investigated by Damjanovich et al., (1997) using flow cytometry FRET measurements with cells fluorescently labelled via antibodies to the receptor subunits. FITC or Cy3 labelled antibodies were used and the FRET signal measured to determine subunit interaction. Antibody-dependent subunit interaction was ruled out by performing the same experiments with labelled Fab fragments of these antibodies. The IL-2 receptor subunits were shown to be co-localized in resting T-cells and the effects of interleukin 2, 7 and 15 on the co-localized subunits described.

Farrar et al., (1999) by expressing combinations of the subunits where an individual subunit was tagged with c-myc, demonstrated the subunit stoichiometry of the cell-surface $GABA_A$ receptor. The fluorescence intensity level of the anti-c-myc, labelled with Europium cryptate, bound for each subunit was examined, and showed the stoichoimetry of the sub-units to be 2α, 2β and 1γ per receptor monomer. This was confirmed by binding the anti-c-myc labelled with europium cryptate, at sub-maximal levels, followed by removal of the excess antibody and replacing it with anti-c-myc-XL665. Energy transfer signals were only obtained when the α or β subunits were labelled, confirming the subunit stoichiometry of 2α, 2β and 1γ.

Interaction between receptor molecules can also be studied using energy transfer and a modified version of FRET, termed BRET, has been used to study the homodimerization of the β_2AR (Angers et al., 2000). This relies on energy transfer between modified receptor proteins containing eYFP or *Renilla* luciferase fused in frame to the C-terminus of the receptor. When both these receptors were expressed in the same cell, after the addition of the luciferase substrate coelentrazine, a BRET signal was obtained. This demonstrated constitutive homodimerization of this receptor, which increased in the presence of agonist.

Immunodetection of receptors studied *in vivo* and *in vitro* indicates receptor homodimerization by the presence of high molecular weight bands corresponding to receptor dimers. Nimchinsky et al., (1997) demonstrated the dopamine D3 receptor in dimeric and trimeric forms in both brain tissue and in transfected cells. Similarly, Zeng and Wess (1999) showed muscarinic M3 receptor dimers in brain tissue. Using FRET to study GPCR homodimerization allows the use of live cells whereas co-immunoprecipitation of differentially tagged receptors which has been used previously to demonstrate GPCR homodimerization (Cvejic and Devi 1997, Hebert et al., 1996), relies on disruption of the cells with detergents. The individual receptor contributions to the properties of a homodimer cannot be distinguished from that of the monomer which may limit pharmacological investigations into homodimers. Heterodimers, however may be studied pharmacologically by comparing the heterodimer pharmacology with that in the presence of selective antagonists of each receptor. The pharmacology of μOR and δOR heterodimers has been investigated using this method (Gomes et al., 2000, George et al., 2000). Rocheville et al., (2000b) demonstrated pharmacologically and by photobleaching FRET, the interaction between the somatostatin SSTR5 and the dopamine D2 receptor.

The δOR has been used in this study as differentially tagged δOR receptors have been shown previously to co-immunoprecipitate (Cvejic and Devi 1997). This has also been described in Chapter 3 figure 3.10. This indicates the likely

presence of constitutive δOR homodimers. Heterodimers between δOR and κOR, but not between μOR and κOR, were demonstrated using co-immunoprecipitation and ligand binding studies by Jordan and Devi (1999). Heterodimerization between δOR and μOR has been demonstrated by Gomes et al. (2000) and George et al. (2000). However data from co-immunoprecipitation studies cannot report where the homodimers are in the cell. Modification of the N-terminal region of the human δOR to contain either the Flag or c-myc epitope tag recognition sequences allows antibody detection of the receptors in live cells. Both FRET and TR-FRET have been used to investigate δOR cell-surface homodimerization. For FRET, antibodies labelled with FITC and Cy3 were used as these have been shown to be a suitable energy transfer pairing by Damjanovich et al., (1997). For TR-FRET, antibodies labelled with EuK and APC were used as these were also shown by Farrar et al., (1999) to be an appropriate TR-FRET pairing. Homogeneous and heterogeneous assay formats were investigated.

4.2 Results

Labelling of anti-Flag antibody with APC makes it a suitable acceptor molecule in TR-FRET assays where Europium is used as the donor fluorophore. Anti-Flag (M5) antibody was labelled with PhycoLink® SMCC-XLAPC as described in section 2.5.2. This cross-linked APC molecule is stable and suitable for protein labelling. The sulfhydryl reactive (maleimide) groups, which have been introduced to the APC, readily react with reduced cysteine groups of proteins.

In figure 4.1A gel filtration of the reduced antibody to remove any excess DTT is shown. Only one peak was obtained, as the DTT does not have an absorbance at 280nm. The protein was eluted from the column after 22ml in a volume of 9ml. After an overnight incubation with the APC the unbound APC was removed from the labelled antibody, again by gel filtration using the Superdex 200 column. The separation of the APC labelled antibody from the free APC is shown in figure 4.1B. The peak of labelled antibody did not return to the baseline before the excess APC began to elute, this indicates that there is likely to be some unbound APC eluted with the labelled antibody. To remove this unbound APC the antibody mixture was concentrated using a Centricon® concentrator with a 100kDa filter.

The absorbance of the labelled antibody was read at 280nm and 650nm and the labelling stoichiometry and antibody concentration was calculated as 0.63 molecules of APC bound per antibody molecule.

The specificity of the anti-Flag-APC was assessed to ensure that the labelling of the antibody with the APC did not inhibit its binding to the Flag sequence expressed on the N-terminus of receptors. The specificity of the anti-Flag-APC antibody was retained after labelling (figure 4.2).

To ensure that the labelled antibody could be used for energy transfer with Europium labelled proteins in close vicinity, increasing concentrations of the APC-labelled antibody were incubated in the presence of 5nM Europium chelate-

protein A. This labelled protein A binds to the APC-labelled anti-Flag antibody generating an energy transfer signal shown in figure 4.3.

Cell lysates that had been used successfully to demonstrate co-immunoprecipitation of the differentially tagged δORs (Chapter 3) were assessed in a homogeneous TR-FRET assay format. Equal amounts of protein (60μg) were added to wells containing both 50nM anti-Flag-APC and 10nM anti-c-myc-EuK antibodies. The TR-FRET signal was monitored and is shown in figure 4.4. No energy transfer above background was observed ($p > 0.05$). The expression level of each tagged receptor could not be measured easily as this assay was performed in solution.

Development of TR-FRET on intact cells was then performed firstly in a homogeneous format. Transiently transfected cells were split 24 h after transfection into wells of a black 96 well plate, ensuring equal numbers of cells were added per well. After a further 24 h to allow the cells to adhere to the surface of the plate, fluorescently labelled antibodies were added. Each well was incubated in the presence of 50nM anti-Flag-APC and 10nM anti-c-myc-EuK. Again no energy transfer signal above background was observed ($p > 0.05$) (figure 4.5).

The fluorescence of the anti-c-myc-EuK antibody was assessed to determine if the level of TR-FRET observed could be resulting from anti-myc-EuK fluorescence alone. The A615nm and A665nm after excitation at 320nm of a standard curve of increasing amounts of anti-c-myc-Eu^{3+} in the presence of 5 x 10^5 HEK293 cells was measured. This demonstrated that the value of TR-FRET signal obtained from the whole cell heterogeneous assay was indeed from the anti-c-myc-EuK antibody alone.

A further experiment was performed in the same manner except that the TR-FRET signal was observed from the antibody associated with the cells. This included a wash step after the incubation with antibodies. The result from this

experiment is shown in figure 4.6 where again no TR-FRET signal was obtained above background.

The lack of an energy transfer signal may simply reflect that the δOR does not form constitutive homodimers at the cell-surface of these cells. The effect of the δOR agonist DADLE was also examined to determine whether agonist activation could result in cell-surface homo-dimerization of the δOR. In no case did DADLE alter the level of TR-FRET observed in these experiments (data not shown).

A further assessment of the assay conditions was then performed. The specificity of the commercially labelled anti-c-myc-EuK was assessed and is shown in figure 4.7. Where the anti-c-myc-EuK was incubated with cells which were either mock transfected or transfected with Flag-δOR or c-myc-δOR, no specific binding was observed. To confirm that this lack of binding was not the result of very low expression of the c-myc-δOR a comparison of the anti-c-myc-EuK binding with anti-c-myc-FITC binding was performed and is shown in figure 4.8. The EuK and the FITC labels were both generated commercially on the rabbit polyclonal 9E10 antibody, therefore any difference in binding obtained must be the effect of the fluorescent label on the antibody. Figures 4.7 and 4.8 show the levels of each antibody binding obtained. The anti-c-myc-FITC antibody binds specifically to cells expressing the c-myc-tagged receptors with high intensity values and the anti-myc-EuK did not. The fluorescent intensities obtained here could reflect the difference in the fluorescent intensity of each probe at the respective conditions used. A standard curve was therefore set up for each antibody to examine the corresponding fluorescence intensities at appropriate wavelengths (535nm after excitation at 490nm for FITC, 620nm after excitation at 320nm for EuK). The fluorescence intensity obtained for the equivalent amount of anti-c-myc-EuK was much higher than that for the anti-c-myc-FITC antibody (figure 4.9). Therefore if equivalent amounts of anti-c-myc-EuK and anti-c-myc-FITC bound to the receptors the fluorescence intensity from the anti-c-myc-EuK would be expected to be higher (at least 100 fold).

These results indicate that either labelling of the anti-c-myc with the europium cryptate has inactivated the antibody or that the antibody was not stored under the appropriate conditions and had broken down in such a way to lose its fluorescent label or lose its specificity. Another batch of the same antibody was not available from the supplier to allow this to be tested.

As the fluorescent EuK donor molecule binding is at such a low level on cells expressing c-myc-tagged receptors, it could not be concluded from the experiments performed if the tagged δOR receptors form constitutive or ligand dependent cell-surface homodimers.

The anti-c-myc-FITC antibody can be used as the fluorescent donor and Cy3 as an acceptor molecule, using FRET to determine the close proximities of the two. Anti-Flag antibody was then labelled according to the manufacturers instructions with Cy3. A labelling stoichiometry of 7.1 molecules of Cy3 per antibody was obtained.

Experiments were then performed in the presence of anti-c-myc-FITC and anti-Flag-Cy3 the results of which are shown in figure 4.10. In A, a FRET signal was achieved apparently demonstrating cell-surface constitutive dimerization of the δOR. However, when the fluorescence emission from the FITC alone was analysed as shown in figure B a large proportion of the apparent energy transfer signal arose from the high level of anti-myc-FITC antibody present and is not "real" energy transfer.

Another source of Europium tagged anti-c-myc antibody was then identified and assessed for specific binding to cells expressing receptors with N-terminal c-myc tag, this is shown in figure 4.11. This anti-c-myc-Eu^{3+} antibody bound specifically to cells that express N-terminal c-myc tags with low binding to cells that were either mock transfected or transfected with a N-terminally Flag-tagged receptor. The specificity of the anti-c-myc-Eu^{3+} is shown in figure 4.12.

Figure 4.1 Gel filtration of anti-Flag antibody labelled with cross-linked allophycocyanin.

A280nm elution profiles of Superdex 200 gel filtration columns. A) After reduction with DTT the antibody was then desalted into 20mM $NaPO_4$, pH 7.5. The protein was eluted after 22ml, in a volume of 9ml. A single protein peak was observed. B) Labelled antibody was separated from unlabelled antibody by gel filtration on a Superdex 200 column, run in PBS with 0.05% Tween20. The elution profile in B shows the first labelled antibody peak after 17ml which was collected up to 24 ml where the unlabelled APC began to elute.

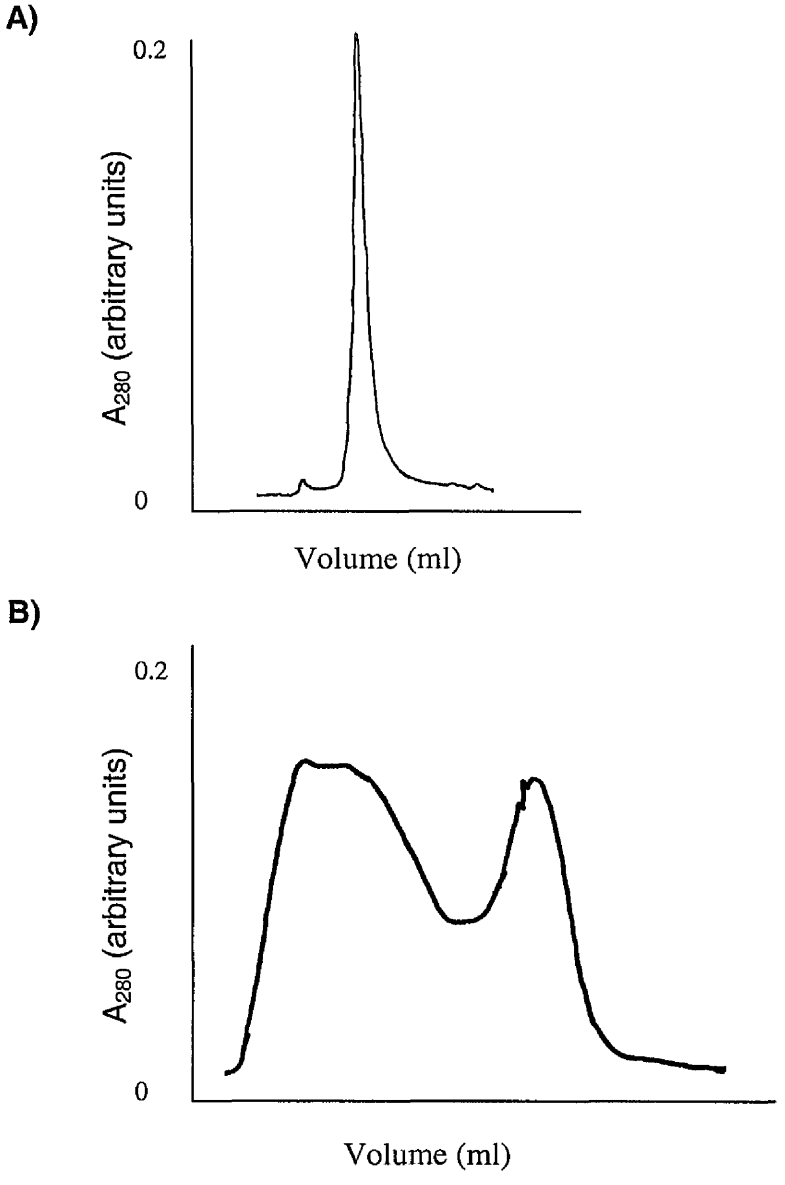

Figure 4.2 Anti-Flag-APC antibody binds specifically to cells expressing N-terminally-tagged Flag receptors.

HEK293 cells were either mock transfected or transfected with Flag-δOR and harvested 48 h after transfection. 5 x 10^5 cells were then incubated with 50nM anti-Flag-APC for one hour at room temperature, before washing 2 x 1ml with PBS. The cells were then re-suspended in 70µl of PBS and read in the Aquest™ fluorescence plate reader. The specific binding of the anti-Flag antibody is clearly demonstrated above the mock transfected cells. This graph is a typical representation of two independent experiments performed in triplicate.

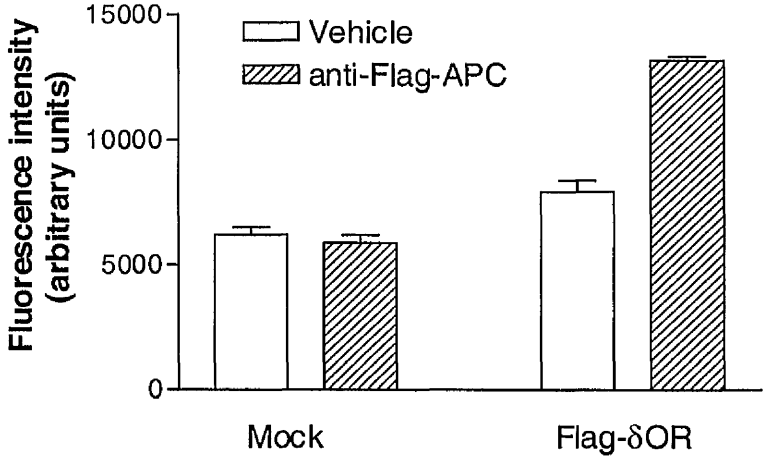

Figure 4.3 Time-resolved Fluorescence Resonance Energy Transfer with protein-A-Eu^{3+} and APC-labelled M5 anti-Flag antibody

The capability of the anti-Flag-APC to interact with protein-A-Eu^{3+} to produce a TR-FRET signal was assessed. Increasing amounts of Anti-Flag-APC were added to 5nM protein-A-Eu^{3+} and the TR-FRET observed on a Victor fluorescence plate reader. The data represent the mean ± SEM. of 3 independent experiments.

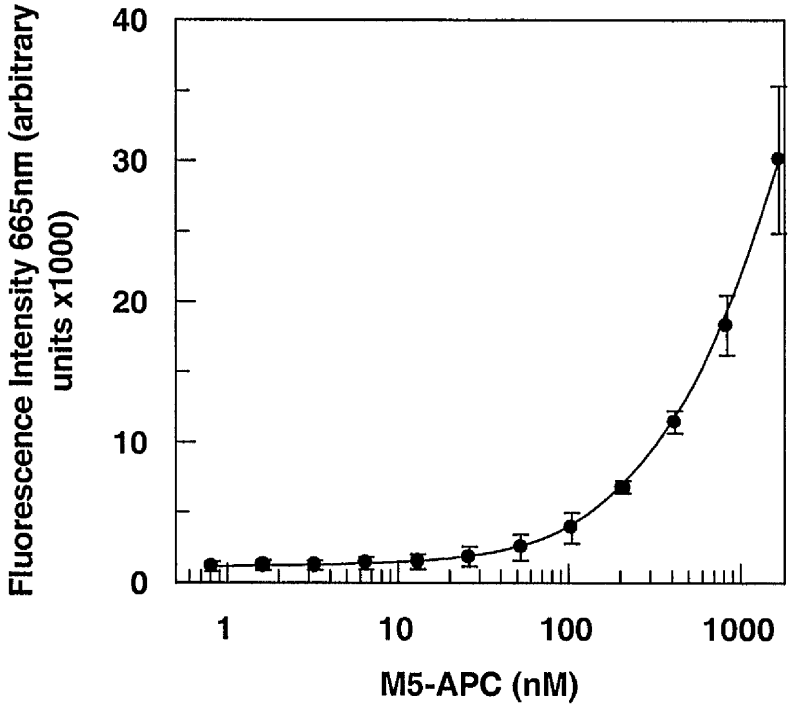

Figure 4.4 No energy transfer signal is obtained with cell lysates previously shown to co-immunoprecipitate Flag-δOR and c-myc-δOR

Cell lysates that had been previously used for co-immunoprecipitation experiments, indicating receptor dimerization, were taken and 60μg of protein incubated with 50nM anti-Flag-APC and 10nM anti-c-myc-EuK for one hour at room temperature. The energy transfer signal was then read in a Victor. No significant energy transfer signal above background was obtained under any of the conditions used ($p > 0.05$). It was not possible to assess the individual antibody binding in this experiment as it was performed in solution. This graph is a typical representation of two independent experiments performed in triplicate.

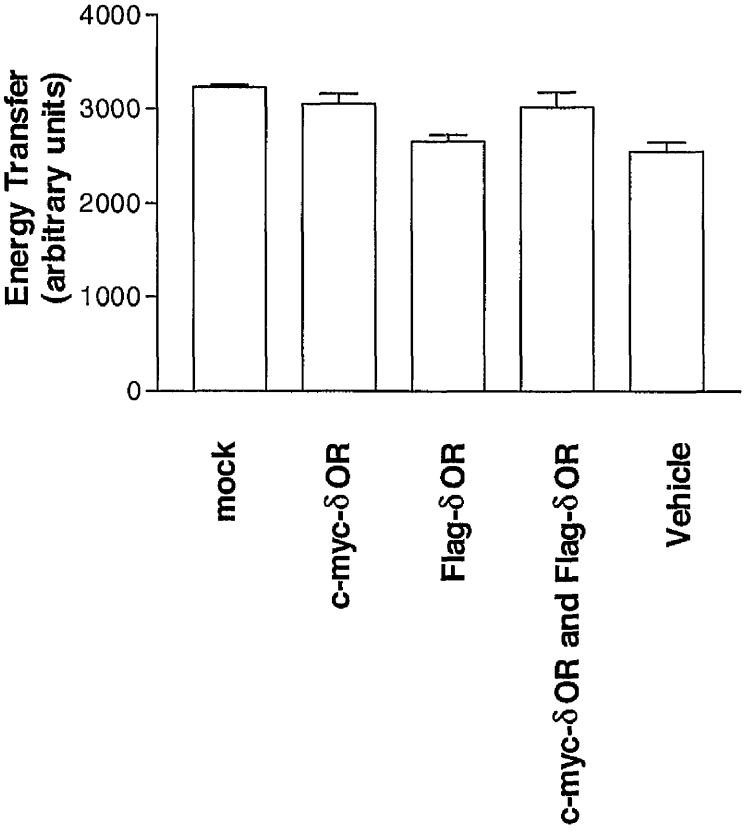

Figure 4.5 No δOR homodimerization was observed in the homogeneous assay fomat in the presence of anti-c-myc-EuK and anti-Flag-APC antibodies.

No TR-FRET was observed with HEK293 cells after transiently transfecting with Flag-δOR or c-myc-δOR alone or expressing both receptors. 24 h after transfection the cells were split into the wells of a 96 well plate with 2.01 ± 0.56 x 10^5 cells per well. No significant energy transfer signal above background was observed after a one hour, room temperature incubation with either 50nM anti-Flag-APC or 10nM anti-c-myc-EuK alone or together ($p > 0.05$).
This graph is a typical representation of two independent experiments performed in triplicate.

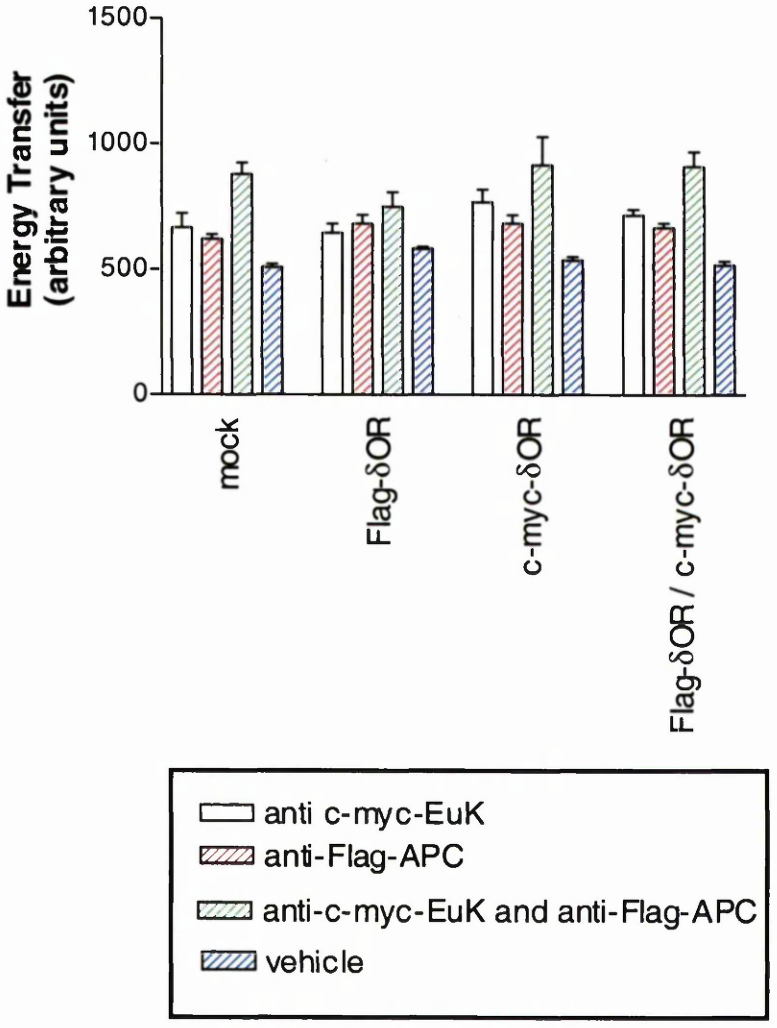

Figure 4.6 No evidence of TR-FRET in cells expressing either Flag-δOR alone or both Flag-δOR and c-myc-δOR

Cells were transiently transfected with either Flag-δOR alone or co-transfected with Flag-δOR and c-myc-δOR and incubated in the presence of 10nM anti-c-myc-EuK antibody and 50nM anti-Flag-APC antibody. The TR-FRET was observed after 1 h and after 14 h at room temperature. No energy transfer was observed above the background. It is likely that this level of background is resulting from fluorescent emission from the EuK alone. This graph is a typical representation of two independent experiments performed in triplicate.

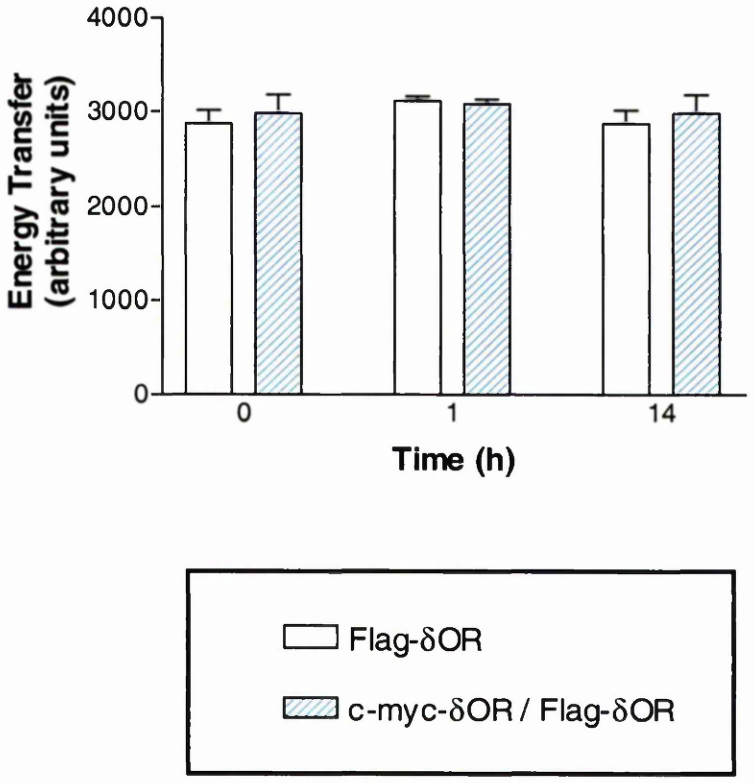

Figure 4.7 Lack of specific anti-c-myc-EuK binding to cells expressing an N-terminal c-myc tagged receptor

HEK293 cells were either mock transfected or transfected with either Flag-δOR or c-myc-δOR. After a 2 h incubation at room temperature, unbound antibody was removed by washing with 2 x 1ml of PBS. The cells were then re-suspended in a 30µl volume and placed in a black 384 well plate and fluorescence intensity read on a Victor^2 fluorescence plate reader.

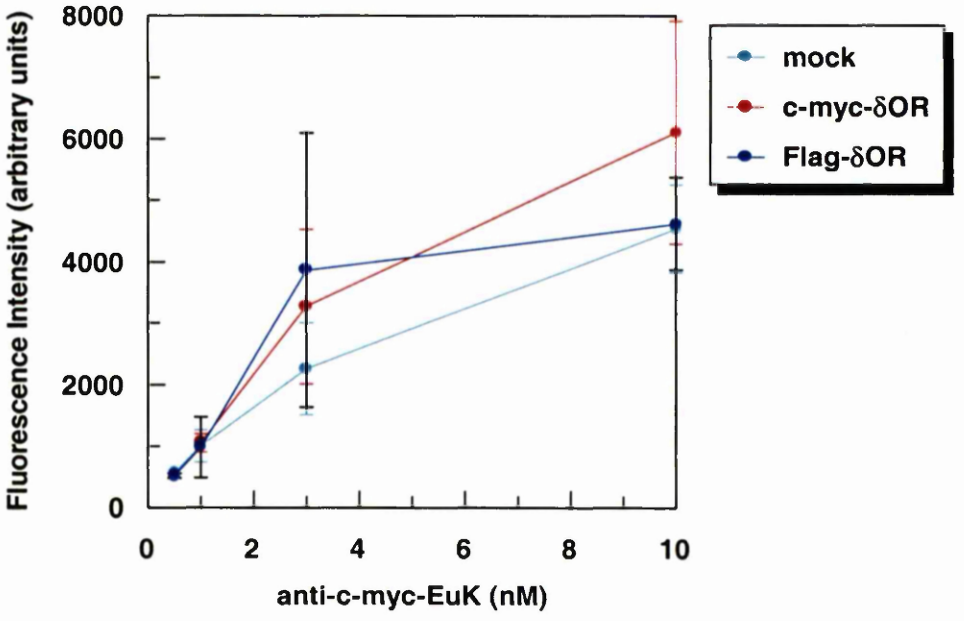

Figure 4.8 Anti-c-myc-FITC antibody binds specifically to cells expressing receptors with an N-terminal c-myc-tag.

The rabbit polyclonal anti-c-myc antibody (9E10), which is commercially available labelled with FITC, was used to measure specific binding on live cells which were either mock transfected or transfected with Flag-δOR or c-myc-δOR.

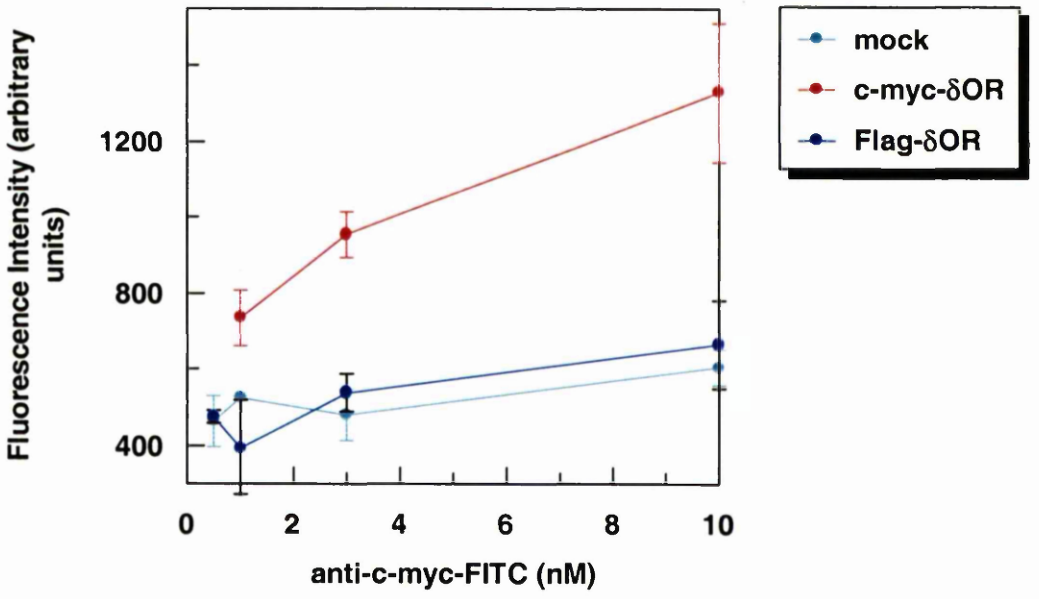

Figure 4.9 **Fluorescence intensity of anti-c-myc antibody labelled with Europium cryptate (EuK) and anti-c-myc antibody labelled with Fluorescein isothiocyanate (FITC).**

Antibodies were diluted in PBS in the presence of 5 x 10^5 HEK293 cells in a total volume of 30µl and the respective fluorescence intensities measured. For EuK the excitation wavelength was 320nm, the emission being measured at 615nm. For FITC the excitation wavelength was 535nm, emission being measured at 590nm. The fluorescence intensity of the EuK labelled antibody is much greater than that of the FITC labelled antibody at the conditions used (the results plotted for the EuK labelled antibody are divided by 100 to allow both sets of data to be plotted on the same graph).

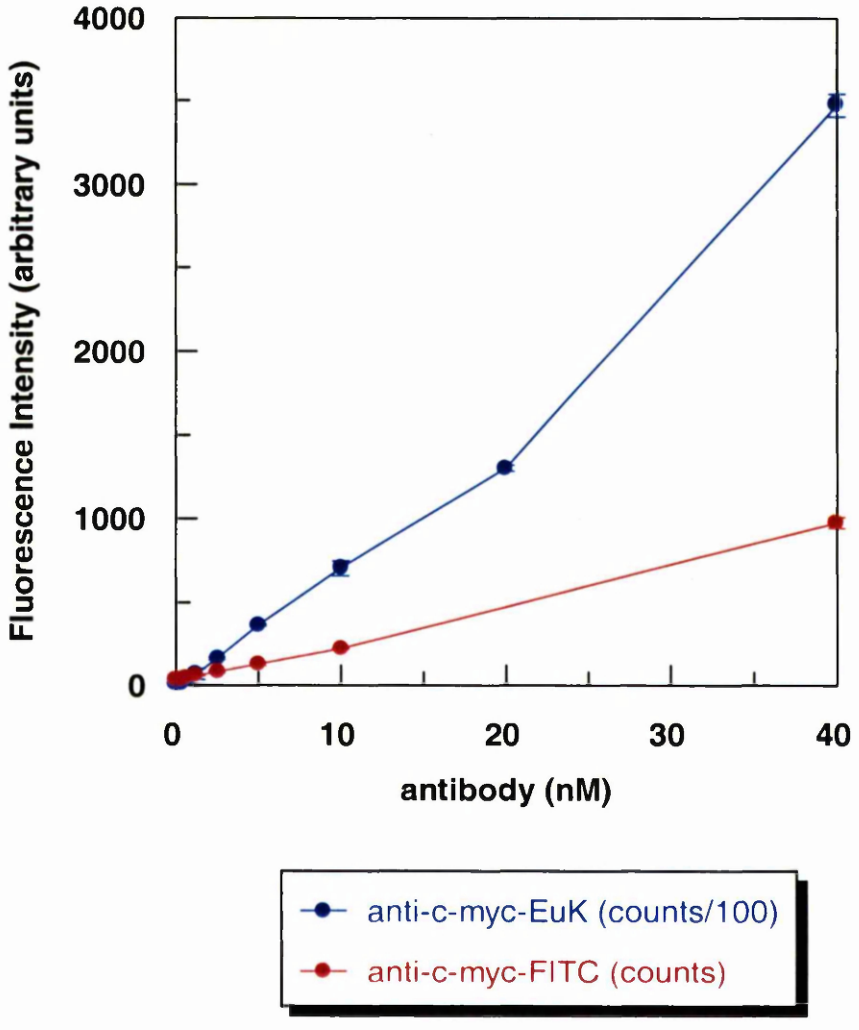

Figure 4.10 No energy transfer signal is obtained from cells expressing both Flag-δOR and c-myc-δOR in the presence of anti-Flag-Cy3 antibody and anti-c-myc-FITC antibody.

HEK293 cells were either mock transfected or transiently transfected with either Flag-δOR alone or with both Flag-δOR and c-myc-δOR and incubated in the presence of 4nM anti-c-myc-FITC antibody and 20nM anti-Flag-Cy3 antibody. The energy transfer signal observed is shown in A. The corresponding FITC fluorescence emission at 535nm is shown in B. The results shown are the mean ± S.E.M. of three independent experiments performed in duplicate.

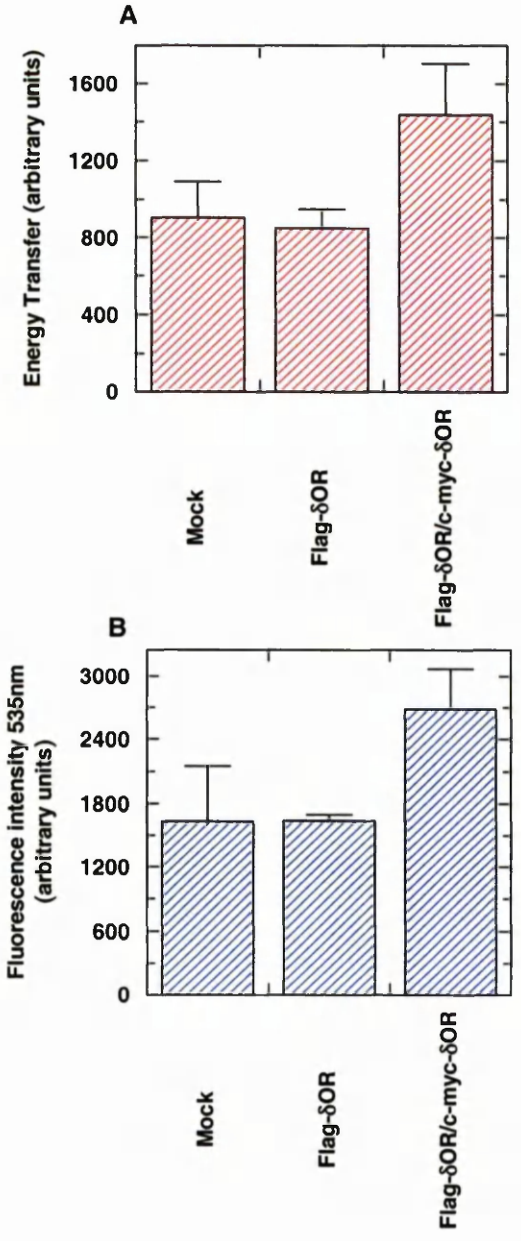

Figure 4.11 Fluorescence intensity of anti-c-myc-EuK alone at 665nm after excitation at 320nm

A standard curve of 0-40nM anti-c-myc-EuK was set-up in the presence and absence of 5 x 10^5 HEK293 cells in a total volume of 30µl PBS. The samples were excited at 320nm and emission measured at 615 and 665nm.

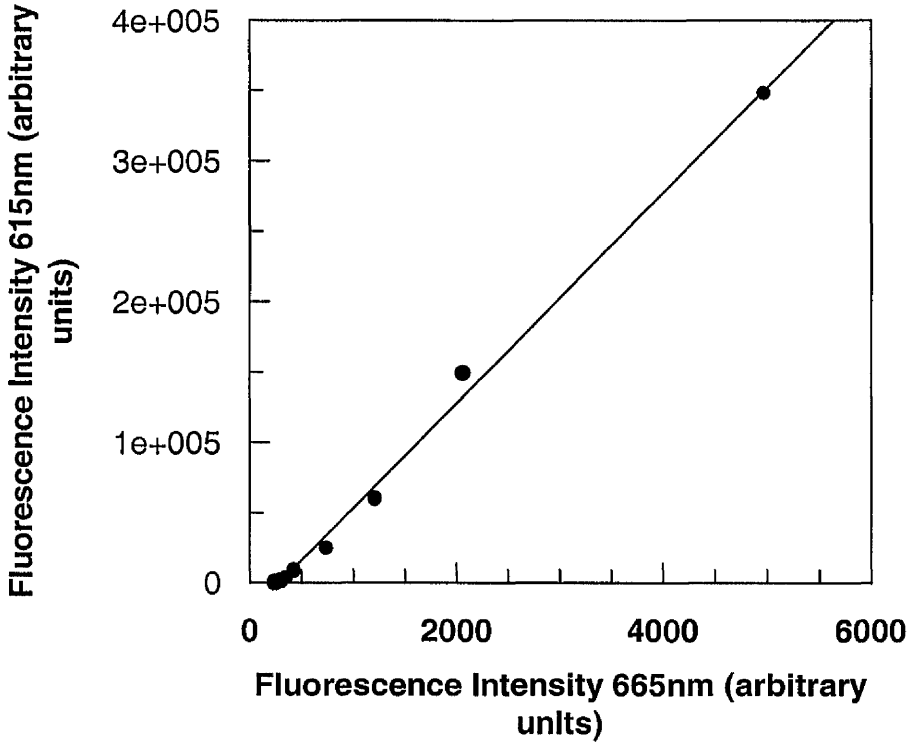

Figure 4.12 Anti-c-myc-Eu^{3+} specifically binds to cells expressing receptors with an N-terminal c-myc-tag.

5 x 10^5 HEK293 cells were either mock transfected or transfected with Flag-δOR or c-myc-δOR, were incubated at room temperature with increasing amounts of anti-c-myc-Eu^{3+}. The fluorescence intensity of the antibody associated with the cells was determined after a 2 hour room temperature incubation after removing the unbound antibody with 2 x 1ml washes with PBS. The fluorescence intensity at **A**. 615nm and **B**. at 665nm are shown.

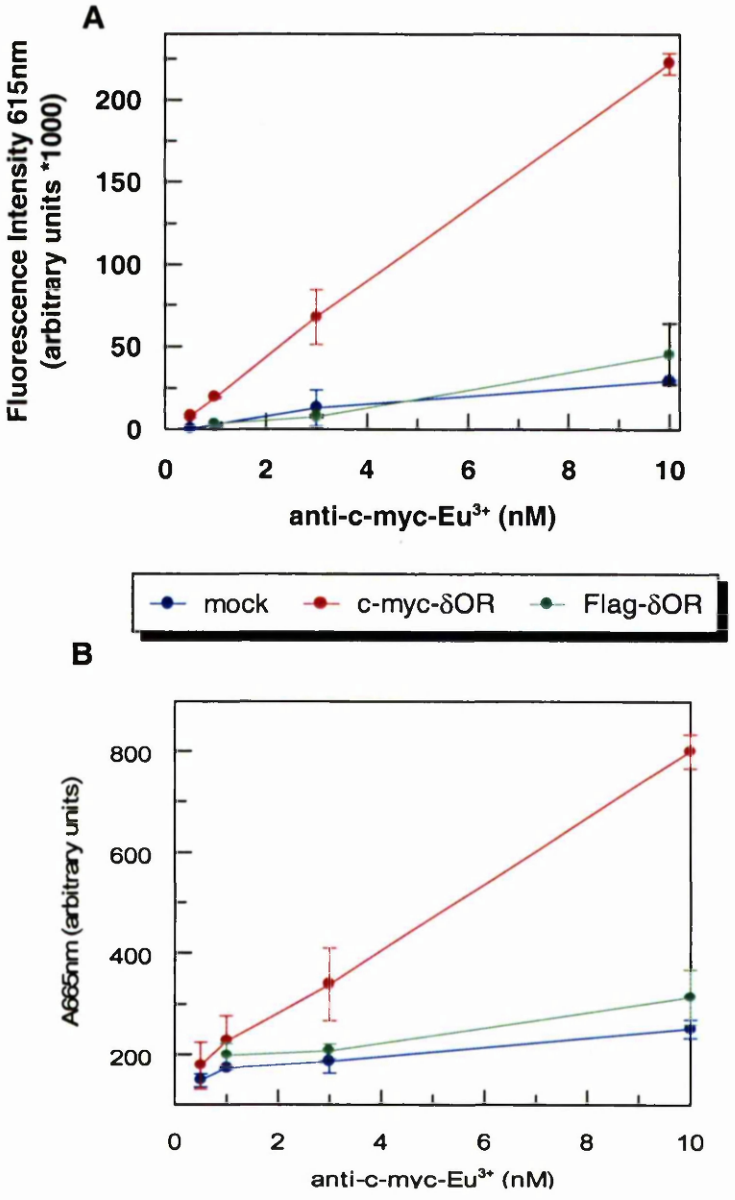

4.3 Discussion

There are only a few methods available that allow protein-protein interactions to be examined within live cells. The yeast Two-Hybrid system has been used successfully to identify intracellular protein-protein interactions (Wang et al., 1995). A drawback to this system is that the interaction has to occur within the yeast nucleus therefore interactions which involve secondary manipulation (e.g. palmitoylation) or compartmentalization are unlikely to be identified using this system. The technique of FRET was chosen here, a related technique known as BRET has previously been used to determine GPCR dimerization. Angers at al. (2000) demonstrated β_2AR homodimerization using BRET, McVey et al. (2001) have also shown homodimerization of the δOR using BRET. The FRET and BRET systems are much more suitable for identifying protein-protein interactions between or with transmembrane proteins such as GPCRs as they can be used in mammalian cells.

The co-immunoprecipitation technique used and described in chapter 3 along with BRET, does not provide any information on where the interaction between the receptors is occurring. Using antibodies which label cell-surface receptors allows the receptor interactions occurring at the cell-surface to be followed in isolation.

The availability of suitable reagents plays a major role in the assay format to be used. At the time when these experiments were performed there was not a commercially available, fluorescently labelled, pair of anti-Flag and anti-c-myc antibodies which could be used for TR-FRET. It was possible, however, to use a commercially available anti-c-myc antibody that was labelled with Europium cryptate ions as the fluorescent donor.

A fluorescent acceptor for Europium is APC and it was possible to obtain APC in a stabilised form, which allowed it to be used to label an anti-Flag antibody. The labelling of the anti-Flag (M5) antibody gave a stoichiometry of 0.63 molecules of APC bound per antibody molecule. This indicates that there is some unlabelled

antibody in this mixture. The value of 0.63 was not included in the calculations for the amount of anti-Flag antibody added to each preparation. Reduction of the antibody molecule results in exposure of free sulfhydryl groups allowing the APC to link covalently via its maleimide group. It is unusual to obtain more than one molecule of APC binding to antibody molecules due to steric hindrances as APC is a large molecule of approximately 100kDa.

It was essential to ensure that the labelling procedure did not alter the binding properties of the anti-Flag antibody and this was shown to be the case (figure 4.2) where specific antibody binding to cells expressing an N-terminally Flag tagged receptor is demonstrated. The specific antibody binding also indicates the sensitivity of the fluorescent antibody as the cells were transiently transfected, (see Chapter 3 about low expression levels with transient expression of opioid receptors).

Only a certain proportion of receptor homodimers can provide a signal using this method. They are those containing both a Flag-δOR and a c-myc-δOR. There will, however, be monomeric receptors as well as homodimers containing the Flag-δOR only and homodimers of the c-myc-δOR only present in the cells. Neither of these combinations can give rise to an energy transfer signal. The proportion of the receptor monomers to dimers is not known.

For TR-FRET assays a homogeneous assay format would be preferred as there would be few manipulations of the cells and no separation of the bound from the free antibody would be necessary. However, the lack of an energy transfer signal in a homogeneous assay did not allow the assessment of individual antibody binding. The level of donor fluorescence used has to be carefully optimized to ensure the emission of the donor itself does not mask any true TR-FRET signal which may occur. A homogeneous assay format was tried using either cell-lysates, which had previously been successfully used in co-immunoprecipitation experiments (figure 3.10), or whole cells which were adhered to the surface of a 96 well plate (figure 4.4). No useful information could be gained from these experiments. It was decided not to continue with this homogeneous assay and

try many variables but to assess the individual components, including individual antibody binding, cell number and antibody concentration in a heterogeneous assay format.

The heterogeneous assay was performed in the wells of a 96 well plate and again no signal was obtained. The lack of signal did not result from loss of cells from the wells as the cells were removed from the wells and counted after measurement of the TR-FRET signal. By assessing the emission of the anti-c-myc-EuK at 665nm after excitation at 340nm (figure 4.5) it was decided that the values obtained derived from the anti-c-myc-EuK only and did not represent energy transfer.

The commercially available anti-c-myc-EuK antibody was assessed for specific binding and was found not to bind specifically to cells expressing N-terminal c-myc tagged opioid receptors. This was confirmed by comparison with an anti-c-myc antibody which was commercially available labelled with FITC. (figures 4.7 and 4.8). The anti-c-myc antibody labelled with EuK or FITC was the widely used polyclonal rabbit antibody 9E10. It can be concluded therefore that the labelling of the antibody with the Europium cryptate has disrupted the antibody binding site or that this antibody was not stored under appropriate conditions and the label was no longer associated with the antibody, or the antibody itself has degraded. The anti-c-myc antibody labelled with Europium cryptate had been used by Farrar et al. (1999) to determine the sub-unit stoichiometry of the $GABA_A$ receptor. Attempts to obtain another batch or more of the same batch failed. Others have also had problems with this antibody (personal communication).

The lack of suitable antibodies for TR-FRET led to the attempt of a FRET assay using anti-c-myc-FITC as the donor with anti-Flag-Cy3 as the fluorescent acceptor. The anti-Flag-Cy3 was labelled according to the maufacturers' instructions. The stoichiometry of labelling was found to be 7.1 molecules of Cy3 per antibody molecule.

Using FRET to determine δOR homodimerization is shown in figure 4.10, and an energy transfer signal was detected for cells which express both Flag-δOR and c-myc-δOR and in the presence of both antibodies. Further investigation into the level of the donor antibody binding and its associated fluorescence intensity at 590nm indicated, however, that the energy transfer signal was a false one and that the energy transfer signal observed was the result of increased anti-c-myc-FITC binding only. It is possible with further assay development and the use of careful controls that this assay format may be used to measure receptor-receptor interaction using live cells. However as another source of anti-c-myc, Europium labelled antibody was identified further work was performed to try again to develop a TR-FRET assay for cell-surface homodimerization of the δOR.

Anti-c-myc-Eu^{3+} binding specificity was assessed (figure 4.12) and specific anti-c-myc-Eu^{3+} binding to cells expressing only c-myc-δOR was demonstrated. The fluorescence emission at 615nm and 665nm of the anti-c-myc-Eu^{3+}, after excitation at 320nm, is shown in 4.12 B. The observed emission at 665nm from the Eu^{3+}-labelled anti-c-myc antibody, though only evident at high levels of antibody, should be considered in design of future assay conditions using this antibody. Further TR-FRET assays can be performed using this new source of anti-c-myc-Eu3+ as the donor and the previously labelled anti-Flag-APC. Such experiments were performed and are presented and discussed in chapter 5.

CHAPTER 5

Investigation of opioid receptor homo- and heterodimerization in intact cells using time-resolved fluorescence resonance energy transfer

CHAPTER 5

Investigation of δ-OR homo and heterodimerization in intact cells using time-resolved fluorescence resonance energy transfer

5.1 Introduction

The existence of opioid receptor dimers *in vivo* was suggested by Hazum et al., (1982) by demonstrating that dimeric morphine and enkephalin agonists bound with higher affinity to the μOR and δOR in membranes. The dimeric forms of agonist also showed higher activity in a guinea-pig ileum assay than the monomeric agonist species. Physical interaction between the opioid receptor species was not demonstrated until much later. δOR receptor homodimerization was demonstrated by Cvejic and Devi (1997) by co-immunoprecipitation of differentially tagged mouse δORs in COS and CHO cell lines. Homodimers of the human δOR have been confirmed in HEK293 cells and have been described in chapter 3. Homodimerization of the rat κOR was shown by Jordan and Devi (1999), who expressed the receptor in HEK293 or COS cells. Homodimerization of the rat μOR was shown in HEK293 cells by George et al. (2000).

The pharmacology for the opioid receptors suggests a larger number of receptor subtypes that have been identified by molecular analysis. This could mean there are opioid receptors not yet identified. It could also indicate that the opioid receptors interact with each other in a functional manner, providing the different receptor pharmacologies. δOR and μOR have been identified in the dorsal root ganglia by Fields et al. (1980) and have been shown to exist in the same plasmalemma of these neurones by Cheng et al. (1997). The κOR has also been identified in similar regions of the brain as the other opioid receptors (Arvidsson et al., 1995). The level of expression of each receptor sub-type and the level of interaction between them *in vivo* may then affect the observed pharmacology.

The first demonstration of physical heterodimerization of the δOR with the κOR was by Jordan and Devi (1999) using HEK293, COS or CHO cells. The heterodimer was shown by co-immunoprecipitation of differentially tagged receptors. The presence of μOR:κOR heterodimers was looked for but no such heterodimer was found. Two independent studies have recently shown a heterodimeric δOR:μOR receptor species, using co-immunoprecipitation techniques (Gomes et al., 2000, George et al., 2000).

Receptor pharmacology of the δOR:κOR heterodimers was investigated in comparison with the individually expressed receptors. By using selective agonists and antagonists the pharmacology of each receptor present in the dimer was investigated. Highly selective δ or κ agonists or antagonists demonstrated poor binding affinity for the δOR:κOR heterodimer. However, partially selective ligands for the individual receptors demonstrated high affinity binding for the δOR:κOR heterodimer. The rank order of ligand binding was also altered for the δOR:μOR heterodimer compared to the monomeric receptor species (Jordan and Devi, 1999). Ligand synergy, when the binding of a ligand to one receptor of the dimer is enhanced by the presence of a ligand to the other receptor, was observed for both the δOR;κOR heterodimer (Jordan and Devi, 1999). The observed synergy for the δOR:μOR heterodimer was ligand specific (Gomes et al., 2000, George et al., 2000). Ligand synergy was also demonstrated in the neuroblastoma cell line SKNSH which endogenously express both δOR and μOR (Gomes et al., 2000). Synergy with two selective antagonists was demonstrated for δOR:κOR heterodimers, however no such synergy was observed when a combination of a κOR selective agonist and a δOR selective antagonist was used. These studies indicate that the opioid receptor heterodimers have a distinct binding site from the individual receptors. This results in the distinct pharmacology of the heterodimer, it has been suggested by Jordan and Devi (1999) that the δOR:κOR heterodimer corresponds to the pharmacology of the κ-2 receptor sub-type described by Zukin et al. (1988).

A possible role for receptor dimerization in receptor trafficking also has been indicated by co-expression of mutant and wild type receptors in the same cell. The data on opioid receptor heterodimers complies with this suggestion in the following manner. δOR is internalized by etorphine when expressed alone but no significant internalization of δOR is evident when it is expressed with κOR. Internalization of the κOR is not induced by etorphine either when expressed alone or with the δOR (Jordan and Devi, 1999) and the rate of internalization of the δOR:μOR heterodimer was different from that for receptors expressed alone (Gomes et al., 2000, George et al., 2000).

As discussed in Chapter 1 there is no consensus in the literature as to regions of receptor directly involved in dimerization. The C-terminus of the δOR was shown to be involved in homodimerization as a15-residue C-terminal truncated form of the receptor did not form homodimers and did not internalize on agonist stimulation (Cvejic and Devi, 1997). This is a further indication that dimerization and internalization may be linked. A heterodimer between δOR and a c-terminally truncated μOR, lacking the last 42 amino acids has been demonstrated by Gomes et al., (2000) suggesting that the C-terminus is not important in the interaction of these two opioid receptors. Clearly further work has to be done to elicudate the regions involved in dimerization of the opioid receptors.

In this chapter homodimerization of the δOR using TR-FRET with differentially tagged receptors and antibodies labelled with Eu^{3+} and APC has been studied. This is a heterogeneous format assay performed on transiently transfected HEK293 cells, unless otherwise stated. Cell-surface heterodimerization between δOR and other GPCRs has also been investigated as well as μOR homodimerization. The development of this assay allows the interaction between N-terminally tagged GPCRs at the cell-surface only to be studied in live cells. Fluorescent antibodies have been utilized, which bind to the N-terminally tagged GPCRs. The time-resolved fluorescence resonance energy transfer signal observed indicates that this is a robust assay with a large signal to noise ratio. Some of these results have been published (McVey et al., 2001). Assay

optimization experiments as well as a description of the development of the TR-FRET assay into a homogeneous format have been included.

5.2 Results

δOR : δOR cell surface homodimerization is shown using Time Resolved – Fluorescence Resonance Energy transfer (TR-FRET)

HEK293 cells transiently transfected with δOR with an N-terminal c-myc epitope tag and with δOR with an N-terminal Flag epitope tag were assessed for homodimerization using TR-FRET as described in section 2.4.5. A statistically significant energy transfer signal ($p < 0.05$) was obtained when both receptors were expressed in the same cell (figure 5.1A). Co-expression of appropriately tagged pairs of δOR and β_2AR was also performed, however, the TR-FRET signal obtained was not statistically significantly ($p > 0.05$) above the background signal from mock transfected cells. The signal observed when each form of the δOR was expressed alone was no different to mock transfected cells. Mixing cells that expressed the individual receptors also did not result in a statistically significant TR-FRET signal above background ($p > 0.05$). This demonstrated that the presence of both receptors is not enough to generate an energy transfer signal, as both receptors have to be expressed in the same cell and in close proximity to generate a TR-FRET signal.

Individual antibody binding to cells expressing each receptor individually or the combination of Flag-δOR with c-myc-δOR or Flag-β_2AR with c-myc-δOR was assessed via their respective fluorescence intensities (figures 5.1B and 5.1C). The specificity of anti-c-myc-Eu^{3+} binding in a statistically significant manner ($p < 0.05$) was observed in cells expressing c-myc-δOR alone or when co-expressed with Flag-δOR or Flag-β_2AR. Neither Flag-δOR nor Flag-β_2AR transfected cells showed any statistically significant anti-c-myc-Eu^{3+} binding over the level of mock transfected cells ($p > 0.05$). The level of anti-c-myc-Eu^{3+} binding in the presence of Flag-receptors is lower than that when expressed alone, although this difference was not statistically significant ($p > 0.05$). The anti-c-myc-Eu^{3+} binding in the presence of c-myc-δOR, co-expressed with Flag-δOR is not significantly different ($p < 0.05$) to that when c-myc-δOR is co-expressed with Flag-β_2AR (figure 5.1B).

Anti-Flag-APC was also shown to bind specifically to cells expressing Flag-tagged receptors alone over mock transfected cells (figure 5.1C). The level of anti-Flag-APC binding is not significantly different ($p > 0.05$) between the cells co-expressing c-myc-δOR with Flag-δOR or c-myc-δOR with Flag-β_2AR.

Excitation of anti-c-myc-Eu^{3+}, in the presence of 5 x 10^5 HEK293 cells resulted in a fluorescent emission at 665nm as well as 615nm (figure 5.2). To assess the level of fluorescence emission from the anti-c-myc-Eu^{3+} alone at 665nm a standard curve of 0 - 40nM anti-c-myc-Eu^{3+} was produced. Excitation was at 320nm with the fluorescence emission being measured at both 615nm and 665nm. The emission signal at 665nm resulting from anti-c-myc-Eu^{3+} was no greater than 250 when concentrations of up to 10nM anti-c-myc-Eu^{3+} were present. This is within the TR-FRET signal obtained for the mock-transfected cells in the TR-FRET experiments (figure 5.1) i.e. background fluorescence. From these data it can be concluded that the emission signal obtained at 665nm is resulting from energy transfer. The emission signal from the anti-c-myc-Eu^{3+} at 665nm for each experiment can be calculated using the graph in figure 5.1.

Effect of ligands on receptor:receptor interactions as measured by TR-FRET.

The effect of ligands on the homodimerization of δOR:δOR and lack of heterodimerization of δOR:β_2AR was investigated using TR-FRET. No statistically significant effect of 100nM DADLE on the δOR homodimerization level was observed ($p>0.05$). The inverse agonist ICI174,864 (Merkouris et al., 1997) also did not affect the δOR homodimerization level (figure 5.3A) ($p>0.05$). The level of each individual antibody binding was not influenced by the presence of ligand in the incubation mixture (figures 5.3B and 5.3C) in a statistically significant manner ($p > 0.05$).

To investigate whether ligand binding would demonstrate heterodimerization between the δOR and β_2AR a TR-FRET assay was performed. Again no statistically significant effect of DADLE, isoprenaline, or a combination of both

was observed ($p > 0.05$), figure 5.4A. The ligands did not affect the level of each individual antibody binding (figures 5.4B and 5.4C).

Ligand binding can occur in the presence of the fluorescently labelled antibodies.

As the binding of fluorescently labelled antibodies to the N-terminal tag of the cell may obstruct ligand binding a [^{3}H] ligand binding assay was performed in the absence and presence of the fluorescent antibodies. The presence of the fluorescently labelled antibodies did not affect the specific binding of [^{3}H]DADLE, or [^{3}H]naltrindole to the δOR (figure 5.5). Binding of [^{3}H]dihydroalprenalol (DHA) and [^{3}H]GCP12,177 to the Flag-β_2AR-GFP in the absence and presence of isoprenaline was also assessed and no affect of antibody on ligand binding was observed (figure 5.6). This confirmed that the ligands can bind to the receptors in the presence of the fluorescently labelled antibodies. Agonist-stimulated inhibition of adenylyl cyclase was also not significantly disrupted by the presence of the fluorescently labelled antibodies ($p > 0.05$) (Table 5.1).

δOR : μOR heterodimerization

Interaction between δOR and μOR receptors was investigated using transiently transfected HEK293 cells. Although there was a clear indication of heterodimerization with this TR-FRET assay on cells co-transfected with Flag-δOR and c-myc-μOR or with Flag-μOR and c-myc-δOR, this did not achieve statistical significance. The μOR homodimerization signal obtained again was not significantly greater ($p > 0.05$) than that for cells transfected with the individual receptors (figure 5.7).

The level of individual antibody binding was assessed for these experiments and the level of anti-c-myc-Eu^{3+} binding to cells expressing c-myc-μOR and Flag tagged δOR or μOR was not significantly different ($p > 0.05$) to that found for c-myc-δOR co-transfected with Flag tagged δOR or μOR (figure 5.7B). The anti-c-myc-Eu^{3+} binding achieved for cells transfected with c-myc-μOR alone was

significantly lower ($p<0.05$) than that for cells transfected with c-myc-δOR alone (figure 5.7B).

The anti-Flag-APC binding in cells expressing Flag-μOR in the presence of c-myc tagged δOR or μOR was not significantly different ($p > 0.05$) from anti-Flag-APC binding to cells expressing Flag-δOR in the presence of c-myc tagged δOR or μOR (figure 5.7C). However, again when the Flag-μOR was expressed alone there was significantly less ($p < 0.05$) anti-Flag-APC binding observed compared to that for cells expressing Flag-δOR alone (figure 5.7C).

Optimization of the TR-FRET signal obtained from this assay was studied by both transfecting varying levels of each epitope tagged receptor into cells and by varying the levels of labelled antibody included in the incubation (figure 5.8). An increase in anti-c-myc-Eu^{3+} binding was observed with increasing levels of c-myc-δOR (figure 5.8B). The energy transfer increased with the level of c-myc-δOR transfected and with the concentration of fluorescent antibody used (figure 5.8A). As the level of anti-c-myc-Eu^{3+} was also increased a larger proportion of this signal would arise from emission directly from the anti-c-myc-Eu^{3+}, taking this into consideration and using the data shown in figure 5.2, the TR-FRET signal was greater when increasing amounts of transfected c-myc-δOR. There was no significant increase in anti-Flag antibody binding when 3nM or 9nM antibody was present in the incubation (figure 5.8C).

A homogeneous format of this assay was set up to avoid the lengthy process of harvesting the cells, washing and then adding to the 384 well plate. This assay was performed in a 96 well format varying the number of cells added per well. The concentrations of antibodies used were 0.5nM anti-c-myc-Eu^{3+} and 5nM anti-Flag-APC (figure 5.9A) or 1nM anti-c-myc-Eu^{3+} and 3nM anti-Flag-APC (figure 5.9B). The TR-FRET signal was measured each hour up to 3 hours after the addition of antibody. δOR homodimerization was evident at each of the conditions used. The TR-FRET signal was greater with the higher concentration of antibodies was used and increased with the number of cells used. No levels of individual antibody binding were obtained using this assay format.

Figure 5.1 δOR homodimerization is demonstrated on live cells via TR-FRET

HEK293 cells were transiently transfected with Flag-δOR, Flag-β_2AR-GFP or c-myc-δOR alone or transfected with both Flag-δOR and c-myc-δOR or Flag-δOR and Flag-β_2AR-GFP. A mix of cells expressing Flag-δOR alone with cells expressing c-myc-δOR alone was also used. 5 x 10^5 cells were incubated for 2 h at room temperature in the presence of 3nM anti-c-myc-Eu^{3+} and 15nM anti-Flag-APC antibody. After washing with 2 x 1ml of PBS the cells were re-suspended in 30µl PBS and the TR-FRET signal read on a Victor^2 fluorescence plate reader.

A) The energy transfer signal presented are mean ± S.E.M. of four independent experiments. Co-expression of Flag-δOR with c-myc-δOR resulted in a statistically significant level of energy transfer ($p < 0.05$). No such signal was observed when c-myc-δOR was co-expressed with Flag-β_2AR-GFP ($p > 0.05$).

B) Specific binding of anti-c-myc-Eu^{3+} to cells expressing an N-terminal c-myc-tag was statistically significant ($p < 0.05$). Data are mean fluorescence intensity ± S.E.M. for four independent experiments.

C) Specific binding of anti-Flag-APC to cells expressing an N-terminal Flag-tag was statistically significant ($p < 0.05$). Data presented are mean fluorescent intensity ± S.E.M. of four independent experiments.

5.1 A)

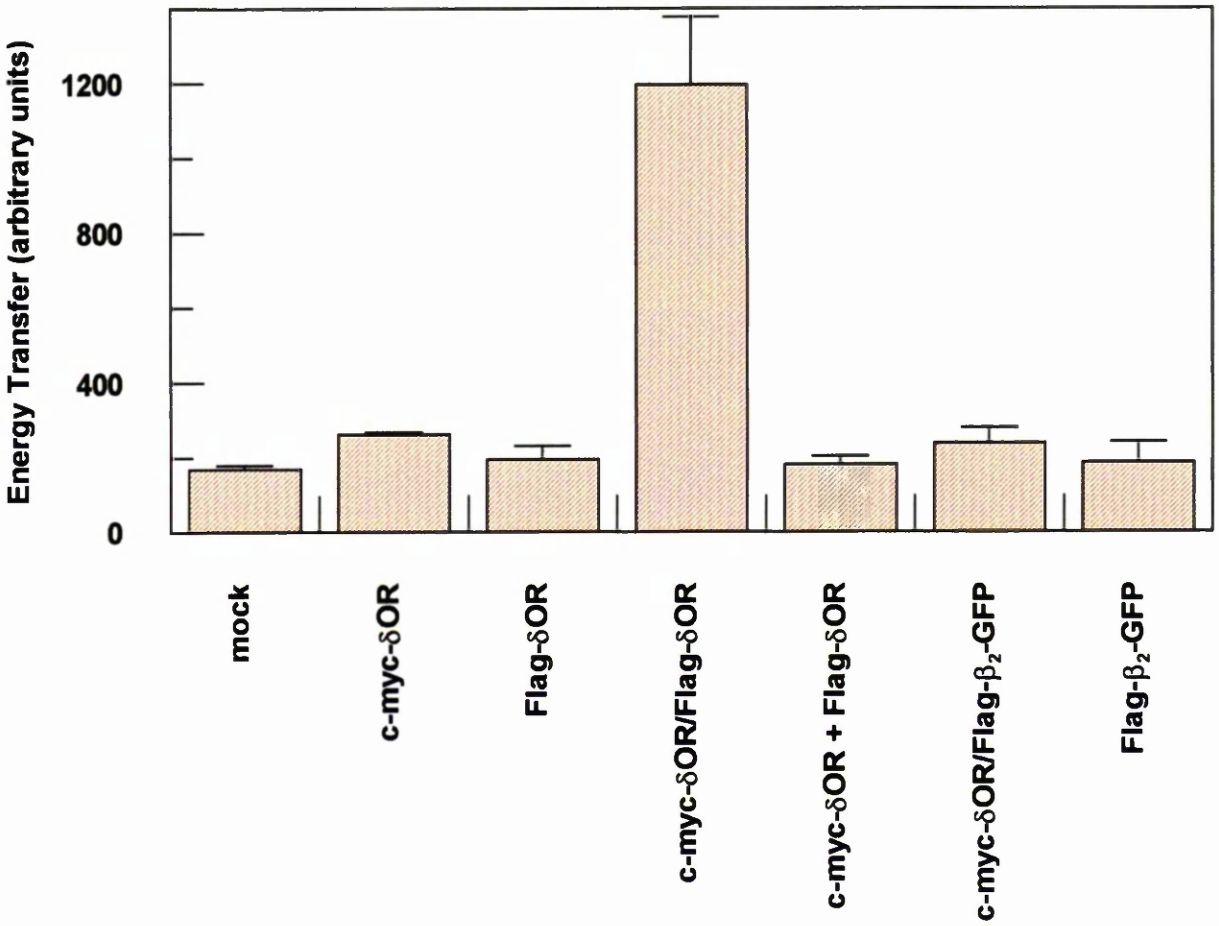
Energy Transfer (arbitrary units)
1200
800
400
0
mock
c-myc-δOR
Flag-δOR
c-myc-δOR/Flag-δOR
c-myc-δOR + Flag-δOR
c-myc-δOR/Flag-β2-GFP
Flag-β2-GFP

5.1 B)

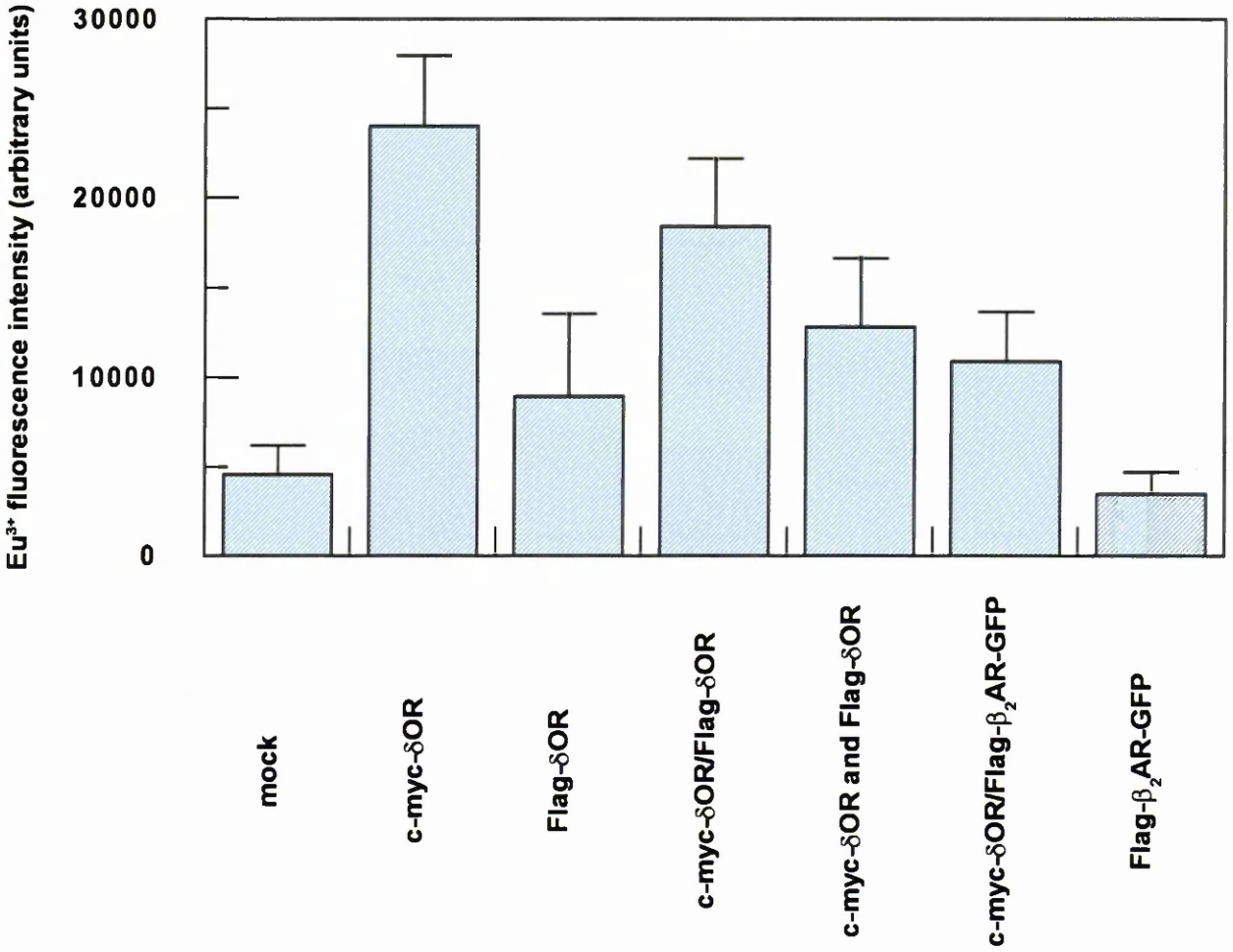
Eu3+ fluorescence intensity (arbitrary units)
30000
20000
10000
0
mock
c-myc-δOR
Flag-δOR
c-myc-δOR/Flag-δOR
c-myc-δOR and Flag-δOR
c-myc-δOR/Flag-β2AR-GFP
Flag-β2AR-GFP

5.1 C)

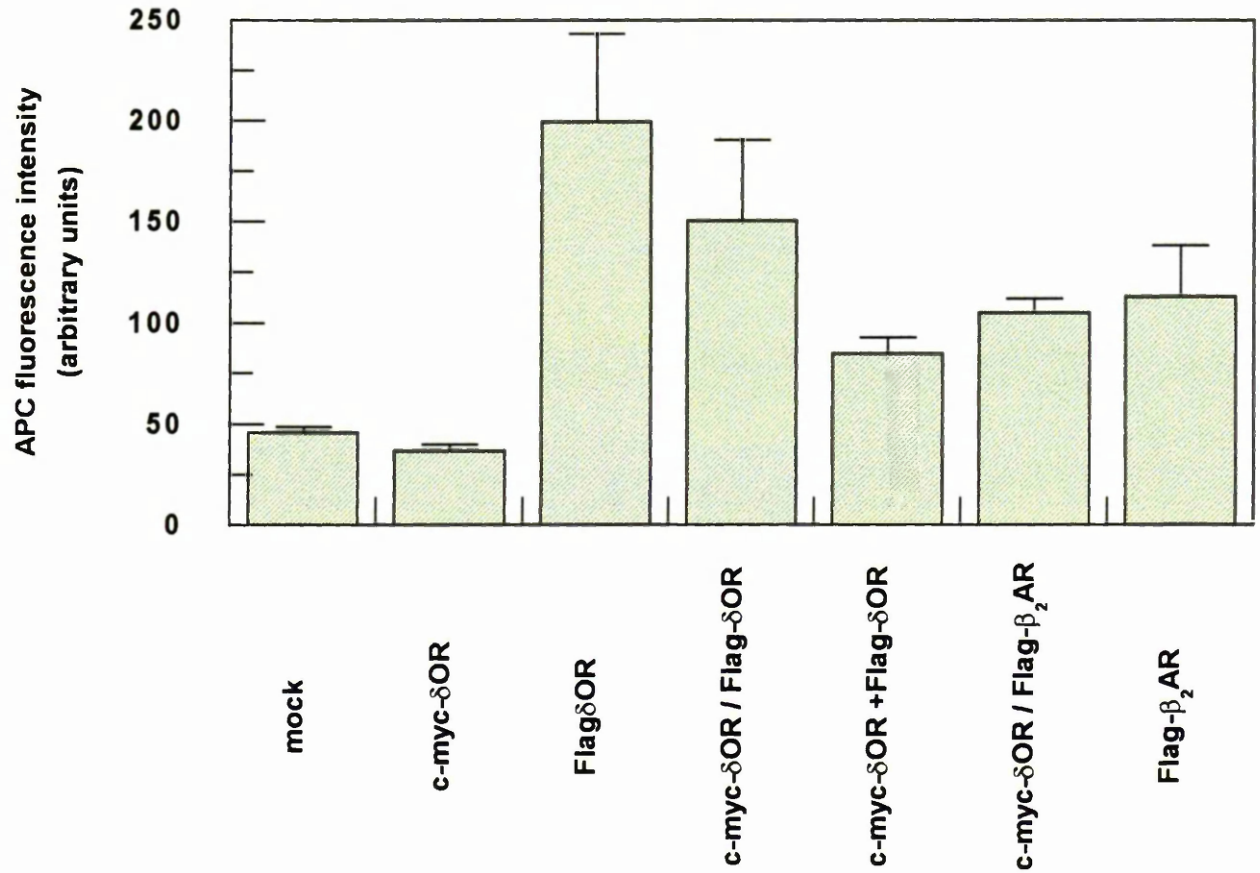
APC fluorescence intensity
(arbitrary units)
250
200
150
100
50
0
mock
c-myc-δOR
FlagδOR
c-myc-δOR / Flag-δOR
c-myc-δOR +Flag-δOR
c-myc-δOR / Flag-β2AR
Flag-β2AR

Figure 5.2 Fluorescence intensity of anti-c-myc-Eu^{3+} at 615nm vs 665nm

A dilution curve of anti-c-myc-Eu^{3+} antibody was set up in a total volume of 30µl in the presence of 5 x 10^5 HEK293 cells. Excitation at 320nm was followed by a 50µs delay and reading for 200µs at both 615 and 665nm. A linear relationship between the emissions at each wavelength exists. This can be used to determine what fraction of the energy transfer signal obtained is from excitation of the Eu^{3+} itself. This value can then be subtracted to give the true energy transfer signal. The data is plotted on a linear scale to show the relationship of the emission at the two wavelengths and on a logarithmic scale to show more clearly the level of anti-c-myc-Eu^{3+} antibody binding needed to give an energy transfer signal of 1000-2000 units under the conditions used.

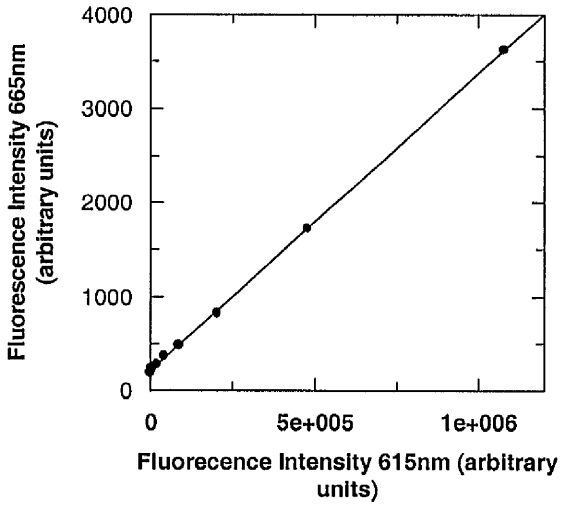

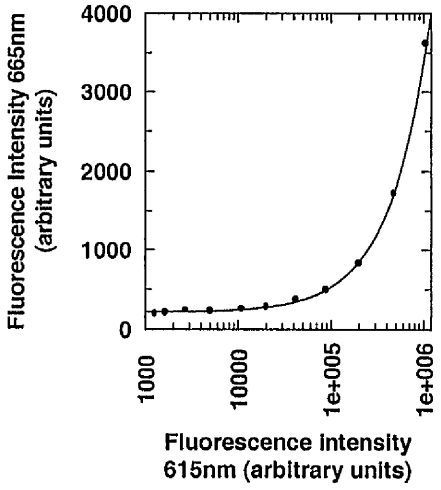

Figure 5.3 Lack of ligand effect on δOR homo-dimerization

5 x 10^5 HEK293 cells transiently expressing Flag-δOR and c-myc-δOR were incubated for 2 h at room temperature in the presence of anti-Flag-APC antibodies and anti-c-myc-Eu^{3+} antibodies. The effect of ligands was investigated by inclusion in the 2 h incubation of the δOR peptide agonist DADLE, the δOR inverse agonist ICI 174,864 or the β_2AR agonist isoprenaline. Each agonist was used at a final concentration of 100nM.

No effect of ligand was demonstrated on :

A) The energy transfer signal, resulting from δOR homodimerization ($p > 0.05$). The data are the mean energy transfer signal ± S.E.M. of three independent experiments performed in triplicate.

B) The anti-c-myc-Eu^{3+} binding to the cells ($p > 0.05$). The data are the mean fluorescence intensity ± S.E.M of three independent experiments performed in triplicate.

C) The anti-Flag-APC antibody binding to the cells ($p > 0.05$). The data are the mean fluorescence intensity ± S.E.M. of three independent experiments performed in triplicate.

5.3 A)

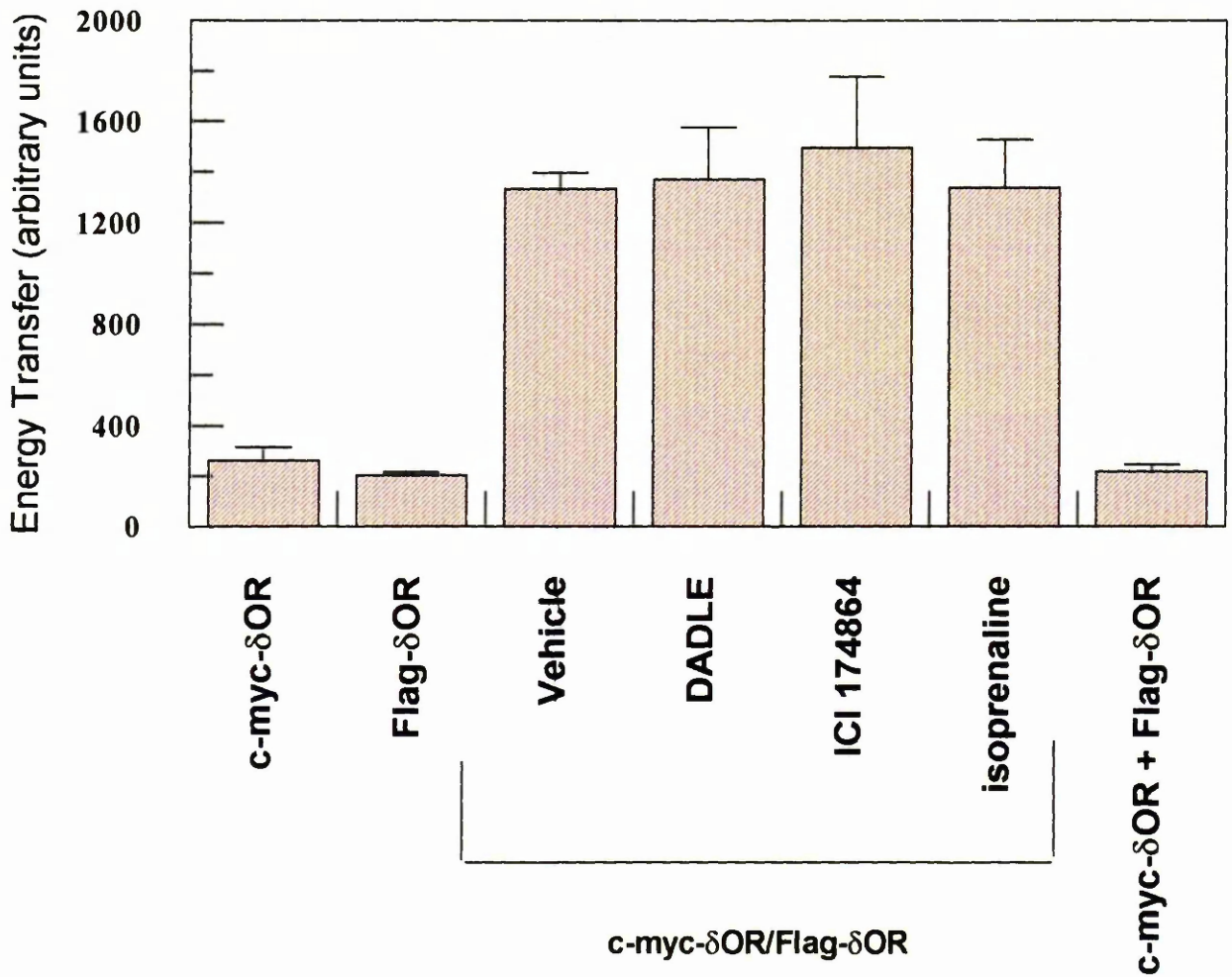
Energy Transfer (arbitrary units)
2000
1600
1200
800
400
0
c-myc-δOR
Flag-δOR
Vehicle
DADLE
ICI 174864
isoprenaline
c-myc-δOR + Flag-δOR
c-myc-δOR/Flag-δOR

5.3 B)

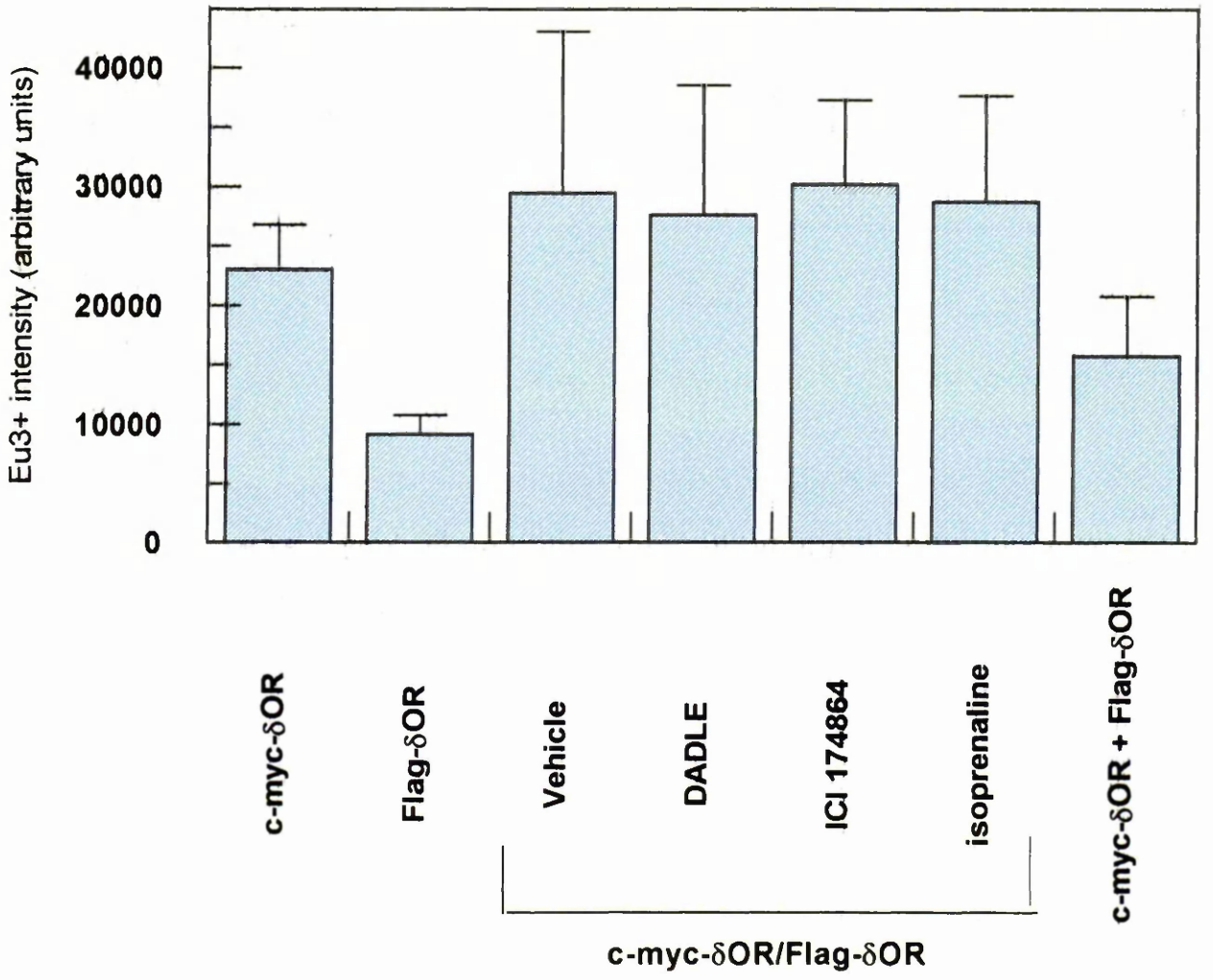
Eu3+ intensity (arbitrary units)
40000
30000
20000
10000
0
c-myc-δOR
Flag-δOR
Vehicle
DADLE
ICI 174864
isoprenaline
c-myc-δOR + Flag-δOR
c-myc-δOR/Flag-δOR

5.3 C)

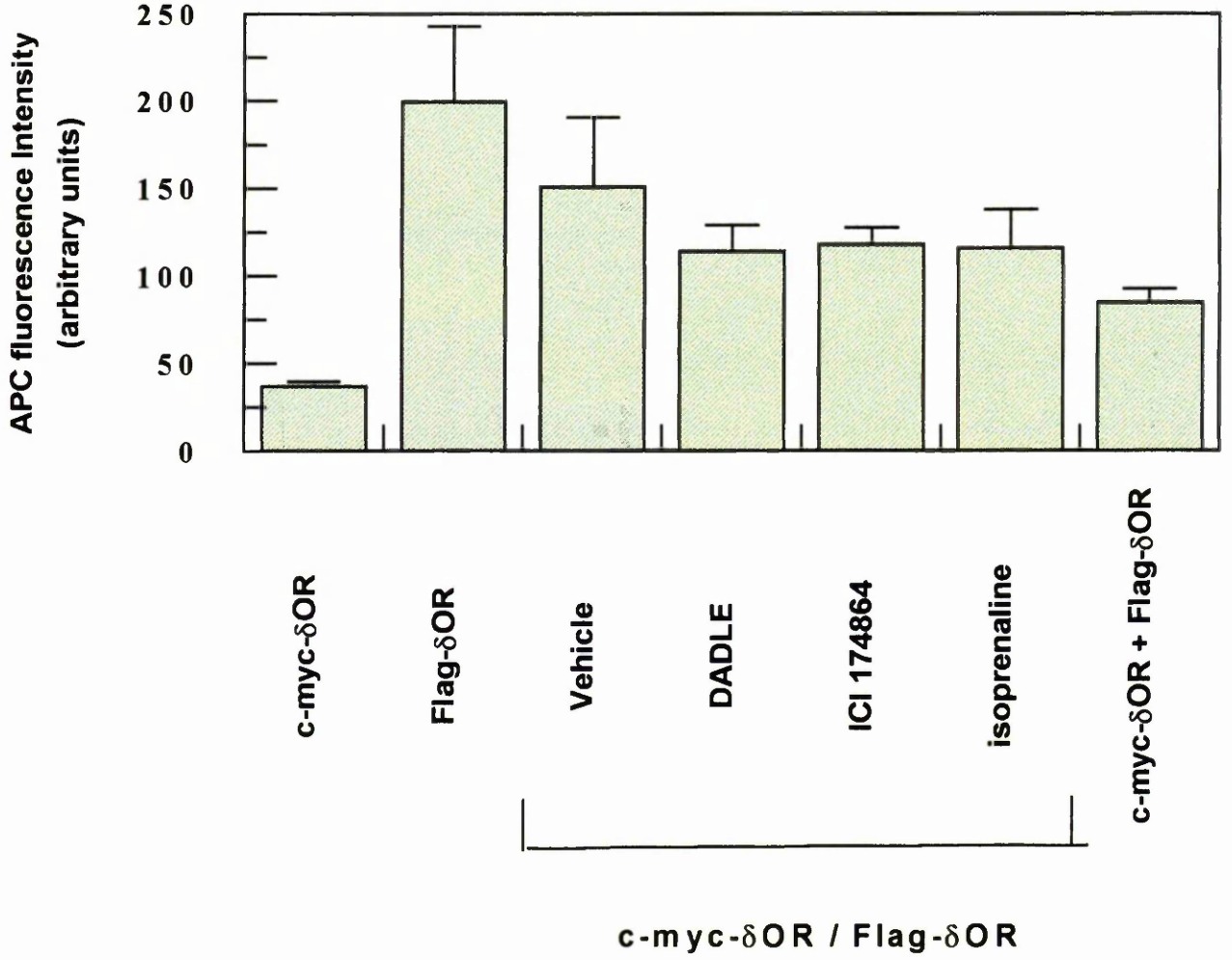
APC fluorescence Intensity
(arbitrary units)
250
200
150
100
50
0
c-myc-δOR
Flag-δOR
Vehicle
DADLE
ICI 174864
isoprenaline
c-myc-δOR + Flag-δOR
c-myc-δOR / Flag-δOR

Figure 5.4 Lack of ligand effect on δOR : β_2AR hetero-dimerization

5 x 10^5 HEK293 cells transiently expressing Flag-β_2AR and c-myc-δOR were incubated for 2 h at room temperature in the presence of anti-Flag-APC antibodies and anti-c-myc-Eu^{3+} antibodies. The effect of ligands was investigated by inclusion in the 2 h incubation of the δOR peptide agonist DADLE, or the β_2AR agonist isoprenaline, or a combination of both DADLE and isoprenaline. Each agonist was used at a final concentration of 100nM.

No effect of ligand was demonstrated on :

A) The energy transfer signal ($p > 0.05$). The data are the mean energy transfer signal ± S.E.M. of three independent experiments performed in triplicate.

B) The anti-c-myc-Eu^{3+} bindng to the cells ($p > 0.05$). The data are the mean fluorescence intensity ± S.E.M. of three independent experiments performed in triplicate.

C) The anti-Flag-APC antibody binding to the cells ($p > 0.05$). The data are the fluorescence intensity ± S.E.M. of three independent experiments performed in triplicate.

5.4 A)

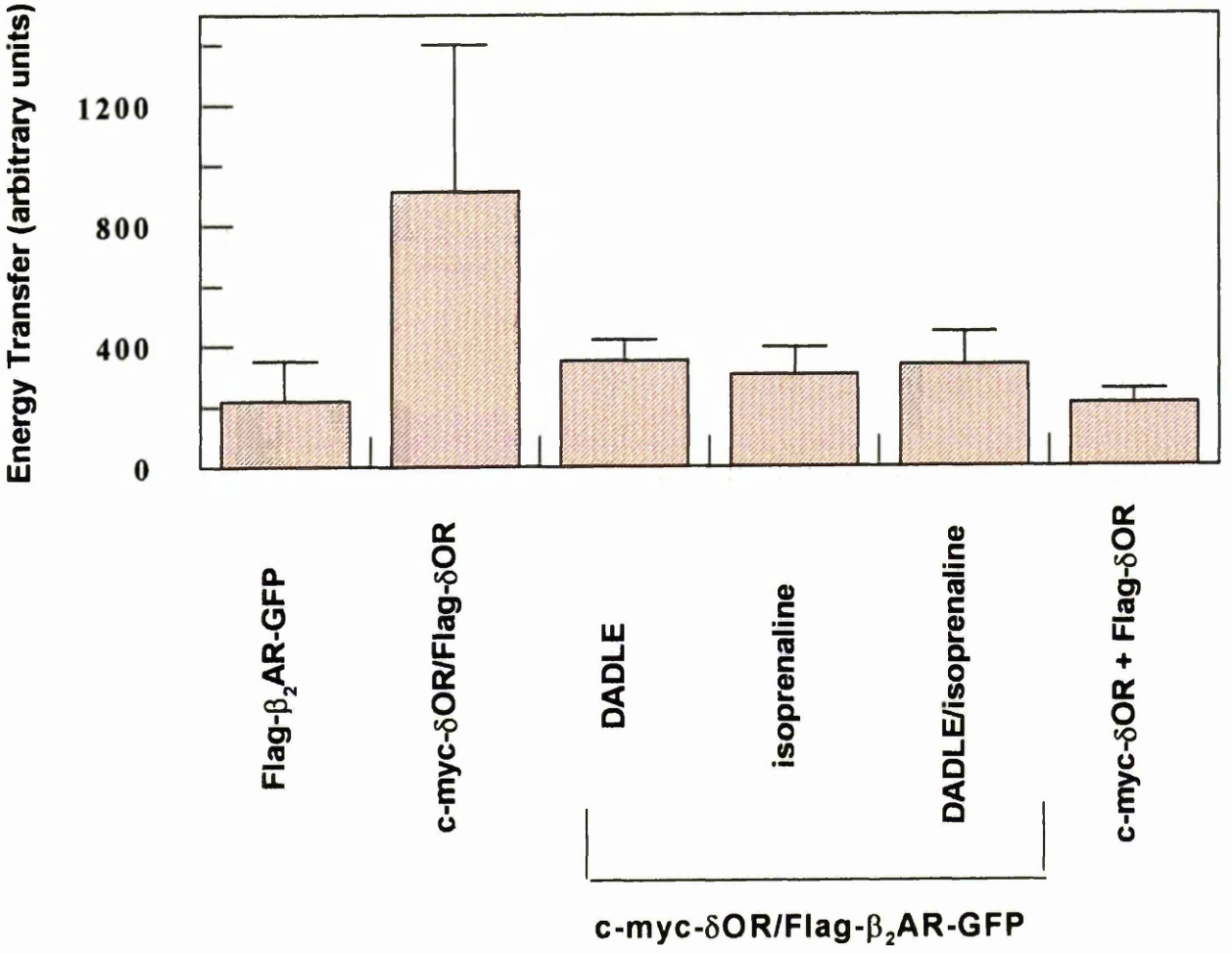
Energy Transfer (arbitrary units)
1200
800
400
0
Flag-β2AR-GFP
c-myc-δOR/Flag-δOR
DADLE
isoprenaline
DADLE/isoprenaline
c-myc-δOR + Flag-δOR
c-myc-δOR/Flag-β2AR-GFP

5.4 B)

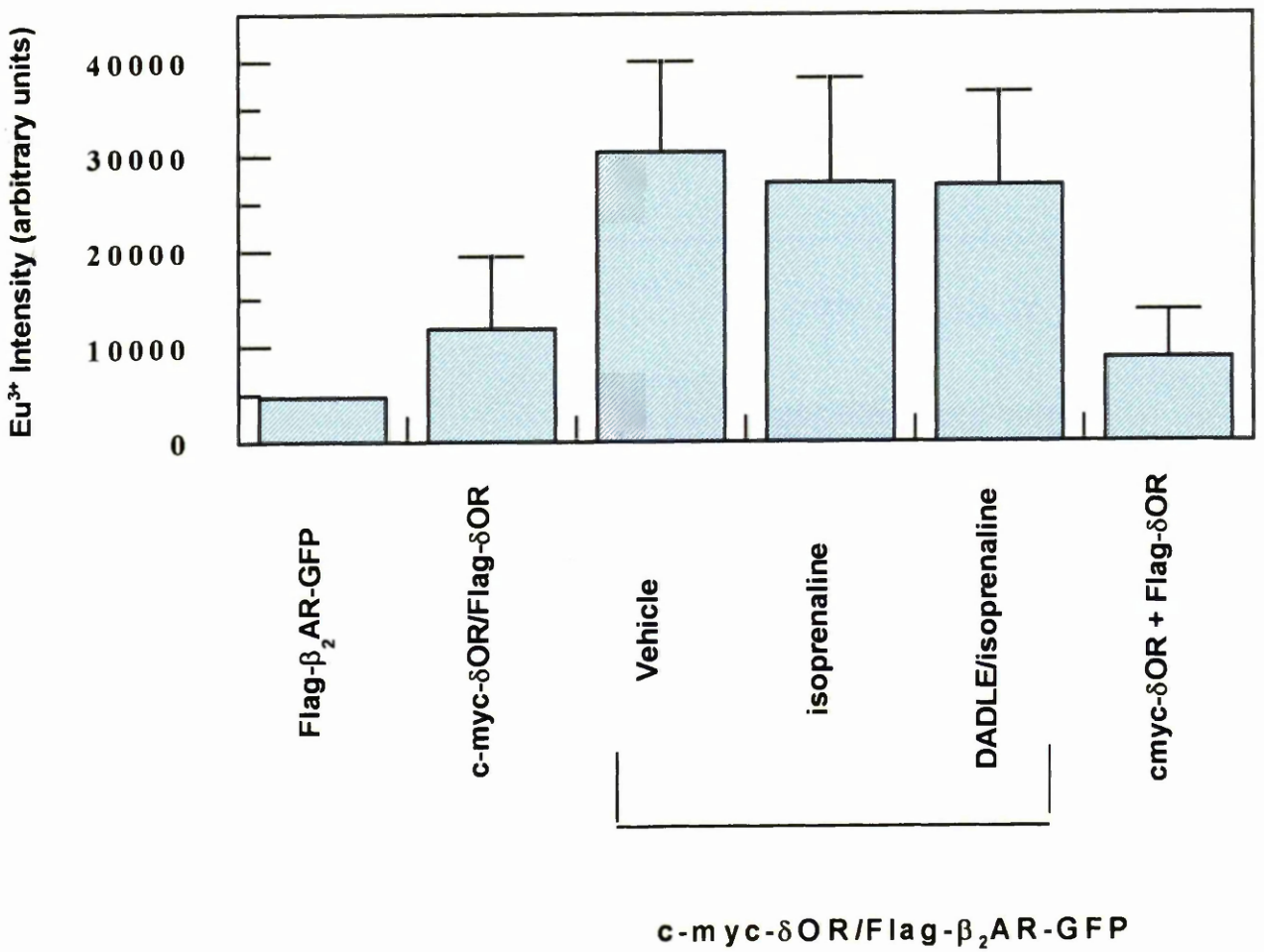
Eu3+ Intensity (arbitrary units)
40000
30000
20000
10000
0
Flag-β2AR-GFP
c-myc-δOR/Flag-δOR
Vehicle
isoprenaline
DADLE/isoprenaline
cmyc-δOR + Flag-δOR
c-myc-δOR/Flag-β2AR-GFP

5.4 C)

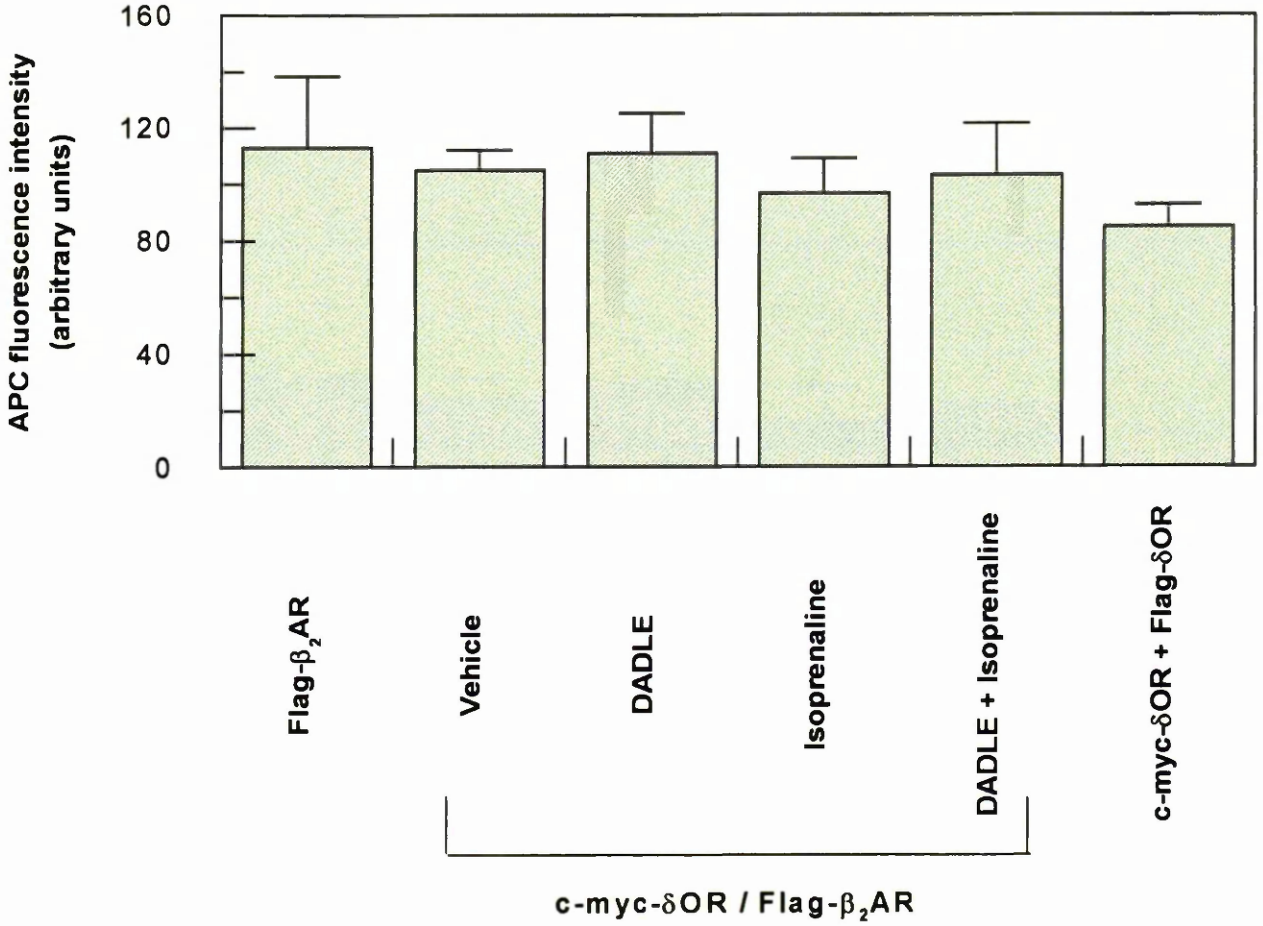
APC fluorescence intensity (arbitrary units)
160
120
80
40
0
Flag-β2AR
Vehicle
DADLE
Isoprenaline
DADLE + Isoprenaline
c-myc-δOR + Flag-δOR
c-myc-δOR / Flag-β2AR

Figure 5.5 Effect of antibodies on [^{3}H]ligand binding to cells expressing δORs

Binding experiments with a single high concentration of the agonist [^{3}H]DADLE (5nM) or the antagonist [^{3}H]naltrindole (5nM) were performed under conditions used for the TR-FRET assay to determine whether the presence of antibodies affected ligand binding. 300μM naloxone was used to determine non-specific binding. The antibodies did not have any significant effect on the level of radioligand binding ($p > 0.05$).

The data shown are the mean ± S.E.M. for three independent experiments.

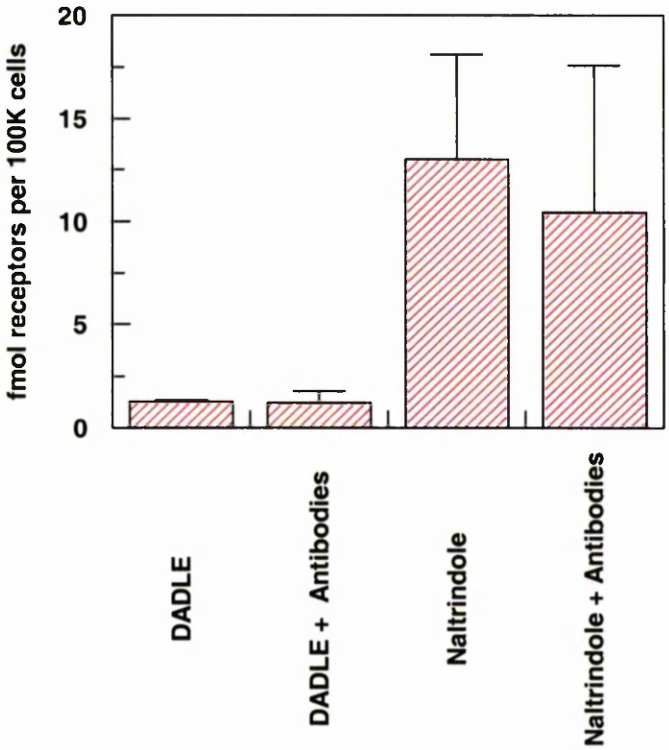

Figure 5.6 Effect of antibodies on [^{3}H] ligand binding to cells expressing δOR and β_2AR-GFP

Saturation binding experiments for the antagonist [^{3}H] CGP12177 (10nM) and [^{3}H] dihydroalprenolol (2nM) were performed under conditions used for the TR-FRET assay to determine whether the presence of antibodies affected ligand binding. CGP12177 being hydrophillic can only label cell surface receptors (McLean and Milligan, 1999) whereas dihydroalprenolol, being hydrophobic can pass through the plasma membrane and therefore can label both internal and cell-surface receptors. The data shown below are the mean ± S.E.M for three independent experiments. The antibodies had no significant effect ($p > 0.05$) on either ligand binding.

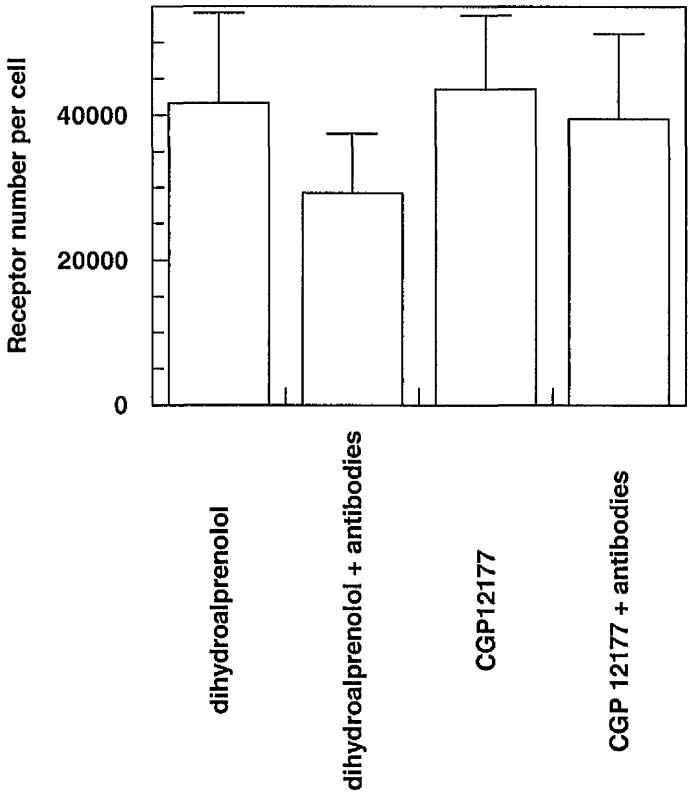

Figure 5.7 μOR homodimerization and heterodimerization with δOR shown via TR-FRET

5×10^5 HEK293 cells transiently transfected with Flag- or c-myc-tagged δOR and Flag- or c-myc-tagged μOR, were incubated in the presence of anti-Flag-APC and anti-myc-Eu^{3+}. After a 2 h room temperature incubation, the cells were washed and re-suspended in PBS before reading the TR-FRET signal and the fluorescence intensity of each bound antibody on a Victor^2. The data are mean ± S.E.M. of three independent experiments performed in triplicate, the exceptions being the Flag-μOR/c-myc-μOR and Flag-δOR/c-myc-μOR which are from two independent experiments performed in triplicate.

A) No significant TR-FRET signal ($p > 0.05$) was observed in the presence of co-expressed Flag-μOR with c-myc-μOR, c-myc-δOR with Flag-μOR or Flag-δOR with c-myc-μOR.

B) Anti-c-myc-Eu^{3+} binding to cells expressing c-myc-μOR and Flag tagged δOR or μOR was not significantly different ($p > 0.05$) to that found for c-myc-δOR co-transfected with Flag tagged δOR or μOR. The anti-c- myc-Eu^{3+} binding achieved for cells transfected with c-myc-μOR alone was significantly lower ($p < 0.05$) than that for cells transfected with c-myc-δOR alone.

C) Anti-Flag-APC binding in cells expressing Flag-μOR in the presence of c-myc tagged δOR or μOR was not significantly different ($p > 0.05$) from anti-Flag-APC binding to cells expressing Flag-δOR in the presence of c-myc tagged δOR or μOR. When Flag-μOR was expressed alone there was significantly less ($p < 0.05$) anti-Flag-APC binding observed compared to that for cells expressing Flag-δOR alone.

5.7 A)

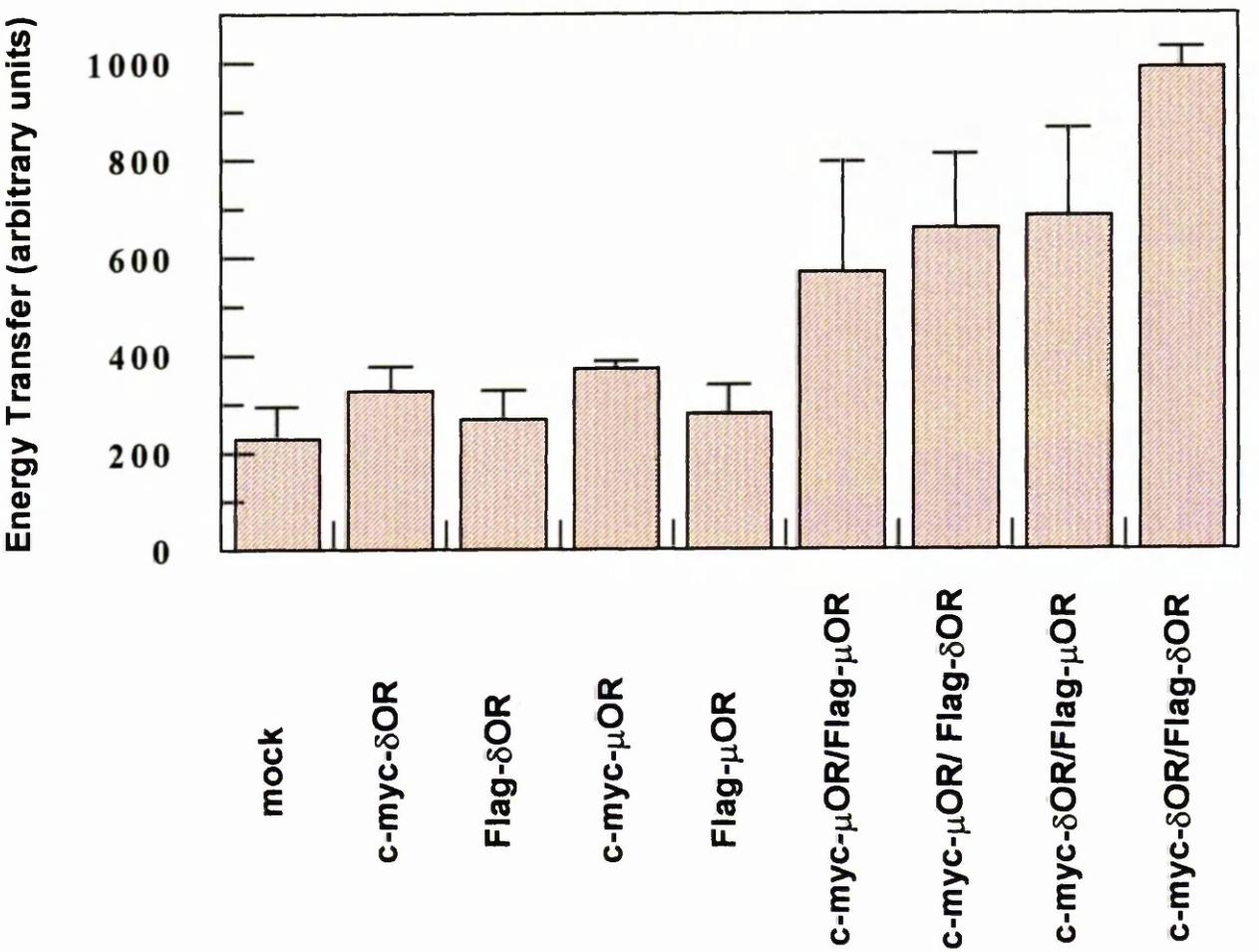
Energy Transfer (arbitrary units)
0
200
400
600
800
1000
mock
c-myc-δOR
Flag-δOR
c-myc-μOR
Flag-μOR
c-myc-μOR/Flag-μOR
c-myc-μOR/ Flag-δOR
c-myc-δOR/Flag-μOR
c-myc-δOR/Flag-δOR

5.7 B)

Eu3+ fluorescence Intensity
(arbitrary units)
0
10000
20000
30000
mock
c-myc-δOR
Flag-δOR
c-myc-μOR
Flag-μOR
c-myc-μOR/Flag-μOR
c-myc-μOR/ Flag-δOR
c-myc-δOR/Flag-μOR
c-myc-δOR/Flag-δOR

5.7 C)

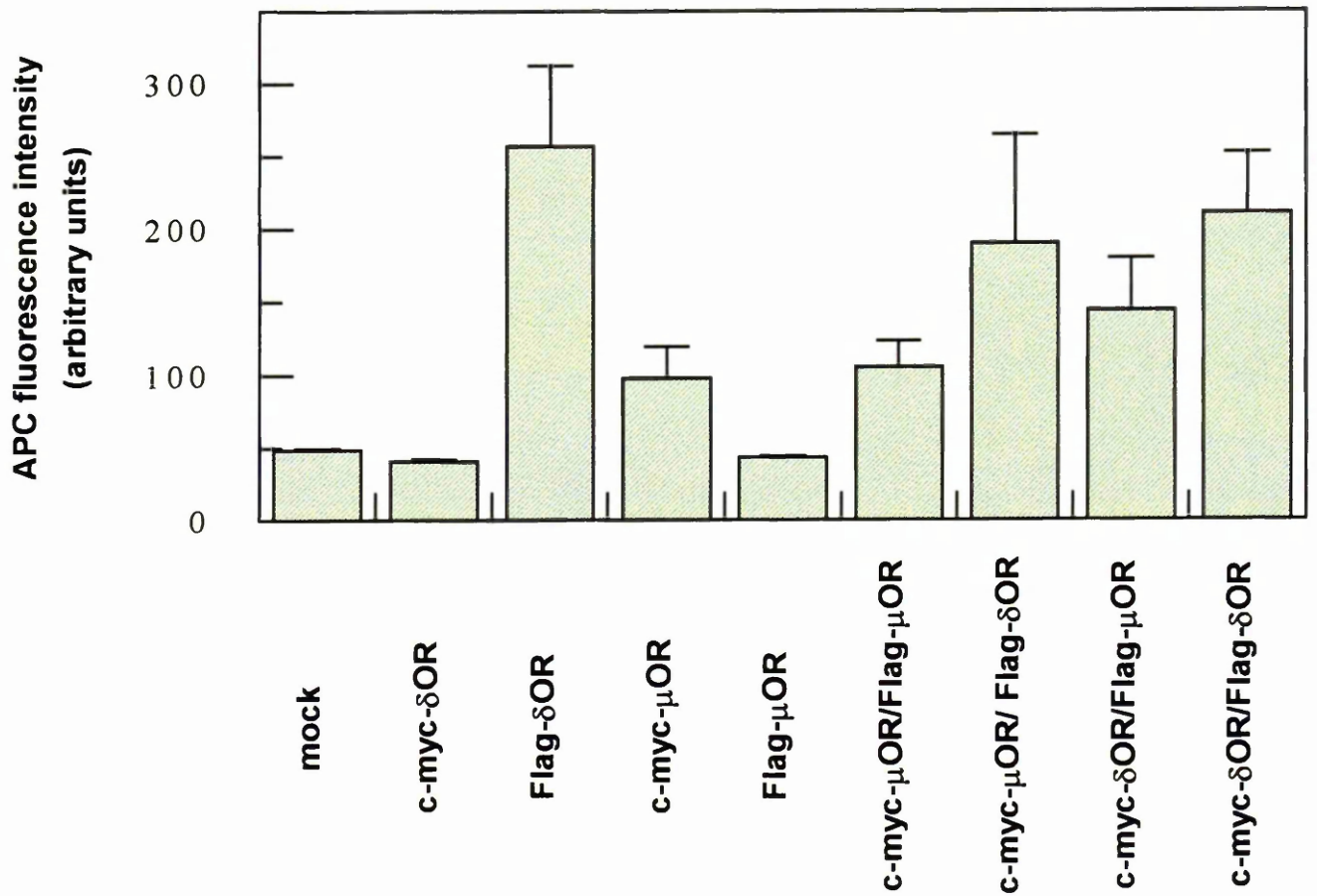
APC fluorescence intensity
(arbitrary units)
300
200
100
0
mock
c-myc-δOR
Flag-δOR
c-myc-μOR
Flag-μOR
c-myc-μOR/Flag-μOR
c-myc-μOR/ Flag-δOR
c-myc-δOR/Flag-μOR
c-myc-δOR/Flag-δOR

Table 5.1 Fluorescently labelled antibodies do not disrupt agonist mediated inhibition of adenylyl cyclase by the δOR.

Intact cell adenylyl cyclase assays as described in section 2.4.3 were performed on HEK293 cells expressing both Flag-δOR and c-myc-δOR.

The effect of 1μM DADLE on the forskolin stimulation of basal cAMP levels was demonstrated in the presence and absence of anti-Flag-APC and anti-c-myc-Eu^{3+}. The results presented are the % of the cAMP levels produced by 50μM forskolin in the absence of antibodies. Results are mean ± S.D. for two independent experiments performed in triplicate. The presence of antibodies did not significantly alter the effect of DADLE ($p > 0.05$).

	No antibody	Plus antibodies
Basal	1.0 ± 0.6	0.9 ± 0.6
Forskolin (50μM)	100	132 ± 19
Forskolin (50μM) plus DADLE (100nM)	29 ± 2	45 ± 14

Figure 5.8 Optimization of TR-FRET assays

5×10^5 HEK293 cells transiently transfected with 0.2 – 1.5μg of c-myc-δOR and 1.5μg Flag-δOR and incubated in the presence of anti-Flag-APC and anti-c-myc-Eu^{3+}. Concentrations of either 3nM of each antibody, 3nM anti-c-myc-Eu3+ and 9nM anti-Flag-APC, 9nM of both antibodies or 15nM of both antibodies were used. After a 2 hour room temperature incubation, the cells were washed and resuspended in PBS before reading the TR-FRET and the fluorescence intensity of each bound antibody on a Victor^2 fluorescence plate reader. This graph is a typical representation of two independent experiments performed in triplicate.

A) TR-FRET signal

B) Fluorescent intensity of anti-c-myc-Eu^{3+} bound to cells

C) Fluorescent intensity of anti-Flag-APC bound to cells

5.8 A)

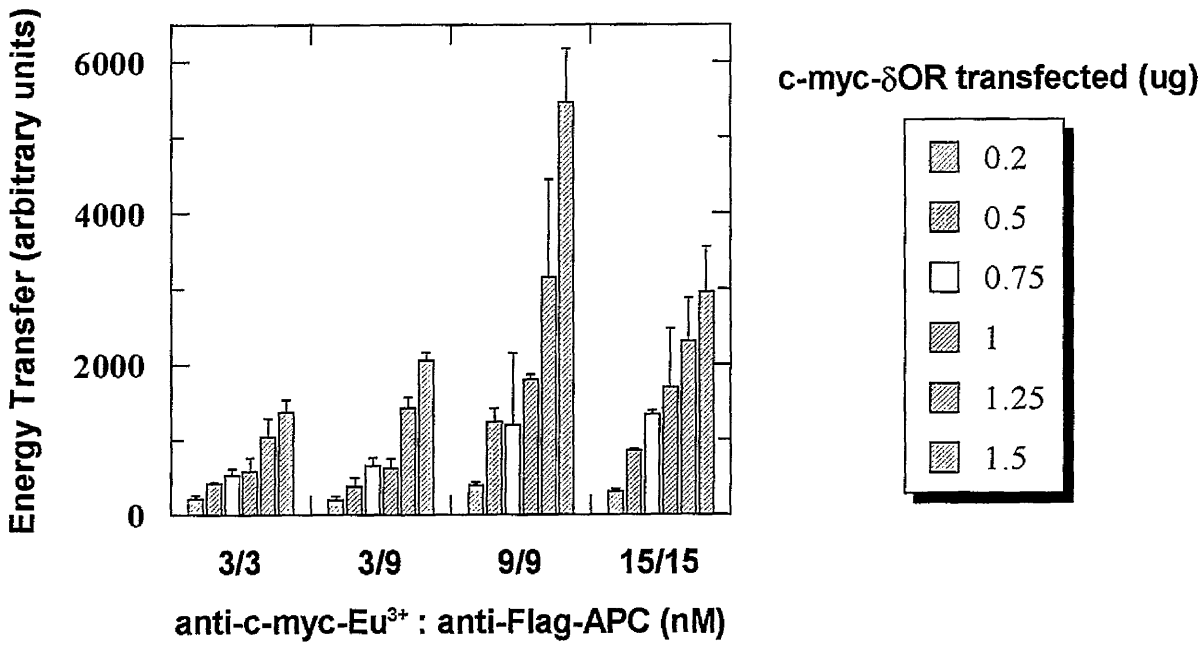
Energy Transfer (arbitrary units)
6000
4000
2000
0
3/3
3/9
9/9
15/15
anti-c-myc-Eu3+ : anti-Flag-APC (nM)
c-myc-δOR transfected (ug)
0.2
0.5
0.75
1
1.25
1.5

5.8 B)

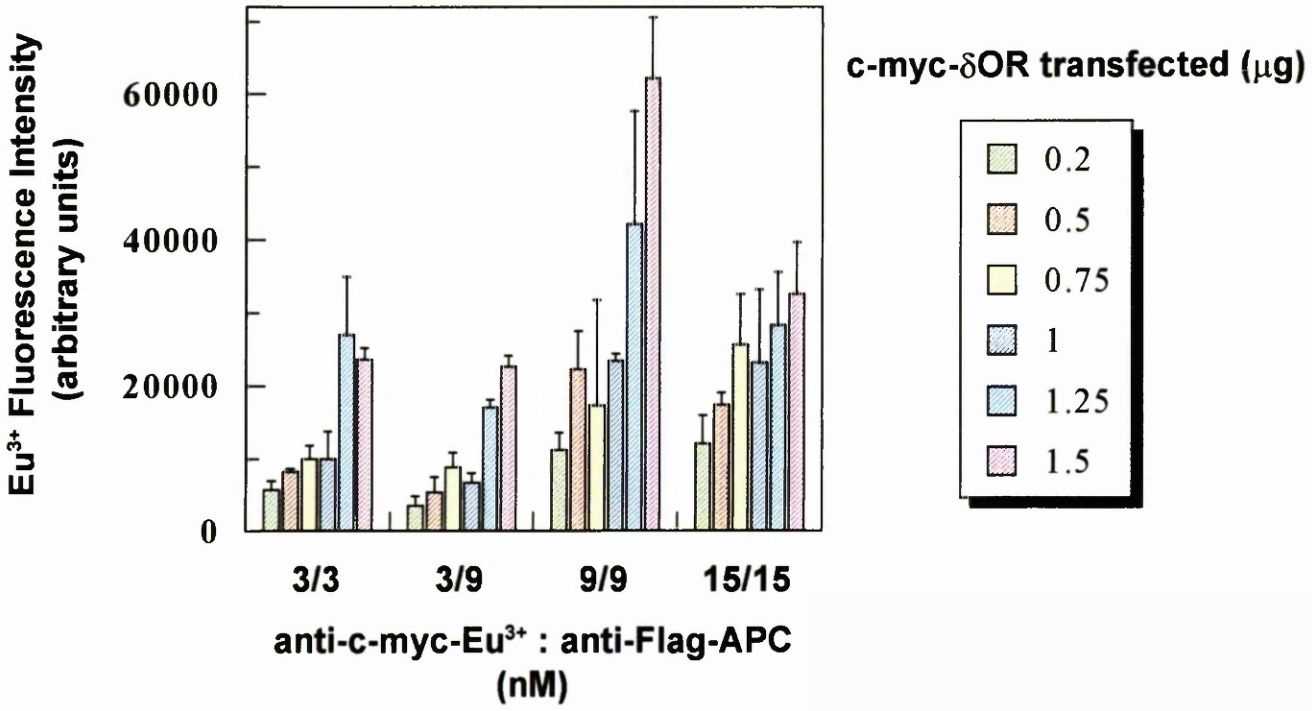
Eu3+ Fluorescence Intensity (arbitrary units)
60000
40000
20000
0
3/3
3/9
9/9
15/15
anti-c-myc-Eu3+ : anti-Flag-APC (nM)
c-myc-δOR transfected (μg)
0.2
0.5
0.75
1
1.25
1.5

5.8 C)

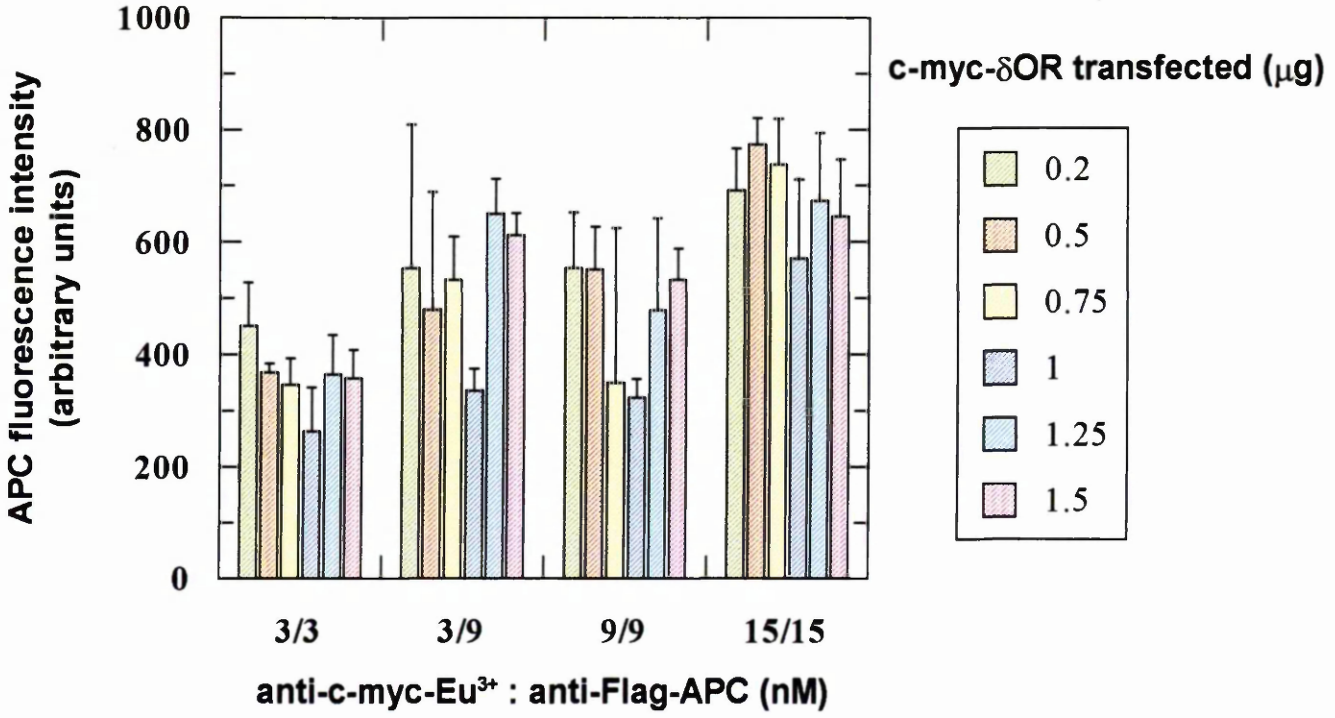
APC fluorescence intensity (arbitrary units)
1000
800
600
400
200
0
3/3
3/9
9/9
15/15
anti-c-myc-Eu3+ : anti-Flag-APC (nM)
c-myc-δOR transfected (μg)
0.2
0.5
0.75
1
1.25
1.5

Figure 5.9 Development of a homogenous assay format for the TR-FRET assay to determine δOR homodimerization

1 – 8 x 10^5 cells transiently transfected with equal amounts of Flag-δOR and c-myc-δOR were incubated in the presence of A) 0.5nM anti-c-myc-Eu^{3+} and 2.5nM anti-Flag-APC or B) 0.5nM anti-c-myc-Eu^{3+} and 5nM anti-c-myc-APC. The TR-FRET signal was measured over a 3 hour time-period on a Victor^2. This graph is a typical representation of two independent experiments performed in triplicate.

5.9 A)

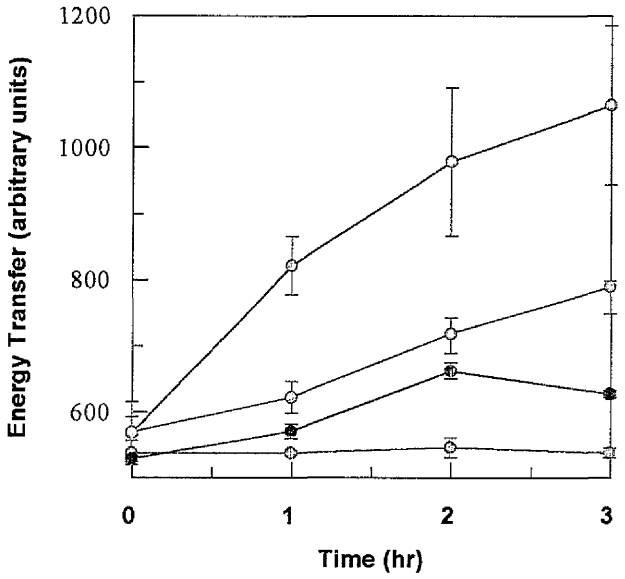
Energy Transfer (arbitrary units)
1200
1000
800
600
0
1
2
3
Time (hr)

5.9 B)

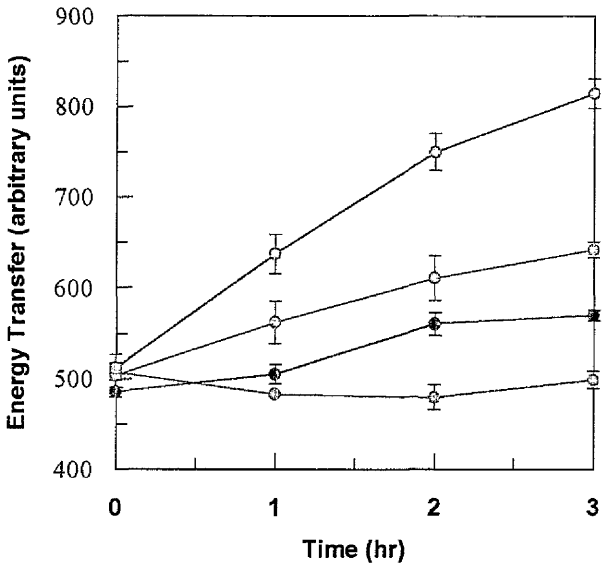
Energy Transfer (arbitrary units)
900
800
700
600
500
400
0
1
2
3
Time (hr)

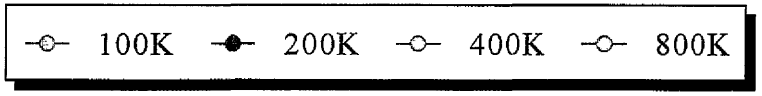
100K
200K
400K
800K

5.3 Discussion

Determination of δOR homodimerization and heterodimerization using live cells was a main aim of this project. Using N-terminal differentially tagged opioid receptors and the fluorescent antibodies described in Chapter 4 has resulted in the development of a heterogeneous cell-surface TR-FRET assay for receptor dimerization which should be applicable to a wide range of GPCRs.

Immunocytochemistry of live or fixed cells as well as flow cytometry has been performed using fluorescently tagged antibodies. These techniques were used to show agonist-stimulated internalization of both the δOR and μOR receptors (Whistler and Von Zastrow, 1999). The lack of suitably labelled specific antibodies led to the in-house generation of an anti-Flag-APC molecule which was described in Chapter 4, however it would be equally feasible to fluorescently label an antibody which had been raised to an external epitope of the receptor. The energy transfer between Eu^{3+} and APC is 50% at a distance of 9.5nm making this pairing suitable to look at protein-protein interactions. (Farrar et al., 1999).

Care has to be taken to ensure that the antibody binding does not directly disrupt or cause receptor dimerization. As Cvejic and Devi (1997) showed that the C-terminus of the δOR is important for dimerization it is unlikely that an antibody to an N-terminal tag would disrupt dimerization of these receptors. Antibodies are bivalent and have been shown to cause aggregation of receptors at the cell surface (Mijares et al., 2000). This is unlikely in this case because if the anti-Flag antibody caused aggregation of receptors it would be of Flag-tagged receptors only. Homodimers of Flag-tagged receptors will not generate an energy transfer signal in this system. Similarly for c-myc-tagged receptors, homodimers of receptors both containing c-myc do not generate an energy transfer signal in this system. Furthermore, Whistler and von Zastrow (1999) used antibodies to N-terminal tags and no receptor aggregation was observed.

A specific fluorescence intensity signal of anti-c-myc-Eu^{3+} and anti-Flag-APC binding over mock transfected cells is demonstrated in figures 4.12 and 4.2 respectively. The level of donor antibody chosen was 3nM to maintain a high level of specific antibody binding over mock transfected cells. The incubation time was set at two hours to ensure the cells were alive and healthy when the TR-FRET signal was measured. Cost was also considered in determining the assay conditions, as the commercially available anti-myc-Eu^{3+} is very expensive. At 3nM, with a 100µl incubation volume, the cost of the anti-c-myc-Eu^{3+} alone is 60p per individual data point, therefore increasing the concentration of the anti-c-myc-Eu^{3+} would substantially increase the cost of these assays. Measuring the fluorescence intensity of the incubation mixture after the removal of the cells showed that there was an excess of anti-c-myc-Eu^{3+} antibody in the incubation mixture. This fluorescent intensity was approximately ten times the level of antibody bound to the cells.

This assay in its present format cannot be fully quantitative as monomeric receptor species and some homodimeric interactions, which do not generate a signal i.e. between Flag-receptor with Flag-receptor and c-myc-receptor with c-myc-receptor, will be present. With this assay an estimation of the level of receptors in each form is not possible. Saturation of all the receptors with antibody was therefore not considered an absolute requirement to observe an informative TR-FRET signal.

Optimisation of cell number, antibody concentration and antibody incubation time used are all necessary to provide a robust assay giving the maximal energy transfer signal at an appropriate cost.

δOR homodimerization is demonstrated using TR-FRET

The TR-FRET signal was measured with cells expressing Flag-tagged or c-myc-tagged receptors alone and cells expressing both receptors. An energy transfer signal was only obtained with cells expressing both receptors (figure 5.1A). These observations demonstrate that constitutive homodimers of δOR are

present on the cell-surface as the antibodies do not have access to receptors present inside the cell. Mixing cells expressing Flag-δOR or c-myc-δOR individually gave no TR-FRET signal (figure 5.1A). This demonstrates that the presence of both receptors and both antibodies in the same mixture is not enough to generate a signal, as both receptors have to be expressed in the same cell to be in sufficiently close proximity. As both antibodies were present in each incubation the possibility of a false positive resulting from non-specific interactions between the antibodies or their respective fluorophores was eliminated.

The co-immunoprecipitation studies described in Chapter 3, generated an unexpected result indicating a possible interaction between the δOR and β_2AR. As the β_2AR-GFP construct also contains an N-terminal Flag tag it was used to look for cell-surface heterodimerization using TR-FRET. No TR-FRET signal was obtained (figure 5.1A) indicating that these receptors do not form a significant level of cell surface heterodimer, this contradicts the co-immunoprecipitation data. The levels of each antibody binding were similar to those observed in the δOR homodimerization experiments (figures 5.1B and 5.1C) therefore the lack of a signal does not represent reduced receptor expression or reduced antibody binding to the Flag-β_2AR.

It is possible that the δOR and β_2AR receptors interact but not at the cell-surface, which would agree with both sets of results found. Indeed recent BRET studies have detected such an interaction (McVey et al., 2001). Cell-surface heterodimers between the δOR and the β_2AR using a co-immunoprecipitation technique have since been demonstrated (Devi et al., 2001). It could be possible that the δOR:β_2AR may interact via an intermediate molecule which hold the receptors in a conformation which is unfavourable for a FRET signal to be observed whereas the co-immunoprecipitation may not be affected by such an interaction.

To confirm that the TR-FRET signal observed from these experiments was not the result of fluorescent "carry-over" from the Eu^{3+}, a standard curve with

increasing amounts of anti-c-myc-Eu^{3+} in the presence of 5 x 10^5 HEK293 cells was set up. It can be seen that the level of anti-c-myc-Eu^{3+} antibody binding necessary to generate the energy transfer that was observed in figure 4.11 would be in the region of 300,000 counts. The fluorescence intensity associated with the cells which were co-transfected with c-myc-δOR and Flag-δOR, for example, shown in figure 5.1B is only approximately one tenth of that value. This confirms that the signal observed is energy transfer to the anti-Flag-APC and not an emission signal from anti-c-myc-Eu^{3+}.

Incubation with δOR ligands does not effect the δOR homodimerization signal.

(Cvejic and Devi, 1997) showed via chemical cross-linking and co-immunoprecipitation that the δOR forms constitutive dimers and that agonist activation leads to monomerization and subsequent internalization of the receptor. It was postulated that if an agonist ligand resulted in monomerisation of the δOR homodimer then an inverse agonist might increase the level of the homodimer. The δOR peptide agonist DADLE and the δOR selective inverse agonist ICI 174,864 were used to look for effects on the TR-FRET signal. As shown in figure 5.3 there was no effect of these ligands or the β_2AR agonist isoprenaline on the δOR homodimerization level. This is consistent with the data described in Chapter 3. As the TR-FRET signal is dependent on the antibody binding to the cells it is vital that ligand binding is not disrupted upon antibody binding. This is shown in figures 5.3B and 5.3C.

The effect of ligands on the lack of heterodimerization between the δOR and the β_2AR was also studied as the lack of significant levels of a constitutive heterodimer does not exclude the possibility that ligand interaction could result in heterodimer formation between δOR and β_2AR. Hebert et al. (1998) demonstrated, via cross-linking and co-immunoprecipitation and Angers et al., (2000) subsequently showed via BRET that agonist activation of the β_2AR leads to increased homodimerization of the receptor. No such demonstration of δOR:β_2AR heterodimerization upon ligand interaction was shown for either the

δOR agonist DADLE, the β_2AR selective agonist isoprenaline or a combination of the two agonists (figure 5.4). Again agonists did not alter the level of antibody binding to the receptors (figures 5.4B and 5.4C). The TR-FRET signal obtained here can only result from interaction between receptors at the cell surface and any internal or internalised receptor will not contribute to the signal obtained. This may explain the differences obtained from the two types of experimental approaches, however, a BRET assay which has been developed for the δOR which can measure δOR interaction within the cell, also showed receptor homodimerization which was not affected by ligands (McVey et al., 2001). Interestingly, a small but significant BRET signal was also found indicative of the formation of δOR:β_2AR heterodimers. Addition of an agonist to either receptor resulted in a further small increase in signal.

The lack of ligand effect on δOR homodimerization is not a result of the antibodies preventing the ligand binding to the receptors as shown in figures 5.5 and 5.6 as ligand binding is not affected by the presence of the antibody. It was also possible that the antibodies used for TR-FRET could modulate receptor function. Thus, the effect of the labelled antibodies on forskolin stimulated increases in cAMP was investigated using an intact cell adenylyl cyclase assay. Activation of the δOR by the agonist DADLE was also tested in the absence and presence of the antibodies as shown in table 5.1. No significant effect of the labelled antibodies on either forskolin stimulation or receptor-mediated inhibition of adenylyl cyclase activity was observed.

μOR homo- and heterodimerization

Statistically significant μOR homodimerization was not demonstrated in this assay (figure 5.7). This conflicts with the results of Gomes et al., (2000) and George et al., (2000) produced via co-immunoprecipitation studies. μOR and δOR are two closely related receptor species have been shown to interact via co-immunoprecipitation (Chapter 3) and by detailed kinetic investigation of the binding of various ligands (Gomes et al., 2000, George et al., 2000).

Although no significant heterodimers between Flag-μOR and c-myc-δOR were observed (figure 5.7) demonstrated by statistical analysis of these data ($p > 0.05$) there was some evidence that at least some heterodimerization was occurring. The level of individual antibody binding shown in figures 5.7B and 5.7C were not significantly lower for the μOR than the δOR or the β_2AR constructs on co-expression, ($p > 0.05$). Further investigations into μOR:δOR heterodimerization may require an increase in receptor expression level and further optimization of assay conditions to detect any cell-surface heterodimer. These results indicate that there is little cell-surface μOR:δOR heterodimer present in the cells transiently transfected with these epitope tagged receptors. The lack of cell-surface expression of this μOR has recently been demonstrated on expression of this receptor with GFP fused to its C-terminus where a significant amount of the receptor was found to present inside the cells, this would explain the lack of a significant TR-FRET signal.

It would be interesting to produce stable cell lines expressing both the μOR and δOR at different ratios and determine the level of heterodimerization and even more interesting if levels of homo and heterodimers could be assessed simultaneously. If appropriate fluorescent labelling of selective antibodies for each receptor and not to an epitope tag it may be possible to use this assay to determine homo and heterodimerization within primary cell lines.

Optimization of TR-FRET signal

For an efficient FRET signal, limiting amounts of fluorescent donor molecule in the presence of excess acceptor is preferred as the energy transfer is dependent on the level of donor molecule. If there is excess acceptor molecule the maximal energy transfer signal will be obtained. To control the levels of donor and acceptor molecule in such experiments is extremely difficult, as this is dependent on the ratio of the c-myc and Flag-tagged receptors and the levels in monomeric and homodimeric forms. To try to optimize the TR-FRET signal obtained two approaches were used. In transient transfections with increasing the level of c-

myc-δOR cDNA transfected, TR-FRET signal was measured at 3 different concentration combinations of anti-c-myc-Eu^{3+} and anti-Flag-APC (figure 5.8). An increase in the overall energy transfer was obtained with increasing amounts of anti-c-myc-Eu^{3+} antibody. No significant difference ($p > 0.05$) in TR-FRET was observed when 3nM, 9nM or 15nM anti-Flag antibody was present in the incubation indicating that 3nM anti-Flag antibody may be saturating in these experiments. The level of energy transfer present with 1.25 and 1.5μg of c-myc-δOR transfected when incubating with 9nM of each fluorescent antibody was higher than the other treatments studied. This higher signal is likely to arise from the increased anti-c-myc-Eu^{3+} binding found with these cells (figure 5.8B). The TR-FRET signal was dependent on the level of c-myc-δOR present in the cells. For complete optimization of these TR-FRET experiments cells a stably transfected cell line would be necessary to ensure a consistent level of each receptor was present in each experiment.

Homogenous assay format

Development of a homogeneous TR-FRET assay format to monitor cell-surface receptor homodimerization was an initial aim of this project. A homogeneous assay does not require any washing procedures to remove the unbound antibody and optimisation of the TR-FRET signal should be achieved quickly as many samples can be assayed under varying conditions simultaneously.

As was shown in Chapter 4 and in figure 5.2 the level of the fluorescent donor has to be decided carefully and empirically as the TR-FRET signal in a homogenous assay format has to be determined in the presence of the donor molecule. High levels of fluorescent donor could easily mask any TR-FRET signal that may occur. Homogenous TR-FRET assays were described in Chapter 4 where cells were plated down onto the surface of the wells of a 96 well plate. To allow a comparison with the heterogeneous system and the results shown in figure 5.10, 1-8 x 10^5 cells were added per well in a volume of 100μl. The energy transfer signal was monitored over 3 h as is shown in figure 5.9. This demonstrated that a homogenous assay format can be developed to determine

TR-FRET. The best conditions determined here were with addition of 0.5 nM donor and 5nM acceptor antibodies with 8 x 10^5 cells in the 100µl volume. Although this assay could demonstrate receptor homodimerization the signal to noise was much less than the heterogeneous assay. A similar loss in sensitivity was found by Blomberg et al., (1999) in the development of a TR-FRET assay when compared to a heterogenous assay format. The homogeneous assay format, however, was much easier to perform as no time-consuming wash steps were involved, and there was no possibility of loss of any cells during washing or transfer into the plate for analysis.

Opioid receptors are very similar, sharing a 65-70% homology (Jordan and Devi, 1998) therefore it is not suprising if they can form homodimers that heterodimers can also be found. The main region of variability between these receptors is at the C-terminus which has been indicated to be important for homodimerization of the δOR (Cvejic and Devi, 1997) but not for heterodimerization between the δOR and a C-terminally truncated µOR (Gomes et al., 2000). The C-terminus of the δOR has been shown to be involved in receptor internalisation as well as dimerization (Cvejic et al. 1996). This is unlikely to be a simple issue because Murray et al., (1998) demonstrated that a mutant δOR which lacks phosphorylation sites in its C-terminus, does not internalize when expressed in CHO cells but does when expressed in HEK293 cells. It would be interesting to assess the level of homo and heterodimerization of mutant opioid receptors lacking the C-terminus via this TR-FRET assay.

Fluorescent techniques, alongside the development of new highly sensitive fluorescent probes, will allow many cell signalling mechanisms to be assayed in a live cell format. This can only be advantageous for the further understanding of these mechanisms.

The lack of suitable antibodies has hindered the development of this assay and the results gained from it. The levels of homodimer versus heterodimer cannot be addressed in this particular assay format. However, using appropriate fluorescently labelled antibodies it may be possible to address this issue in the

future. The number of suitable fluorescent probes and antibodies is growing at great speed as such assays become more widely used. There are now other antibodies available, which could be used for this TR-FRET assay. An anti-Flag-Eu^{3+} antibody is now available and it would be interesting to confirm these data with the anti-Flag antibody as a donor and anti-c-myc antibody as acceptor. This would allow further optimization of the TR-FRET assay. Investigations into the cell-surface presence of κORs would be of interest. The use of fluorescent ligands has already been developed for opioid (Arttamangkul et al., 2000, Kshirsagar et al., 2001, Maeda et al., 2000) and other GPCRs (Heithier et al. 1994) and the use of fluorescent ligands has been recently reviewed by McGrath et al. (1996). It may be possible to employ TR-FRET assays to look at receptor dimerization, and fluorescent ligand binding assays to examine alterations in receptor pharmacology in parallel.

CHAPTER 6

Final Discussion

Final Discussion

GPCR homodimerization, heterodimerization and oligomerization have all been suggested. The lack of a robust assay which allows the detection of receptor:receptor interaction in live cells has hindered the progress of investigations of such interactions.

Pharmacological data have been presented for heterogeneous receptor systems, which affect each other both *in vivo* and *in vitro*. This however, does not demonstrate any physical interaction between the contributing GPCRs. Identification of constitutive and agonist-modulated homodimers (Angers et al., 1996, Cvejic and Devi, 1997) and hetero-dimers (George et al., 2000, Gomes et al., 2000) has been reported. Co-immunoprecipitation experiments of differentially tagged GPCRs have been used to determine such interactions although care has to be taken while producing cell lysates for co-immunoprecipitation. The length of time used for film exposure to the ECL has to be taken into consideration to ensure each interaction is fully identified.

Co-immunoprecipitation of differentially tagged GPCRs has been used to demonstrate dimerization, and indeed oligomerization, of many GPCRs (Hebert et al., 1996, Cvejic and Devi, 1997, Pfeiffer et al.,2001). This method may generate artifactual results as discussed in Chapter 3. The solubilization of proteins from cellular membranes can depend on the detergents used. However, with proper controls this method can demonstrate protein-protein interactions. One drawback to this system is the lack of information provided on where the interactions occur within the cell as all the cellular membranes are assayed and not just those of the plasma membrane.

The Yeast Two-Hybrid system has also been used successfully to identify protein-protein interactions as discussed by Milligan and White (2001). This system has the drawback that the protein-protein interaction has to occur within the Yeast nucleus, therefore interactions which involve secondary manipulation

(e.g. palmitoylation) or compartmentalisation are unlikely to be identified using this system.

In this study the challenge to develop an appropriate technique which would allow detection of GPCR homo and heterodimers in intact cells was undertaken. Transient transfection of epitope-tagged GPCRs allowed their specific labelling at the cell surface with appropriate antibodies that were fluorescently labelled. The use of fluorescent molecules has increased in biological applications as new fluorophores with high quantum yields and a variety of excitation and emission wavelengths have been developed in parallel with the production of sensitive and affordable equipment for the detection of fluorescence. In the study of GPCRs, fluorescent ligands in place of the more traditional radiolabelled ones (Maeda et al., 2000, Arttamangkul et al., 2000, Kshirsagar et al., 1998) have been used to make assays safer. GPCRs themselves have also been directly labelled with fluorophores (Gether et al., 1995) to identify the conformational changes associated with ligand binding.

Fluorescent energy transfer arises as a fluorescent donor transfers excitation energy in a non-radiative way, by dipole-dipole interaction, to an acceptor molecule. The emission spectrum of the donor molecule must overlap the excitation spectrum of the acceptor molecule for the energy transfer to be possible. The acceptor molecule does not have to be fluorescent and in this case the energy transfer is observed by the quenching of the emission from the donor molecule. For successful energy transfer, the donor and acceptor molecules have to be in very close proximity 10-100Å, depending on the fluorophores used. Lanthanide chelate molecules have a long fluorescence lifetime in comparison to more traditional fluorophores allowing their emission signal to be measured after a short lag period, by the end of which any autofluorescence from the sample will have decayed, increasing the signal to noise ratio for such time-resolved fluorescence. TR-FRET is an appropriate technique to study the cell-surface expression of N-terminal epitope tagged GPCRs using fluorescently tagged antibodies. Eu^{3+} and APC were the fluorescent tags used in this study as they have appropriate spectral overlap and the Eu^{3+} has a long-lived fluorescence emission signal.

Constitutive homodimerization of δORs was demonstrated at the cell surface using this technique. As the presence of GPCRs at the cell surface is an indication of their correct folding, glycosylation and trafficking, it is advantageous to be able to identify the cell-surface receptors only. The related technique of BRET also detects constitutive homodimerization of δORs although BRET does not indicate the site of receptor interaction as this signal is derived from receptors within intracellular compartments as well as at the plasma membrane. Agonist stimulation of constitutive mouse δOR homodimers has been shown previously to increase the monomerization of these receptor homodimers (Cvejic and Devi, 1997). This was not the case for the constitutive homodimers detected using TR-FRET or BRET (McVey et al., 2001). Agonist activation of GPCRs has been demonstrated to vary from having no effect, increasing the levels of dimerization or causing monomerization of constitutive homodimers. The lack of a consensus of agonist effect may be, in part, the result of the different techniques used to study these interactions or may reflect true variations in the GPCR signalling.

Heterodimerization between the human δOR and β_2AR was demonstrated using the co-immunoprecipitation technique however this was not replicated when using the TR-FRET assay even in the presence of ligands to either or both receptors. The related BRET assay did however, demonstrate a small but statistically significant increase in signal in the presence of ligand to either receptor (McVey et al., 2001). Subsequently Jordan et al. (2001) have demonstrated interactions between these two GPCRs. The lack of consensus may be due in part to the different techniques used to identify GPCR dimerization and again highlights the care that has to be taken when interpreting the data from them.

Heterodimerization between δOR and μOR has been shown by Gomes et al. (2000) and George et al. (2000). Interaction between these receptors on transient transfections was indicated but not confirmed in a significantly

significant manner using the TR-FRET technique. This may be due to the lack of cell surface expression of the μOR as discussed in chapter 5.

Other methods are being developed to look at receptor dimerization within live cells. One such method is ICAST where the proteins of interest are tagged with β-galactosidase deletion mutants. As the proteins interact the β-galactosidase components also interact resulting in β-galactosidase activity, which being enzymatically amplified, can be measured in a number of spectrometric, fluorescent or chemiluminescent methods (Blakely et al., 2000).

The development of the TR-FRET assay to determine GPCR dimerization has been accomplished. There are, however, further challenging aspects for the future development of this assay which time did not allow me to address. These include stoichiometry of GPCR monomers, homodimers and heterodimers and the development of new fluorescent probes.

References

Abdalla, S., Lother, H. and Quitterer, U. (2000) Nature **407**, 94-98

Abdalla, S., Zaki, E., Lother, H. and Quitterer, U. (1999) J. Biol. Chem. **274**, 26079-26084

Allouche, S., Polastron, J., Hasbi, A., Homburger, V. and Jauzac, P. (1999) Biochem. J. **342**, 71-78

Ammer, H. and Schulz, R. (1997) J. Pharmacol. Exper. Ther. **280**, 512-520

Angers, S., Salahpour, A., Joly, E., Hilairet, S., Chelsky, D., Dennis, M. and Bouvier, M. (2000) Proc. Natl. Acad. Sci. U.S.A. **97**, 3684-3689

Arden, J. R., Segredo, V., Wang, Z. and Sadee, W. (1995) J. Neurochem. **65**, 1636-1645

Arttamangkul, S., Alvarez-Maubecin, V., Thomas, G., Williams, J. T. and Grandy, D. K. (2000) Mol. Pharmacol. **58**, 1570-1580

Arvidsson, U., Dado, R. J., Riedl, M., Lee, J. H., Law, P. Y., Loh, H. H., Elde, R., Wessendorf, M. W. (1995) J. Neurosci. **15**, 1215-1235

Auer, M., Moore, K, J., Meyer-Almes, F. J., Guenther, R., Pope, A.J. and Stoeckli, K. A. (1998) Drug Disc. Today. **3**, 457-465

Avissar, S., Amitai, G and Sokolovsky, M. (1983) Proc. Natl. Acad. Sci. U.S.A. **80**, 156-159

Bai, M., Trivedi, S., Kilfor, O., Quinn, S. J. and Brown, E. M. (1999) Proc. Natl. Acad. Sci. U.S.A. **96**, 2834-2839

Bai, M., Trivedi, S. and Brown, E. M. (1998) J. Biol. Chem. **273**, 23605-23610

Baird, G. S., Zacharias, D. A. and Tsien, R. Y. (2000) Proc. Natl. Acad. Sci. U.S.A. **97**, 11984-11989

Barak, L. S., Ferguson, S. S. G., Zhang, J. and Caron, M. G. (1997) J. Biol. Chem. **272**, 27497-27500

Barak, L. S., Warabi, K., Feng, X., Caron, M. G. and Kwatra, M. M. (1999) J. Biol. Chem. **274,** 7565-7569

Barbier, P., Colelli, A., Bolognesi, M. L., Minarini, A., Tumiatti, V., Corsini, G.U., Melchiorre, C. and Maggio, R. (1998) Eur. J. Pharmacol. **355**, 267-274

Barrett, R. and Vaught, J. (1982) Eur. J. Pharmacol. **80**, 427-430

Barritt, G. J. and Gregory, R. B. (1997) Cell. Signal. **9**, 207-218.

Befort, K., Tabbara, L., Kling, D., Maigret, B. and Kieffer, B. L. (1996) J. Biol. Chem. **271**. 10161-10168.

Befort, K., Zilliox, C., Filliol, D., Yue, S., Kieffer, B. L. (1999) J. Biol. Chem. **274**, 18574-18581

Billinton, N. and Knight, A. W. (2001) Anal. Biochem. **291,** 175-197

Blakely, B. T., Rossi, F. M. V., Tillotson, B., Palmer, M., Estelles, A. and Blau, H.M. (2000) Nature Biotechnology. **18**, 218-222

Blomberg, K., Hurskainen, P. and Hemmilä, I. (1999) Clin. Chem. **45**, 855-861

Bockaert, J and Pin, J. P. (1999) EMBO **18,** 1723-1729

Böhm, S. K., Grady, E. F. and Bunnett, N. W. (1997) Biochem. J. **322**, 1-18

Bouvier, M. (2001) Nature Reviews **2**, 274-285

Bradbury, A., Smyth, D., Snell, C., Birdsall, N. and Hulme, E. (1976) Nature **260**, 793-795

Brandt, W., Golbraikh, A., Tager, M. and Lendeckei, U. (1999) J. Biochem. **261**, 89-97

Brock, R., Vàmosi, G., Vereb, G. and Jovin, T. M. (1999) Proc. Natl. Acad. Sci. U.S.A. **96**, 10123-10128

Burt, A. R., Carr, I. C., Mullaney, I., Anderson, N. G. and Milligan G. (1996) Biochem. J. **320**, 227-235

Caplan, S., Dell'Angelica, E. C., Gahl, W. A. and Bonifacine, J. S. (2000) Immunol. Letts. **72**, 113-117

Carman, C. V., Som, T., Kim, C. M. and Benovic, J. L. (1998) J. Biol. Chem. **273,** 20308-20316

Chambers, J. A. A. and Rickwood, D. (1993) Biochemistry LabFax, Blackwell Scientific Publications Ltd.

Chang, K. and Cuatrecasas, P. (1979) J. Biol. Chem. **254**, 2610-2618

Chen, C. A. and Manning, D. R. (2001) Oncogene **20**, 1643-1652

Chen, Y., Mestek, A., Liu, J., Hurley, J. A., and Yu, L. (1993) Mol Pharmacol **44,** 8-12

Cheng, Z. J., Fan, G. H., Zhao, J., Zhang, Z., Wu, Y. L., Jiang, L. Z., Zhu, Y., Pei, G. and Ma, L. (1997) Neuroreport **8**, 1913-1918

Cheng, Z., Yu, Q., Wu, Y., Ma, L. and Pei, G. (1998) J. Biol. Chem. **273**, 24328-24333

Chu,P., Murray, S., Lissin, D and von Zastrow, M. (1997) J. Biol. Chem. **272**, 27124-27130

Claude, P., Wotta, D., Zhang, X., Prather, P., McGinn, T., Erickson, L., Loh, H. and Law, P. (1996) Proc. Natl. Acad. Sci. U.S.A. **93**, 5715-5719

Cornea, A., Janovick, J., Maya-Núñez, G. and Conn, M. (2001) J. Biol. Chem. **276**, 2153-2158

Cox, B., Goldstein, A. and Li, C. (1976) Proc. Natl. Acad. Sci. U.S.A. **73**, 1821-1823

Cvejic, S. and Devi, L.A., (1997) J. Biol. Chem. **272**, 26959-26964
Cvejic, S., Trapaidze, N., Cyr, C. and Devi, L. A. (1996) J. Biol. Chem. **271**, 4073-4076

Daaka, Y., Luttrell, L.M. and Lefkowitz, R. J. (1997) Nature **390**, 719-722

Damjanovich, S., Bene, L., Matkó, J., Alileche, A. and Goldman, C. K., (1997) Proc. Natl. Acad. Sci. U.S.A. **94**, 13134-13139

De Angelis, D. A., Miesenböck, G., Zemelman, B. V. and Rothman, J.E. (1998) Proc. Natl. Acad. Sci. U.S.A. **95**, 12312-12316

Dixon, R. A., Kobilka, B. K., Strader, D. J., Benovic, J. L., Dohlman, H. G., Frielle, T., Bolanowski, M. A., Bennet, C. D., Rands, E., Diehl, R. E., Mumford, R. A., Slater, E., Sigal, E., Caron, M. G., Lefkowitz, R. J. and Strader, C.,D. Nature (1986) **321**, 75-79

Drmota, T., Gould, G. W. and Milligan, G. (1998) J. Biol. Chem. **273**, 24000-24008

Eagan, T. and North, R. (1981) Science **214**, 923-924

Ehrlich, G. K., Andria, M L., Zheng, X., Kieffer, B., Gioannini, T L., Hiller, J. M., Rosenkranz, J. E., Veksler, B. M., Zukin, R. S. and Simon, E. J. (1998) Can. J. Physiol. Pharmacol. **76,** 269-277

Eigen, M. and Rigler, R. (1994) Proc. Natl. Acad. Sci. U.S.A. **91,** 5740-5747

Evans, C.J., Keith, D.E., Jr., Morrison, H., Magendzo, K., and Edwards,R.H. (1992) Science **258**, 1952-1955

Fan, G., Ray, K., Zhao, X., Goldsmith, P. K. and Spiegel, A. M. (1998) FEBS Letts. **436**, 353-356

Fancy, D. A. and Kodadek, T. (1999) Proc. Natl. Acad. Sci. U.S.A. **96**, 6020-6024

Farndale, R. W., Allan, L. M., and Martin, B. R. (1991) in: Signal Transduction A Practical Approach, Oxford University Press, U.K., 75-103

Farrar, S. J., Whiting, P. J., Bonnert, T. P. and McKernan, R. M., (1999) J. Biol. Chem. **274**, 10100-10104

Farrens, D. L., Altenbach, C., Yang, K., Hubbell, W. L. and Khorana, H. G. (1996) Science **274**, 768-770

Fattori, D., Urbani, A., Brunetti, M., Ingenito, R., Pessi, A., Prendergast, K., Narjes, F., Matassa, V. G., De Francesco, R. and Steinkühler, C. (2000) J. Biol. Chem. **275,** 15106-15113

Ferre, S., Fuxe, K. and Franco, R. (2000) Proc. Nacl. Acad. Sci. U.S.A. **97**, 8606-8611

Fields, H., Emson, P., Leigh, B., Gilbert, R and Iversen, L. (1980) Nature **284**, 351-353

Franco, R., Ferré, S., Agnati, L., Torvinen, M., Ginés, S., Hillion, J., Casadó, V., Lledó, P., Zoli, M., Lluis, C and Fuxe, K. (2000) Neuropsychopharmacol. **23**, S4

Franek, M., Pagano, A., Kaupmann, K., Bettler, B., Pin, J. and Blahos, J. (1999) Neuropharmacol. **38**, 1657-1666

Fukuda, K., Kato, S., Morikawa, H., Shoda, T. and Mori, K. (1996) J. Neurochem. **67**, 1309-1316

Fukushima, Y., Asano, T., Saitoh, T., Anai, M., Funaki, M., Ogihara, T., Katagiri, H., Matsuhashi, N., Yazaki, Y. and Sugaro, K. (1997) FEBS letts. **409**, 283-286

Garzon, J., Juarros, J., Castro, M. and Sanchez-Blazquez, P. (1995) Mol. Pharmacol. **47**, 738-744

George, S. R., Lee, A. P., Varghese, G., Zeman, P. H., Seeman, P., Ng, G. Y. K. and O'Dowd, B. F. (1998) J. Biol. Chem. **273**, 30244-30248

George, S. R., Fan, T., Xie, Z., Tse, R., Tam, V., Varghese, G. and O'Dowd, B. F. (2000) J. Biol. Chem. **275**, 26128-26135

Georgoussi, Z., Merkouris, M., Mullaney, I., Megaritis, G., Carr, C., Zioudrou, C. and Milligan, G. (1997) Biochem. Biophys. Acta. **1359**, 263-274

Gervaix, A., West, D., Leoni, L.M., Richman, D. D., Wong-Staal, F. and Corbeil, J. (1997) Proc. Natl. Acad. Sci. U.S.A. **94,** 4653-4658

Gether, U. and Kobilka, B. K. (1998) J. Biol. Chem. **273**, 17979-17982

Gether, U., Ballesteros, J. A., Seifert, R., Sanders-Bush, E., Weinstein, H. and Kobilka, B. K. (1997) J. Biol. Chem. **272**, 2587-2590

Ghanouni, P., Steenhuis, J. J., Farrens, D. L. and Kobilka, B. K. (2001) Proc. Natl. Acad. Sci. U.S.A. **98**, 5997-6002

Gierschik, P., Bouillon, T., and Jakobs, K. H. (1994) Methods Enzymol. **237**, 13-26

Gines, S., Hillion, J., Torvinen, M., Le Crom, S., Casado, V., Canela, E. I., Rondin, S., Lew, J. Y., Watson, S., Zoli, M., Agnati, L. F., Vernier, P., Lluis, C., Gioannini, T. L., Liu, Y. F., Park, Y. H., Hiller, J. M. and Simon, E. J. (1989) J. Mol. Recog. **2,** 44-48

Giuliani, S., Lecci, A. and Maggi, C. A. (2000) Peptides. **21**, 977-984

Goldstein, A., Fischli, W., Lowney, L., Hunkapiller, M. and Hood, L. (1981) Proc. Natl. Acad. Sci. U.S.A. **78**, 7219-7223

Gomes, I., Jordan, B. A., Gupta, A., Trapaidze, N., Nagy, V. and Devi, L.A. (2000) J. Neurosci. **20**, 1-5

Gouldson, P. R., Higgs, C., Smith, R. E., Dean, M. K., Gkoutos, G. V. and Reynolds, A. (2000) Neuropsychopharmacol. **23**, S60-S77

Grosse, R., Schoneberg, T., Scultz, G. and Gudermann, T. (1997) Mol. Endocrinol. **11**, 1305-1318

Guo, J., Wu, Y., Zhang, W., Zhao, J., Devi, L. A., Pei, G. and Ma, L. (2000) Mol. Pharmacol. **58,** 1050-1056

Ha, T., Enderle, Th., Ogletree, D. F., Chemla, D. S., Selvin, P.R. and Weiss, S. (1996) Proc. Natl. Acad. Sci. U.S.A. **93**, 6264-6268

Hamm, H. E. and Gilchrist, A. (1996) Curr. Biol. **8**, 189-196

Hamm, H. E. (1998) J. Biol. Chem. **273**, 669-672

Hamm, H. E. (2001) Proc. Natl. Acad. Sci. U.S.A. **98**, 4819-4821

Hazum, E., Chang, K. and Cuatrecasas, P. (1979) Nature **282**, 626-628

Hazum, E., Chang, K., Leighton, H. J., Lever, W. Jr. and Cuatrecasas, P. (1982) Biochem. and Biophys. Res. Com. **104**, 347-353

Hebert, T. E., Loisel, T. P., Adam, L., Ethier, N., St. Onge, S. and Bouvier, M. (1998) Biochem. J. **330**, 287-293

Hebert, T. E., Moffett, S., Morello, J., Loisel, T. P., Bichet, D. G., Barret, C. and Bouvier, M. (1996) J. Biol. Chem. **271**, 16384-16392

Heither, H., Hallmann, D., Boege, F., Reiländer, H., Dees, C., Jaeggi, K. A., Arndt-Jovin, D., Jovin, T. M. and Helmreich, E. M. J. (1994) Biochem. **33**, 9126-9134

Heldin, C. (1995) Cell **80**, 213-223

Henderson, G. and McKnight, A. T. (1997) Trends Pharmacol. Sci. **18**, 293-300.

Heyduk, E and Heyduk, T. (1997) Anal. Biochem. **248,** 216-227

Heyman, J., Vaught, J., Mosberg, H., Haaseth, R. and Porreca, F. (1989) Eur. J. Pharmacol. **165**, 1-10

Higashi, H., Sato, K., Ohtake, A., Omori, A., Yoshida, S. and Kudo, Y. (1997) FEBS letts. **414** 55-60

Higashijima, T., Ferguson, K. M., Smigel, M. D. and Gilman, A. G. (1987) J. Biol. Chem. **262,** 757-761

Hovius, R., Vallotton, P., Wohland, T. and Vogel, H. (2000) Trends Pharmacol. Sci. **21**, 266-273

Huang, C., Duncan, J.A., Gilman, A. G. and Mumby, S. M. (1999) Proc. Natl. Acad. Sci. U.S.A. **96**, 412-417

Hughes, J., Smith, T., Kosterlitz, H., Fothergill, L., Morgan, B and Morris, H. (1975) Nature **258**, 577-579

Jakubik, J. and Wess, J. (1999) J. Biol. Chem. **274**, 1340-1358

Javitch, J. A., Fu, D., Liapakis, G. and Chen, J. (1997) J. Biol. Chem. **272**, 18546-18549

Ji, R. R., Zhang, Q., Law, P. Y., Low, H. H., Elde, R., Hökfelt T. (1995) J. Neurosci. **15**, 8156-8166

Ji, T. H., Grossmann, M. and Ji, I. (1998) J. Biol. Chem. **273**, 17299-17302

Jiang, Q., Bowen, W., Mosberg, H., Rothman, R. and Porreca, F. (1990) J. Pharmacol. Exp. Ther. **255**, 636-641

Jockers, R., Angers, S., Da Silva, A., Benaroch, P., Strosberg, A. D., Bouvier, M. and Marullo, S. (1999) J. Biol. Chem. **274**, 28900-28908

Jordan, B. A., Cvejic, S. and Devi, L. A. (2000) Neuropsychopharmacol. **23**, S4

Jordan, B. A. and Devi, L. A. (1999) Nature **399**, 697-700

Jordan, B. A., Trapaidze, N., Gomes, I., Nivarthi, R. and Devi, L.A. (2001) Proc. Natl. Acad. Sci. U.S.A. **98**, 343-348

Kakidani, H., Furutani, Y., Takahashi, H., Noda, M., Morimoto, Y., Hirose, T., Asai, M., Inayama, S., Nakanishi, S. and Numa, S. (1982) Nature **298**, 245-249

Kallal, L., Gagnon, A. W., Penn, R. B. and Benovic, J. L. (1998) J. Neurosci. **273**, 322-328

Kamikubo, K., Murase, H., Matsuda, M. and Miura, K. (1988) J. Neurochem. **50,** 503-509

Karpa, K. D., Lin, R., kabbani, N. and Levenson, R. (2000) Mol. Pharmacol. **58**, 677-683

Kask, P., Palo, K., Ullmann, D. and Gall, K. (1999) Proc. Natl. Acad. Sci. U.S.A. **96,** 13756-13761

Kaupmann, K., Malitschek, B., Schuler, B., Heid, J., Froestl, W., Beck, P., Mosbacher, J., Bischoff, S., Kulik, A., Shigemoto, R., Karschin, A. and Bettler, B. (1998) Nature. **396**, 683-687

Keith, D. E., Murray, S. R., Zaki, P. A., Chu, P. C., Lissin, D. V., Kang, L., Evans, C. J. and von Zastrow, M. (1996) J. Biol. Chem. **271**, 19021-19024

Kieffer, B.L., Befort, K., Gaveriaux-Ruff, C., and Hirth, C.G. (1992) Proc. Natl. Acad. Sci. U.S.A. **89,** 12048-12052

Kieffer, B.L. (1999) Trends Pharmacol. Sci. **20**, 19-26

Kilpatrick, G.J., Dautzenberg, F. M., Martin, G. R. and Eglen, R.M. (1999) Trends Pharmacol. Sci. **20**, 294-301

Kong, H., Raynor, K., Yasuda, K., Moe, S., Portoghese, P., Bell, G. and Reisine, T. (1993) J. Biol. Chem. **268**, 23055-23058

Kovoor, A., Celver, J., Abdryashitov, R. I., Chavkin, C. and Gurevich V. V. (1999) J. Biol. Chem. **274**, 6831-6834

Kovoor, A., Nappey, V., Kieffer, B. L. and Chavkin, C. (1997) J. Biol. Chem. **272**, 27605-27611

Kramer, H. K., Andria, M. L., Esposito, D. H. and Simon, E. J. (2000) Biochem. Pharmacol. **60**, 781-792

Krause, G., Hermosilla, R., Oksche, A., Rutz, C., Rosenthal, W. and Schülein, R. (2000) Mol. Pharmacol. **57**, 232-242

Kroeger, K. M., Hanyaloglu, A. C., Seeber, R. M., Miles, L. E. C. and Eidne, K. A. (2001) J. Biol. Chem. **276**, 12736-12743

Kshirsagar, T., Nakano, A. H., Law, P. Y., Elde, R. and Portoghese, P. S. (1998) Neurosci. Lett. **249**, 83-86

Kunishima, N., Shimada, Y., Tsuji, Y., Sato, T., Yamamoto, M., Nakanishi, S., Jingami, H. and Morikawa, K. (2000) Nature **407**, 971-977

Lämmli, U. K. (1970) Nature. **227**, 680-685

Law, P., Kouhen, O. M., Solberg, J., Wang, W., Erickson, L. J. and Loh, H. H. (2000) J. Biol. Chem. **275**, 32057-32065

Law, P. Y., Wong, Y. H. and Loh, H. H. (1999) Biopolymers **51**, 440-455

Lee, N., Leybin, L., Chang, J. and Loh, H. (1980) Eur. J. Pharmacol. **68**, 181-185

Lee, S. P., O'Dowd, B. F., Ng, G. Y. K., Varghese, G., Akil, H., Mansour, A., Nguyen, T and George, S. R. (2000a) Mol. Pharmacol. **58**, 120-128

Lee, S. P., Xie, Z., Varghese, G., Nguyen, T., O'Dowd, B. F. and George, S. R. (2000b) Neuropsychopharmacol. **23**, S4

Leurs, R., Smit, M J., Alewijnse, A. E. and Timmerman, H. (1998) Trends Pharmacol. Sci **23**, 418-422

Li, J., Benivic, J. L. and Liu-Chen, L. (2000) Mol. Pharmacol. **58,** 795-801

Liu, R., Paxton, W. A., Choe, S., Ceradini, D., Martin, S. R., Horuk, R. M., MacDonald, M. E., Stuhlmann, H., Koup, R. A. and Landau, N. R. (1996) Cell **86**, 367-377

Lord, J., Waterfield, A., Hughes, J. and Kosterlitz, H. (1977) Nature **267**, 495-499

Lupus, A. (1996) Trends Biologi. Sci **21**, 375-382

Machelska, H. and Stein, C. (2000) Clini. Experi. Pharmacol. and Physiol. **27**, 533-536

Maeda, D.Y., Berman, F., Murray, T. F. and Aldrich, J. V. (2000) J. Med. Chem. **43**, 5044-5049

Maggio, R., Vogel, Z. and Wess, J. (1993a) FEBS letts. **319**, 195-200

Maggio, R., Vogel, Z. and Wess, J. (1993b) Proc. Natl. Acad. Sci. U.S.A. **90**, 3103-3107

Maggio, R., Barbier, P., Fornai, F and Corsini, G. U. (1996) J. Biol. Chem. **271**, 31055-31060

Manzanares, J., Corchero, J., Romero, J., Fernández-Ruiz, Ramos, J. A. and Fuentes J. A. (1999) Trends Pharmacol. Sci **20**, 287-293

Margeta-Mitrovic, M., Jan, Y.N. and Jan, L.Y. (2000) Neuron **27**, 97-106

Marshall, F. H., Jones, K. A., Kaupmann, K. and Bettler, B. (1999) Trends Pharmacol. Sci **20**, 396-399

Marshall, F. H. (2001) Curr. Opinion Cell. Biol. **1**, 1-5

Matthes, H., Maldonado, R., Simonin, F., Valverde, O., Slowe, S., Kitchen, I., Befort, K., Dierich, A., Le Meur, M., Dolle, P., Tzavara, E., Hanoune, J., Roques, B. and Keiffer, B (1996) Nature **383**, 819-823

Matthes, H. W. D., Smadja, C., Valverde, O., Vonesch, J. L., Foutz, A. S., Boudinot, E., Denavit-Saubié, M., Severini, C., Negri, L., Roques, B. P., Maldonado, R. and Kieffer, B. L. (1998) J. Neurosci. **18**, 7285-7295

McFadyen, I. J., Houshyar, H., Liu-Chen, L., Woods, J. A. and Traynor, J. R. (2000) Mol. Pharmacol. **58,** 669-676

McGrath, J. C., Arribas, S. and Daly, C. J. (1996) Trends Pharmacol. Sci. **17**, 393-399

McLatchie, L. M., Fraser, N. J., Main, M. J., Wise, A., Brown, J., Thomson, N., Solari, R., Lee, M. L. and Foord, S. M. (1998) Nature **393,** 333-339

McLean, A. J., Bevan, N., Rees, S. and Milligan, G. (1999) Mol. Pharmacol. **56**, 1182-1191

McLean, A. J. and Milligan, G. (2000) Br. J. Pharmacol. **130**, 1825-1832

McVey, M., Ramsay, D., Kellett, E., Rees, S., Wilson, S., Pope, A. J. and Milligan, G. (2001) J. Biol. Chem. **276**, 14092-14099

Meng, F., Hoversten, M. T., Thompson, R. C., Taylor, L., Watson, S. J. and Akil, H. (1995) J. Biol. Chem. **270**, 12730-12736

Meng, F., Wei, Q., Hoversten, M.T., Taylor, L.P. and Akil, H. (2000) J. Biol. Chem. **275**, 21939-21945

Merkouris, M., Dragatsis, I., Megaritis, G., Konidakis, G., Zioudrou, C., Milligan, G. and Georgoussi Z. (1996) Mol. Pharmacol. **50**, 985-993

Merkouris, M., Mullaney, I., Georgoussi, Z. and Milligan, G. (1997) J. Neurochem. **69**, 2115-2122

Metzger, T. G. and Ferguson D. M. (1995) FEBS Letts. **375**, 1-4

Michaely, P., Kamal, A., Anderson, R. G. W. and Bennett, V. (1999) J. Biol. Chem. **274**, 35908-35913

Mijares, A., Lebesgue, D., Wallukat, G. and Hoebeke, J. (2000) Mol. Pharmacol. **58**, 373-379

Milligan, G., Carr, C., Gould, G.W., Mullaney, I and Lavan B.E. (1991) J. Biol. Chem. **266**, 6447-6455

Milligan, G. (2001) J. Cell Sci. **114**, 1265-1271

Milligan, G. and Rees, S. (2000) Annu. Rep. Med. Chem. **35**, 271-279

Milligan, G. (2000) Science **288**, 65-67

Milligan, G. (1998) Trends Endrocrin. Metab. **9**, 13-19

Milligan, G. and White, J. H. (2001) Trends Pharmacol. Sci. **22**, 513-518

Miyawaki, A., Llopis, J., Heim, R., McCaffery, J. M., Adams, J. A., Ikura, M. and Tsien, R. Y. (1997) Nature. **388**, 882-887

Mogil, J. S., Grisel, J. E., Hayward, M. D., Bales, J. R., Rubinstein, M., Belknap, J. K. and Low, M. J. (2000) Neuroscience. **101**, 709-717

Möhler, H and Fritschy, J. (1999) Trends Pharmacol. Sci **20**, 87-89

Monnot, C., Bihoreau, C., Conchon, S., Curnow, K. M., Corvol, P. and Clauser, E. (1996) J. Biol. Chem. **271**, 1507-1513

Moon, H., Cavalli, A., Bahia, D. S., Hoffmann, M., Massotte D. and Milligan, G. (2001) J. Neurochem. **76**, 1805-1813

Morello, J. P., Salahpour, A., Laperriere, A., Bernier, V., Arthus, M. F., Lonergan, M., Petaja-Repo, U., Angers, S., Morin, D., Bichet, D. G. and Bouvier, M. (2000) J. Clin. Invest. **105**, 887-895

Mullaney, I., Shah, B.H., Wise, A. and Milligan, G. (1995) J. Neurochem. **65**, 545-553

Murray, S. R., Evans, C. J. and von Zastrow, M. (1998) J. Biol. Chem. **273**, 24987-24991

Nakagawa, T., Masuda, T., Watanabe, T., Minami, M. and Satoh, M. (2000) Eur. J. Pharmacol. **390**, 257-266

Nakanishi, S., Inoue, A., Kita, T., Nakamura, M., Chang, A., Cohen, S and Numa, S. (1979) Nature **278**, 423-427

Nakanishi-Matsui, M., Zheng, Y-W., Suiciner, D. J., Weiss, E. J., Ledeman, M. J and Coughlin, S. R. (2000) Nature **404**, 609-613

Naray-Fejes-Toth, A. and Fejes-Toth, G. (1996) J. Biol. Chem. **271**, 15436-15442

Nathans, J. and Hogness, D. S. (1983) Cell **34**, 807-814

Ng, G. Y., Mouillac, B., George, S. R., Caron, M, Dennis, M. and Bouvier, M. (1994) Eur. J. Pharmacol. **267**, 7-19

Ng, G. Y. K., O'Dowd, B. F., Lee, S. P., Chung, H. T., Bran, M. R., Seeman, P. and George, S. R. (1996) Biochem. and Biophys. Res. Com. **227**, 200-204

Nimchinsky, E. A., Hof, P. R., Janssen, W. G. M., Morrison, J. H. and Schmauss, C. (1997) J. Biol. Chem. **272**, 29229-29237

Noda, M., Furutani, Y., Takahashi, H., Toyosato, M., Hirose, T., Inayama, S., Nakanshini, S. and Numa, S. (1982) Nature **295**, 202-206

Oakley, R. H., Laporte, S. A., Holt, J. A., Barak, L. S. and Caron, M. G. (1999) J. Biol. Chem. **274**, 32248-32257

O'Brien, P. J., Prevost, N., Molino, M. M., Hollinger, K., Woolkalis, M. J., Woulfe, D. S. and Brass, L. F. (2000) J. Biol. Chem. **275**, 13502-13509

Offermanns, S., Mancino, V., Revel, J. and Simon, M. (1997) Science. 275, 533-536

Onaran, H. O. and Gürdal, H. (1999) Trends Pharmacol. Sci **20**, 274-278

Oswald, B., Lehmann, F., Simon, L., Terpetschnig, E. and Wolfbeis, O. S. (2000) Anal. Biochem. **280,** 272-277

Overton, M. C. and Blumer, K. L. (2000) Curr. Biol. **10**, 341-344

Palczewski, K., Kumasaka, T., Hori, T., Behnke, C. A., Motoshima, H., Fox, B. A., Le Trong, I., Teller, D., Okada, T., Stenkamp, R. E., Yamamoto, M. and Miyano, M. (2000) Science **289**, 739-745

Pan, Y., Xu, J., Bolan, E., Abbadie, C., Chang, A., Zuckerman, A., Rossi, G and

Pasternak, G. W. (1999) Mol. Pharmacol. **56**, 396-403

Pasternak, G., Simantov, R. and Snyder, S. (1976) Mol. Pharmacol. **12**, 504-513

Pei, G., Kieffer, B. L., Lefkowitz, R. J. and Freedman, N. J. (1995) Mol. Pharmacol. **48**, 173-177

Pepin, M., Yue, S. Y., Roberts, E., Wahlestedt, C. and Walker, P. (1997) J. Biol. Chem. **272**, 9260-9267

Pert, C. and Snyder, S. (1973) Science **179**, 1011-1014

Petäjä-Repo, U. E., Hogue, M., Laperrière, A., Walkers, P and Bouvier, M. (2000) J. Biol. Chem. **275**, 13727-13736

Peybay-Peyroula, E., Rummel, G., Rosenbusch, J and Landau, E. (1997) Science **277**, 1676-1681

Pfeiffer, M., Koch, T., Schröder, H., Klutzny, M., Kirscht, S., Hreienkamp, H., Hölt, V and Schulz, S. (2001) J. Biol. Chem. **276**, 14027-14036

Pierce, K. L., Luttrell, L. M. and Lefkowitz, R. J. (2001) Oncogene **20**, 1532-1539

Pogozheva, I.D., Lomize, A.L. and Mosberg, H.I. (1998) Biophys.J. **75**, 612-634

Pope, A. J., Haupts, U. M. and Moore, K. J. (1999) Drug. Disc. Today. **4,** 350-362

Porreca, F., Takemori, A., Sultana, M., Portoghese, P., Bowen, W. and Mosberg, H. (1992) J. Pharmacol. Exp. Ther. **263**, 147-152

Powell, K. J., Ma, W., Sutak, M., Doods, H., Quirion, R. and Jhamandas, K. (2000) Brit. J. Pharmacol. **131**, 875-884

Quitterer, U. and Lohse, M. J. (1999) Proc. Natl. Acad. Sci. U.S.A. **96,** 10626-10631

Quock, R. M., Burkey, T. H., Varga, E., Hosohata, Y., Hosohata, K., Cowell, S. M., Slate, C. A., Ehlert, F. J., Roeske, W. R. and Yamamura, H. I. (1999) Pharmacol. Reviews. **51**, 503-532

Ray, K. and Hauschild, B. C. (2000) J. Biol. Chem. **275**, 34245-34251

Remmers, A. E. (1998) Anal. Biochem. **257,** 89-94

Remmers, A. E., Clark, M. J., Liu, X, Y. and Medzihradsky, F. (1998) J. Pharmacol. Experi. Therap. **287**, 625-632

Rodríguez-Frade, J. M., Vila-Coro, A. J., De Anna, A. M., Albar, J. P., Martínez, A. C. and Mellado, M. (1999) Proc. Natl. Acad. Sci. U.S.A. **96,** 3628-3633

Romano, C., Yang, W. and O'Malley, K. L. (1996) J. Biol. Chem. **271**, 28612-28616

Rosomer, V. A., Ball, R. and Smrcka, A. V. (1996) J. Biol. Chem. **271**, 25071-25078

Rosomer, V. A., Hinkle, P. M. and Persechini, A. (1997) J. Biol. Chem. **272**, 13270-13274

Rocheville, M., Lange, D. C., Kumar, U., Sasi, R., Patel, R. C. and Patel, Y. C. (2000a) J. Biol. Chem. **275**, 7862-7869

Rocheville, M., Lange, D. C., Kumar, U., Patel, D. C. and Patel, Y. C. (2000b) Science **288**, 154-157

Ruehr, M. L., Zakhary, D. R., Damron, D. S. and Bond, M. (1999) J. Biol. Chem. **274,** 33092-33096

Salahpour, A., Angers, S and Bouvier, M. (2000) Trends Endocrin. Metab. **11**, 163-168

Salomon, Y., Londos, C., and Rodbell, M. (1974) Anal. Biochem. **58**, 541-548

Scarselli, M., Armogida, M., Chiaccho, S., DeMontis, M. G., Colzi, A., Corsini, G. U. and Maggio, R. (2000) Eur. J. Pharmacol. **397**, 291-296

Scheer, A., Fanelli, F., Costa, T., De Benedetti, P. G. and Cottecchia, S. (1996) Proc. Natl. Acad. Sci. U.S.A. **94**, 808-813

Schiller, P., Fundytus, M., Merovitz, L., Weltrowska, G., Nguyen, T., Lemieux, C., Chung, N. and Coderre, T (1999) J. Med. Chem. **42**, 3520-3526

Schöbeberg, T., Yun, J., Wenkert, D. and Wess, J. (1996) EMBO J. **15**, 1283-1291

Schulz, A., Grosse, R., Schulz, G., Gudermann, T and Schöneberg, T. (2000) J. Biol. Chem. **275**, 2381-2389

Seifert, R., Wenzel-Seifert, K. and Kobilka, B. K. (1999) Trends. Pharmacol. Sci. **20**, 383-389

Simon, J., Hiller, J. and Edelman, I. (1973) Proc. Natl. Acad. Sci. U.S.A. **70**, 1947-1949

Sora, I., Funada, M. and Uhl, G. R. (1997) Eur. J. Pharmacology **324**, 1-2
Stadel, J.M., Wilson, S. and Bergsma, D. J. (1997) Trends Pharmacol. Sci. **18**, 430-436

Stenroos, K., Hurskainen, P., Eriksson, S., Hemmilä, I., Blomberg, K. and Lindqvist, C. (1998) Cytokine. **10,** 495-499

Stone, L.S., MacMillan, L. B., Kitto, K. F., Limbird, L. E., Wilcox, G. L. (1997) J. Neurosci. **17**, 7157-7165

Strahs, D. and Weinstein, H. (1997) Protein Engineering. **10**, 1019-1038.

Tanner, K. G. and Kyte, J. (1999) J. Biol. Chem. **274**, 35985-35990

Tarasova, N. I., Rice, W. G. and Michejda, C. J. (1999) J. Biol. Chem. **274,** 34911-34955

Tarasova, N. I., Stauber, R.H., Choi, J. K., Hudson, E. A., Czerwinski, G., Miller, J. L., Pavlakis, G. N., Michejda, C. J. and Wank, S. A. (1997) J. Biol. Chem. **272,** 14817-14824

Terenius, L. (1973) Acta. Pharmacol. Toxicol **32**, 317-319

Tsien, R. Y. (1998) An. Rev. Biochem. **67,** 509-544

Tsuji, Y., Shimada, Y., Takeshita, T., Kajimura, N., Nomura, S., Sekiyama, N., Otomo, J., Usukura, J., Nakanishi, S. and Jingami, H. (2000) J. Biol. Chem. **275**, 28144-28151

Turcatti, G., Vogel, H. and Chollet, A. (1995) Biochemistry. **34**, 3972-3980

Ulloa-Aguirre, A., Stanislaus, D., Janovick, J. A. and Conn, P. M. (1999) Arch. Med. Res. **30**, 420-435

Valiquette, M., Vu, H., Yue, S., Wahlestedt, C. and Walker, P. (1996) J. Biol. Chem. **271**, 18789-18791

Vanderklish, P. W., Krushel, L. A., Holst, B. H., Gally, J. A. and Crossin, K. L. (1999) Proc. Natl. Acad. Sci. U.S.A. **97,** 2253-2258

Vaughan, M. (1998) J. Biol. Chem. **273**, 667-668

Vaught, J. and Takemori, A. (1979) J. Pharmacol. Exp. Ther. **208**, 86-94

Vickery, R. V. and von Zastrow, M. (1999) J. Cell Biol. **144,** 31-43

Vila-Coro, A. J., Mellado, M., Martin, de Ana, A., Lucas, P., del Real, G., Martinez, A. C. and Rodriguez-Frade, J. M. (2000) Proc. Natl. Acad. Sci. U.S.A **97**, 3388-3393

Vila-Coro, A. J., Rodriguez-Frade, J. M., Martin, de Ana, A., Moreno-Ortiz, M. C., Martinez-A, C. and Mellado, M. (1999) FASEB J. **13**, 1699-1710

Wang, C., Zhou, D., Cheng, Z., Wei, Q., Chen, J., Li, G., Pei, G. and Chi, Z. (1998) Biochem. Biophys. Res. Comm. **249**, 321-324

Wang, H., Peters, G. A., Zeng, X., Tang, M., Ip, W. and Khan, S. A. (1995) J. Biol. Chem. **270**, 23322-23329

Wells, J. L., Bartlett J. L., Ananthan, S. and Bilsky, E.J. (2001) J. Pharmacol. Exp. Therap. **297**, 597-605

Weng, G., Bhalla, U. S. and Iyengar, R. (1999) Science. **284,** 92-96
Wess, J. (1997) FASEB J. **11**, 346-354

Whistler, J. L., Chuang, H., Chu, P., Jan, L. Y. and von Zastrow M. (1999) Neuron. **23**, 737-746

Whistler J. L. and von Zastrow M. (1999) J. Biol. Chem. **274**, 24575-24578

White, J. A., Wise, A., Main, M. J., Green, A., Fraser, N. J., Disney, G. H., Barnes, A. A., Emson, P., Foord, S. M. and Marshall, F. H. (1998) Nature. **396**, 679-682

Whitehead, I. P., Zohn, I. E. and Der, C. J. (2001) Oncogene **20**, 1547-1555

Willars, G. B., Heding, A., Vrecl, M., Sellar, R., Blomenrohr, M., Nahorski, S. R. and Eidne, K. A. (1999) J. Biol. Chem. **274**, 30146-30153

Winkler, T., Kettling, U., Koltermann, A. and Eigen, M. (1999) Proc. Natl. Acad. Sci. U.S.A. **96**, 1375-1378

Wong, Y. H. (1994) Methods Enzymol. **238**, 81-94

Wu, P and Brand, L. (1994) Anal. Biochem. **218,** 1-13

Xu, Y., Piston, D. W. and Johnson, C.H. (1999) Proc. Natl. Acad. Sci. U.S.A. **96**, 151-156

Yang, Q. and Lanier, S. M. (1999) Mol. Pharmacol. **56**, 651-656

Yasuda, K., Raynor, K., Kong, H., Breder, C. D., Takeda, J., Reisine, T., and Bell, G. I. (1993) Proc. Natl. Acad. Sci. U.S.A. **90,** 6736-6740

Yasunaga, T., Motoyama, S., Nose, T., Kodama, H., Kondo, M. and Shimohigashi, Y. (1996) J. Biochem. **120,** 459-465

Yesilaltay, A. and Jenness, D. D. (2000) Mol. Biol. Cell **11**, 2873-2884

Zeng, F. and Wess, J. (1999) J. Biol. Chem. **274**, 19487-19497

Zernicka-Goetz, M., Pines, J., McLean, H. S., Dixon, J. P., Sieming, K. R., Haseloff, J. and Evans, M. J. (1997) Development **124**, 1133-1137

Zhang, J., Ferguson, S.S.G., Barak, L.S., Ménard L. and Caron, M. G. (1996) J. Biol. Chem. **271**, 18302-18305

Zhang, J., Barak, L. S., Anborgh, P. H., Laporte, S. A., Caron, M. G. and Ferguson, S. S. G. (1999) J. Biol. Chem. **274**, 10999-11066

Zhang, J., Tongming, C., Nguyen, S. H. and Oldenburg, K, R. (2000) Anal. Biochem. **281**, 182-186

Zhu, J., Yin, J., Law, P., Claude, P. A., Rice, K. C., Evans, C. J., Chen, C., Yu, L. and Liu-Chen, L. (1996) J. Biol. Chem. **271**, 1430-1434

Zhu, X. and Wess, J. (1998) Biochemistry **37**, 15773-15784

Zimprich, A., Simon, T and Hollt, V. (1995) FEBS letts. **359**, 142-146

Zitzer, H., Honck, H., Bachner, D., Richter, D. and Kreienkamp, H. (1999) J. Biol. Chem. **274**, 32997-33001

Zuck, P., Zhege, L., Skwish, S., Glickman, J. F., Yang, K., Burbaum, J. and Inglese, J. (1999) Proc. Natl. Acad. Sci. U.S.A. **96**, 11122-11127

Zukin, R. S., Echbali, M., Olive, D., Unterwald, E. M. and Tempel, A. (1998) Proc. Natl. Acad. Sci. 4061-4065